# ATF3 Expression as a Marker of Response to Histone Deacetylase Inhibition of Bladder Cancer Progression

BY

## Dhanya Sooraj

**Supervisors:**

**Prof. Bryan R G Williams**

**Dr. Dakang Xu**

A thesis submitted for fulfilment of the requirements for the degree of

DOCTOR OF PHILOSOPHY

2016

*Centre for Cancer Research*

*Hudson Institute of Medical Research*

*Faculty of Medicine, Nursing and Health Sciences*

# Copyright Notice

## Notice 1

## Notice 2

# *TABLE OF CONTENTS*

# *DECLARATION*

**General Declaration**

**Monash University**

In accordance with Monash University Doctorate Regulation 17.2 Doctor of Philosophy and Research Master's regulations the following declarations are made:

I hereby declare that this thesis contains no material which has been accepted for the award of any other degree or diploma at any university or equivalent institution and that, to the best of my knowledge and belief, this thesis contains no material previously published or written by another person, except where due reference is made in the text of the thesis. The central theme of the thesis is reactivating ATF3 has therapeutical utility in advanced bladder cancer. The ideas, development and writing up of thesis were principle responsibility of myself, the candidate, working within the Hudson Institute of Medical Research under the supervision of Prof. Bryan RG Williams and Dr. Dakang Xu.

Signed

Name: Dhanya Sooraj

Date: 23/08/2016

# *ACKNOWLEDGEMENTS*

This thesis covers a body of work performed over the past three years, and this should not have been possible without the guidance, experience and supports provided my supervisors, collaborators, colleagues, friends and family.

First and foremost I would like to thank my supervisor, Professor Bryan Williams for providing me a wonderful opportunity to undertake my postgraduate studies under his guidance and supervision. I am so honoured to have Bryan as my supervisor, who always inspires me with his wealth of knowledge, and passion and commitment to research. He always finds time in his busy schedules (being the Director of the Hudson) to discuss my research findings and promptly correcting my documents, and all those discussions we had helped me grow my confidence and independency. I am so privileged to have Bryan as my supervisor in my important research journey and I will always be grateful for all the precious advice and support given to me in the past years and would like to continue this association in my journey ahead.

I would also like to thank my other supervisor, Dr. Dakang Xu for his continued support and advice. Dr. Daniel Gold, our respected collaborator, I would like to thank for your advice and feed backs during this study.

I would also acknowledge my gratitude to Dr. Jason Cain, for his generous act of accommodating me in his tight schedules. Your advice and support gave me a head-start in my research journey and I will always be grateful for providing me a profound insight into some technical aspects of this study. Jason, always happy to discuss my research findings and conversation with him keep me excited.

# *PUBLICATIONS*

1. **Sooraj D,** Xu D, Cain JE, Gold DP, Williams BR Activating Transcription Factor 3 expression as a marker of response to the histone deacteylase inhibitor Pracinostat. Molecular Cancer Therapeutics. 2016 Apr 25. doi: 10.1158/1535-7163-MCT-15-0890. PubMed PMID: 27196751

## *ABSTRACTS*

**Dhanya Sooraj**, Dakang Xu, Jason Cain, Daniel Gold, and Bryan R. Williams. Activating transcription factor 3 (ATF-3) expression is a potential marker of tumor response to the HDAC inhibitor Pracinostat. Proceedings: AACR Annual Meeting 2014; April 5-9, 2014; San Diego, CA. **Cancer Research** October 1, 2014   74; 387

## **AWARDS**

Australian Postgraduate Award:  2012 - 2015

# THESIS PREFACE

The work presented in this thesis contains unpublished results arising from this study. Chapter 1 of this thesis details the molecular landscape with particular emphasis on the epigenetic modulations associated with the clinical development and progression of bladder cancer and the current treatment options. This chapter also details the dichotomous role of Activating Transcription Factor 3 (ATF3) in human cancers and discuss the pharmacological benefits and potency of Pracinostat - the histone deacetylase inhibitor (HDACi) used for further studies. Chapter 2 contains general experimental methods for experiments performed as a part of this thesis. Specialised methods are provided in the relevant chapters. Chapter 3 is an experimental chapter describing the role of Pracinostat in reactivating ATF3 expressions and significance of this reactivation using *in vitro* bladder models. Chapter 4 confirms the findings made from chapter 3 using animal models. The anti-tumor efficacy of Pracinostat and the consequences of ATF3 reactivation comprehensively illustrated using xenograft models. Chapter 5 defines the pivotal role of ATF3 in defining the sensitivity to HDACi mediated therapy using *in vivo* and *in vitro* tumor models. This chapter also identify Retinoblastoma (RB1) as a potential target of ATF3 and describe the role of ATF3 in regulating the RB1 expression. Chapter 6 explores translated ribosome affinity purification (TRAP)-mRNA method to identify the key partner proteins of ATF3 in regulating the non-malignant phenotypes. Chapter 7, final chapter is a general discussion of all the results presented in the thesis with relevant conclusions and future directions.

# *ABBREVIATIONS*

5-ALA                5-aminolevulinic acid

AIHW                 Australian institute of health and welfare

ANOVA                Analysis of variance

ATCC                 American type culture collection

ATF3                 Activating transcription factor 3

ATP                  Adenosine tri-phosphate

BBN                  N- butyl N- nitrosamine

BCA                  Bicinchoninic acid assay

BCG                  *Bacillus Calmette - Guerin*

BCL-2                B-cell CLL/lymphoma 2

BRCA1                Breast cancer 2

BRCA2                Breast cancer 2

bZIP                 Basic region leucine zipper

CBP                  Cyclic-AMP response element binding protein

CCL4                 Chemokine (C-C motif) ligand 4

CDKN2A               Cyclin-dependent kinase inhibitor 2A

cDNA                 Complementary DNA

| | |
|---|---|
| CHD6 | Chromodomain helicase DNA binding protein 6 |
| ChIP | Chromatin Immuno-Precipitation |
| CIS | Carcinoma *in situ* |
| CMV | *CytoMegaloVirus* |
| CREBBP | CREB binding protein |
| CRPC | Castration resistant prostate cancer |
| CTC | Circulating tumor cell |
| CTC | Circulating tumor cells |
| CTCL | Cutaneous T-cell lymphoma |
| CYP3A4 | Cytochrome P450 family 3 subfamily A member 4 |
| CYPIA2 | Cytochrome P450 family 1 subfamily A member 2 |
| DAPI | 4',6-Diamidino-2-phenylindole |
| DAPK | Death-associated protein kinase 1 |
| dH2O | Distilled water |
| DMEM | Dulbecco's minimal essential medium |
| DMSO | Dimethyl sulfoxide |
| DNA | Deoxyribonucleic acid |
| dNTPs | Deoxynucleotide triphosphate |
| DR-5 | Death receptor-5 |

| | |
|---|---|
| DTT | Dithiothreitol |
| E2F | E2F transcription factor 1 |
| EGFR | Epidermal Growth Factor Receptor |
| EP300 | E1A binding protein p300 |
| ERBB2 | erb-b2 receptor tyrosine kinase 2 |
| ESR1 | Estrogen receptor 1 |
| EZH2 | Enhancer of zeste 2 polycomb repressive complex 2 subunit |
| FBS | Feotal bovine serum |
| FDA | Food and drug administration |
| FGFR3 | Fibroblast growth factor receptor |
| GCNT | GCN-related N-acetyl transferase |
| GSTM1 | glutathione S-transferase-$\mu$1 |
| GSTP1 | Glutathione S-transferase pi 1 |
| HAL | hexaminolevulinic acid |
| HATs | Histone acetyl transferases |
| HDACi | Histone deacetylase inhibitor |
| HDACs | Histone deacetylases |
| HDMs | Histone demethylases |
| HMTs | Histone methyl transferases |

| | |
|---|---|
| H-ras | v -Ha- Ras- Harvey rat sarcoma viral oncogene |
| hTERT | Human telomerase reverse transcriptase |
| IL1β | Interleukin 1 beta |
| KDa | Kilodalton |
| KDM6A | Lysine demethylase 6A |
| lncRNA | Long non-coding RNA |
| MAPK | Mitogen activated kinase-like protein |
| mGFP | Monomeric green fluorescent protein |
| MGMT | O-6-methylguanine-DNA methyltransferase |
| MIBC | Muscle invasive bladder cancer |
| miRNA | microRNA |
| ml | Milliliter |
| MLH1 | Mut L homolog 1 |
| MLL | Lysine methyltransferase 2A |
| MLL2 | Myeloid/lymphoid or mixed-lineage leukemia 2 |
| MTD | Maximum tolerated dosage |
| mTOR | Mechanistic target of rapamycin ( serine/ threonine kinase) |
| M-VAC | Methotrexate, Vinblastine, Doxorubicin (Adriamycin) and Cisplatin |
| MYST | Monocytic leukaemia zinc finger protein |

NAT2            N-acetyl transferase 2

NCOR1           Nuclear receptor corepressor 1

NF-κB           Nuclear factor of kappa light polypeptide gene enhancer in B-cells 1

NMIBC           Non-muscle invasive bladder cancers

NSCLC           Non-small cell lung cancer

PBS             Phosphate buffered saline

PI              Propidium iodide

PI3K            Phosphoinositide-3 kinase

PIK3Ca          Phosphatidylinositol-4,5-bisphosphate 3-kinase catalytic subunit alpha

PIK3CA          phosphoinositide-3-kinase, catalytic, alpha polypeptide

PSA             Prostate specific antigen

PTEN            Phosphatase and tensin homologue

PVDF            Polyvinylidene fluoride

RARB            Retinoic acid receptor beta

RAS             Resistance to audiogenic seizures

RB1             Retinoblastoma 1

RIPA            Radio immunoprecipitation assay

RLU             Relative light unit

RNA             Ribonucleic acid

| | |
|---|---|
| RNA-seq | Ribonucleic acid sequencing |
| RPL10 | Ribosomal protein L10 |
| RPs | Ribosomal proteins |
| rRNA | Ribosomal RNA |
| RTK | Receptor tyrosine kinase |
| SCID | Severe combined immune deficient |
| SDS-PAGE | Sodium dodecyl sulphate-polyacrylamide gel electrophoresis |
| shRNA | small hairpin Ribonucleic Acid |
| siRNA | small interfering RNA |
| snoRNA | small nuclear RNA |
| SP1 | Sp1 transcription factor |
| STAT1 | Signal transducer and activator of transcription 1 |
| TACC3 | Transforming acidic coiled-coil containing protein 3 |
| TCC | Transitional cell carcinoma |
| TGF-β1 | Transforming growth factor beta 1 |
| TGI | Tumor growth inhibition |
| TIMP3 | TIMP metallopeptidase inhibitor 3 |
| TIP60 | Tat interactive protein |
| TNF | Tumor necrosis factor |

| | |
|---|---|
| TNM | Tumour-node-metastasis |
| TP53 | Tumor protein 53 |
| TRAP | translating ribosome affinity purification |
| tRNAs | Ribosomal ribonucleic acid |
| TRX | Thioredoxin |
| TURBT | Transurethral resection of bladder tumour |
| UCC | urothelial cell carcinomas |
| UTX | Utx histone demethylase |
| VEGF | Vascular endothelial growth factor |
| α-SMA | alpha- Smooth muscle actin |
| γH2AX | Gamma histone variant H2AX |

# *ABSTRACT*

Improved treatment strategies are required for bladder cancer, due to frequent recurrence of low-grade tumors and poor survival rate from high-grade tumors with current therapies. Histone deacetylase inhibitors (HDACi), approved as single agents for specific lymphomas, have shown promising preclinical results in solid tumors but could benefit from identification of biomarkers for response. Loss of activating transcription factor 3 (ATF3) expression is a feature of bladder tumor progression, and correlates with poor clinical survival. This study investigated the utility of measuring ATF3 expression as marker of response to the HDACi Pracinostat in bladder cancer models. Pracinostat treatment of bladder cancer cell lines reactivated expression of ATF3, correlating with significant alteration in proliferative, migratory and anchorage-dependent growth capacities. Pracinostat induced growth arrest at the G0/G1 cell cycle phase, coincident with activation of tumor suppressor genes. Pracinostat treatment also induced sensitivity of bladder cancer cells to chemotherapy *in vitro*. In mouse xenograft bladder cancer models, Pracinostat treatment significantly reduced tumor volumes compared to controls, accompanied by re-expression of ATF3 in non-proliferating cells from early to late stage of therapy, and in parallel induced anti-angiogenesis and apoptosis. Importantly, cells in which ATF3 expression was depleted were less sensitive to Pracinostat treatment *in vitro*, exhibiting significantly higher proliferative and migratory properties. *In vivo*, control xenograft tumors were significantly more responsive to treatment than ATF3 knockdown xenografts. This study also identified a potential target of ATF3 - RB1, a key tumor suppressor, in regulating the non-malignant phenotype. Mechanistic studies revealed that overexpression of ATF3 upregulated RB1 expression, concomitant with cell cycle arrest.

I conclude that the reactivation of ATF3 is pivotal in determining sensitivity to Pracinostat treatment, both *in vitro* and *in vivo,* and could serve as a potential biomarker of response, and provide a rationale for therapeutic utility in HDACi-mediated treatments for bladder cancer.

# CHAPTER -1

## INTRODUCTION

A report from the Australian Institute of Health and Welfare (AIHW) published in 2014 suggests that cancer is the leading illness causing death and accounts for about 3 in 10 deaths. The report estimated that nearly 45,780 people succumbed to death in 2014 from cancer [1] [2]. Furthermore, it was estimated that 123,920 Australians were diagnosed with cancer in 2014 and more than half of cancers (55%) were diagnosed in males. The five most commonly reported cancers are prostate, bowel (colorectal), breast, melanoma and lung cancers. The report also suggested that the number of new cases being diagnosed has more than doubled in the last two decades, mainly due to the ageing and increasing size of populations, improved diagnosis through screening programs, and improvements in techniques and technologies for identifying and diagnosing cancers. Similarly, survival rates have also improved over the past 5 years, although the improvements are not consistent across all cancers, with the largest survival gains in prostate and kidney cancers, and non-Hodgkin lymphoma.

## 1.1 Bladder Cancer

Bladder cancer is the most common cancer of the urinary tract, with ~150,000 deaths and ~380,000 new cases worldwide each year [3]. It ranks fifth among cancers in men in Western countries. In Australia, 2014 AIHW reported that the incidence rates were higher in males, with approximately 2,060 new cases diagnosed, whereas less than half of the cases reported were in females (~675 new cases). The five year relative survival rate at the end of 2012 was 55% in males and 47% in females, according to the report.

## 1.2 Risk Factors for Bladder Cancer

Many epidemiological studies have identified a range of environmental and genetic risk factors associated with the development of bladder cancer [4-7]. Age is the most significant risk factor for bladder cancer and the median age at diagnosis is ~70 years. According to the

latest estimate in Australia, the incidence risk to age 75 years for males is 1 in 115, which substantially increases to 1 in 43 at the age of 85 [8]. Although men are more likely to develop bladder cancer, women often present with more advanced disease, with a less favourable prognosis [9-11].

Smoking is another key risk factor; the chances of developing bladder cancer are three times higher in smokers compared to non-smokers [12]. Tobacco smoke contains aromatic amines such as β-naphthylamine, and polycyclic aromatic hydrocarbons known to cause bladder cancer [13]. Workplace exposure to certain chemicals, including aromatic amines ( benzidine, polycyclic hydrocarbons) used mainly in industries such as leather, dye, rubber, textiles and paint, and consumption of arsenic-contaminated water are known environmental risk factors that contribute to the development of bladder cancer[14, 15]. Additionally, chronic inflammation of the bladder, infection with *Schistosoma* species and previous urological cancer treatment, especially with ionizing radiation or therapy with phenacetin-containing analgesic, are also listed as risk factors for bladder cancer [9, 16].

Genetic and familial background also contributes to the risk of developing bladder cancer; the risk of bladder cancer is two-fold higher in first degree relatives of bladder cancer patient [17]. Somatic mutations in several genes including FGFR3, H-ras (gain) RB1, TP53 and PTEN (loss) were identified in bladder cancer development and progression [18-20]. Inherited polymorphisms in two carcinogen-detoxifying genes – N-acetyl transferase 2 (NAT2) and glutathione S-transferase-μ1 (GSTM1) are often associated with bladder cancer accounting for up to 30% of bladder cancer cases because of their high prevalence [21] [17]. Meta-analysis of clinical data using transitional bladder cancer samples showed that the GSTM1 null genotype increases the overall risk of bladder cancer while the NAT2 genotype increases the risk particularly in cigarette smokers.[22].

## 1.3 Types and Staging of Bladder Cancer

The majority of bladder cancers are urothelial cell carcinomas (UCC), which start in the inner epithelial layer/lumen of the bladder and account for >90% of carcinomas. They are clinically subdivided into superficial non-muscle invasive bladder cancers (NMIBCs) and muscle invasive bladder cancers (MIBCs). At the time of diagnosis, the majority (~60%) of the UCC are low-grade NMIBCs and the remaining 40% are high-grade MIBCs. NMIBCs (spread only in the epithelial basement membrane) frequently recur at a rate of 50-70%, but infrequently (10-15%) progress to high-grade invasive cancers [23]. MIBCs are believed to develop via carcinoma *in situ* (CIS) or flat dysplasia. UCC are staged using the TNM (tumour-node-metastasis) system according to their cellular characteristics [9] (Figure 1.1).
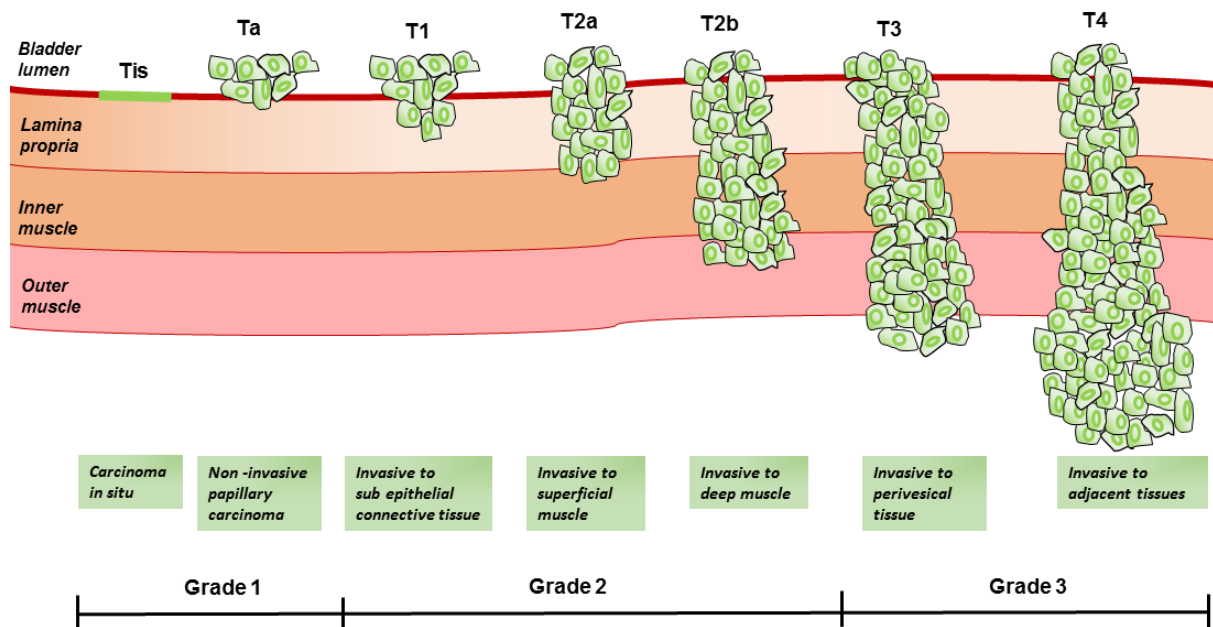


**FIGURE 1.1**: *Schematic representation of bladder cancer staging and grading according to the tumour-node-metastasis (TNM) system, adapted and modified* **[9]***.*

At the time of presentation, NMIBCs are in stage T1 and have a good prognosis, resulting in ~90% survival 5 years after treatment. MIBCs are mainly at stage T2 and above, resulting in a less favourable prognosis, with a survival rate of <50% five years after surgery [24]. The survival rates significantly drop to 34% for those with disease that has spread locally beyond the bladder (to the adjacent lymph nodes) and to 6% for patients with distant metastases [25]. The remaining histological types of bladder cancer are squamous cell carcinoma (1-2%), adenocarcinoma (1%), small cells (1%) micropapillary, and plasmacytoid.

## 1.4 Treatment and Management of Bladder Cancer

### 1.4.1        Surgery

Standard treatment for NMIBC tumours involves transurethral resection of bladder tumour (TURBT), followed by intravesical installation of chemotherapeutic agent or immunotherapeutic agent to delay recurrence [26] [27]. TURBT is not effective in CIS, because the disease is diffuse in nature and is difficult to visualize for complete surgical removal [28]. White light has traditionally been used for visualising neoplastic lesions and bulk tumour for resection. Due to the high recurrence rates (31-78%) of NMIBC, patients need to undergo multiple resections over many years, with constant monitoring to reduce morbidity. Photodynamic diagnosis is an emerging option that utilises the photodynamics of certain compounds (5-aminolevulinic acid - 5-ALA, hexaminolevulinic acid - HAL) to better visualise tumour lesions for resection. Use of this photodynamic technology results in improved outcomes and reduces the recurrence rate to >10% reduction compared to white-light resection [29].

Radical cystectomy (partial or complete removal of the bladder) followed by radiation or chemotherapy is the first-line treatment for patients with muscle invasive disease, mainly in stage T2-T4 [30] [31]. Cystectomy is also appropriately used to treat some high-risk NMIBC

tumours, including CIS. Radical cystectomy for men is known as cystoprostatectomy and for women it is anterior pelvic exenteration; both of these procedures include dissection of the regional lymph nodes [32]. At the time of radical cystectomy, ~25% of patients are diagnosed with lymph node metastasis, in which case bilateral pelvic lymphadenectomy (PLND) is also performed.

### 1.4.2 Intravesical immunotherapy and chemotherapy

Patients with low-grade, low-stage disease are expected to benefit from a single installation of intravesical immunotherapy or chemotherapy, followed by the TURBT. Immunotherapy with BCG (*Bacillus Calmette - Guerin*) was found to be effective in patients with T1 and CIS, though it did not improve the recurrence rate [33]. Interferon alpha/gamma has also been used in combination with immunotherapy for treating Ta, T1 and CIS urothelial carcinoma [34].

The most common chemotherapeutic agents used in intravesical chemotherapy are mitomycin (alkylating agent), epirubicin and doxorubicin (intercalating agents). The treatment is initiated from 6 hours after resection to prevent seeding of tumour cells, till 2-4 weeks post-resection to remove residual neoplastic and pre-neoplastic cells, depending on the type of agent [35].

### 1.4.3 Chemotherapy for advanced bladder cancer

Cisplatin-based neoadjuvant chemotherapy is the standard treatment for MIBC with tumour grade T2 or more. Chemotherapy prior to radical cystectomy is shown to have several potential benefits, including a reduction in the primary tumour burden resulting in effective local surgery, effective treatment for micro-metastatic disease, pathologic down staging and improved survival outcomes [36]. Although there is compelling evidence in support of neoadjuvant chemotherapy, with a proportionate increase in survival rate, adjuvant

6

chemotherapy is also used in clinical settings in advanced bladder cancer. The adjuvant chemotherapy is beneficial for patients who undergo up-front radical cystectomy and have extensive tumour invasion of the bladder wall or lymph node involvement [37].

In metastatic bladder cancer, platinum-based chemotherapy is the standard of care, in the combination of Methotrexate, Vinblastine, Doxorubicin (Adriamycin) and Cisplatin (M-VAC). This treatment regime has been shown to increase the survival rate significantly where there is a complete response. M-VAC therapy is less effective in patients with Epidermal Growth Factor Receptor (EGFR) overexpression (poor prognostic marker), renal impairment or cardiac diseases, and thus alternative targeted therapies have been shown to be of benefit. Gemcitabine and Cisplatin (GC) is a newer regime that has been shown to be as effective as M-VAC, but with less toxicity. Gefitinib, a receptor tyrosine kinase inhibitor for EGFR, has been found to be more effective in patients overexpressing EGFR in Phase 2 clinical trials [38].

The treatment regime for localised small cell carcinoma is neoadjuvant chemotherapy followed by radical cystectomy [39]. Patients with stage 3 (T3) and stage 4 (T4) disease are treated with adjuvant chemotherapy with radical cystectomy and chemotherapy using platinum-based protocol, as applied to metastatic disease [40].

In adenocarcinoma, chemotherapy-based treatment options are less effective and thus radical cystectomy is the treatment of choice. Squamous cell carcinomas are generally responsive to a treatment regime with radical cystectomy and pelvic lymph node dissection [34]. The current treatment options for bladder cancer are summarised in **Table 1.1**

Due to the history of a high-frequency recurrence rate (37-78%), as well as a moderate progression rate (2-45%) to MIBC, a rigid 5-year follow-up plan is required to manage patients with NMIBC. The follow-up strategy is to monitor the recurrence and grade/stage

progression in order to facilitate timely intervention and ablation. Currently, the combination of bladder cystoscopy, imaging and urine sedimentation examination is standard surveillance care [41]. Disease recurrence may occur even after several years, and thus the need for lifetime surveillance and repeated treatment of recurrent disease has an adverse impact on the quality of life. Because of the poor survival rate from high-grade tumours and the economic burden from the management of low-grade tumours, there is a greater demand for better alternative therapies, accompanied by biomarkers to predict treatment outcomes, and for improving the therapeutic management of bladder cancer.

| Bladder tumor | Non-muscle invasive | | Muscle invasive | | Metastatic | |
|---|---|---|---|---|---|---|
| Treatment | TURBT | Intravesical Chemo/BCG | Cystectomy | Neo-adjuvant Gem/Cis | Cystectomy | M-VAC |
| Benefit | ❖ Elimination of primary tumor<br>❖ Prevent/ delay recurrence<br>❖ Prevent/delay MIBC | | ❖ Elimination of tumor to prevent/ delay recurrence<br>❖ Prevent/delay metastasis | | ❖ Palliative treatment to slow decline of patients | |

**TABLE 1.1**: *Summary of the current treatment options and benefits for patients with bladder cancer.*

### 1.5 Molecular Scenery of Bladder Cancer

Mounting evidence from clinical and pre-clinical studies suggests that both genetic and epigenetic events are playing crucial roles in different stages of bladder cancer, from early neoplastic lesions to the progression to advanced disease.

A major difference between NMIBC and MIBC is the extent of genetic and chromosomal instability. Low-grade, NMIBCs are commonly near-diploid with limited genomic rearrangements or mutations, whilst the high-grade MIBCs evolve with progressive and extended genomic alterations and chromatin re-arrangements, resulting in the activation of

oncogenes together with the inactivation of tumour suppressor genes [42] [43]. Gain of function mutation of fibroblast growth factor receptor 3 (FGFR3) is associated with the majority of low-grade NMIBCs, while it is less (~12%) prevalent in MIBC [44]. Kinase signalling pathways, mainly receptor tyrosine kinase (RTK) and phosphoinositide-3 kinase (PI3K), have been found to be implicated in MIBCs. Approximately 44% of MIBCs have alterations in PI3K-mTOR or RAS-RTK-MAPK with oncogenic activation-associated genes such as PIK3Ca, AKT3, EGFR, ERBB2 (Her2) and FGFR3 [45]. A recent Cancer Genome Atlas study reveals that genes encoding for TP53 and RB1 are altered in the majority of high-grade cancers, with deletion and/or mutation of the TP53 gene in ~50% of MIBCs [20]. Other key players involved in genomic aberrations are hTERT (telomerase - promoter activation), CDKN2A (homozygous deletion and inactivation), and Cyclins D1and E1 (amplification mutation results in loss of cell cycle control) [46].

Chromosomal rearrangement and chromatin restructuring also have significant roles in pathogenic bladder cancer. A recurrent novel intra-chromosomal translocation has been identified on chromosome 4, involving FGFR3 and TACC3, resulting in a fusion protein that is implicated in MIBCs. Genes involved in epigenetic regulation have also been found to be significantly mutated, including MLL2 (encodes H3K4 methyl transferase) and KDM6A (encoding H3K27), suggesting that such genes may have a crucial role in carcinogenesis [20].

### 1.6 Epigenetic Changes in Bladder Cancer

In addition to genetic alterations, epigenetic changes are widely implicated in the development and progression of solid tumours, including bladder cancer [47] [46]. By definition, epigenetics is the establishment of heritable changes in DNA without alterations in the DNA sequences. Epigenetic changes are indispensable in normal developmental process, including embryonic development, cellular differentiation, genetic imprinting, adult cell

9

renewal and X-chromosome inactivation [48] [49]. The main processes responsible for epigenetic changes are DNA methylation, chromatin remodelling by core histone modifications and post-translational gene regulation by non-coding RNAs. It is evident from a large number of publications that disruption of these processes has a fundamental role in the development of various pathogeneses, including metabolic processes, immune system, neurological impairment and cancer. In cancer, aberrant epigenetic patterns cause alterations in gene expression and subsequently gene function, which play a critical role in the initiation and development of tumours, and subsequent malignant progression [50] [49] [51].

Methylation of DNA is a covalent modification of the cytosine ring at the 5' position of a CpG dinucleotide by addition of a methyl group to the $5^{th}$ carbon of the ring with the aid of S-adenosyl methionine as a methyl donor. These changes include hyper-methylation of gene-associated CpG islands and hypo-methylation of genomic DNA [52]. The majority of the studies in bladder cancer over the last 20 years were on hyper-methylation and CpG-island promoters as candidate genes, and their implications on urothelial carcinoma [53-55]. Genes involved in essential biological pathways such as cell cycle regulation (CDKN2A, P16-INK4A, P14, CyclinD2 and RB1), DNA repair enzymes and genes (MGMT, MLH1, GSTP1, TP53, BRAC1 and BRCA2), genes associated with apoptosis (DAPK) and candidates linked to the invasion process (TIMP3, LAM, ESR1 and RARB) were found to be hyper-methylated at a higher frequency in bladder cancer and have been shown to be correlated with poor prognosis and clinical outcomes. These hyper-methylated genes have also been shown to be of benefit for diagnosis and therapy outcome, as the methylation markers can be detected by urine-based assays [56].

Non-coding RNAs are categorized into small RNAs (<200 nucleotides) and large RNAs (>200 nucleotides), and have been found to be heavily involved in the regulation of

chromatin structure and gene function [57]. These non-coding RNAs are increasingly found to be associated with normal development and are altered in many cancers, including bladder cancer. The small non-coding RNAs, including microRNA (miRNA), small interfering RNA (siRNA) and small nuclear RNA (snoRNA), are involved in transcriptional and post-transcriptional gene silencing through specific base paring with their target genes [58]. Of the above non-coding RNAs, miRNAs are widely studied, as they are vital for normal physiological processes and their aberrant expression is linked to several diseases, including cancer [51].  For example, miR-127 was found to be epigenetically silenced in urothelial cancers and is induced upon treatment with 5-Aza-CdR (DNA de-methylating agent)/PBA (HDACi) with downregulation of proto-oncogene BCL6 [59]. Expression of miR-205 was epigenetically silenced by a long non-coding RNA (HOTAIR), by breaking the balance of histone modifications between H3K4me3 and H3K27me3 on miR-205 promoters [60]. miRs 370, 1180 and 1236 were shown to be downregulated in bladder cancer and positively correlated with the expression of p21 by directly targeting the promoter of p21 [61]. Conversely, the miR 183-96-182 cluster and miR-210 were shown to play an oncogenic role in bladder cancer [62]. Long non-coding RNA (lncRNA) AB074778 was found to be upregulated in urothelial cancer cells and in tumour tissue samples, compared to normal urothelial cells and non-cancerous tissue samples [63].

Histone modification is a covalent post-translational modification to histone proteins that includes methylation, acetylation, phosphorylation, ubiquitylation or sumoylation. In eukaryotes, chromatin is a highly ordered structure that packages DNA into highly coiled fibre-like structures wrapped around an octamer of histone protein. Histones are small basic proteins with molecular weights between 11 and 20 KDa, and contain a high percentage of positively charged amino acids, mainly lysine and arginine [64]. Eukaryotic cells contain four core histone proteins (H2A, H2B, H3 and H4) and a histone linker protein (H1). All four core

proteins share similar structures with a central 'fold' structure and terminal 'tail' structures (amino or carboxyl) [65]. These terminal 'tails' are the main target for post-translational modifications and are highly crucial in regulating normal cellular processes, including transcription and replication [66]. The enzymes involved in histone modifications are histone methyl transferases (HMTs) and histone demethylases (HDMs); there is also some evidence showing that kinases and phosphatases, ubiquitin ligases and deubiquitinases, and sumoligases and proteases are also involved in these modification processes [67].

Amongst the various post-translational modifications associated with epigenetic changes, acetylation and deacetylation are well characterized in pathogenesis, as this process is vital to regulation of chromatin remodelling and thus gene expression (Figure 1.2).
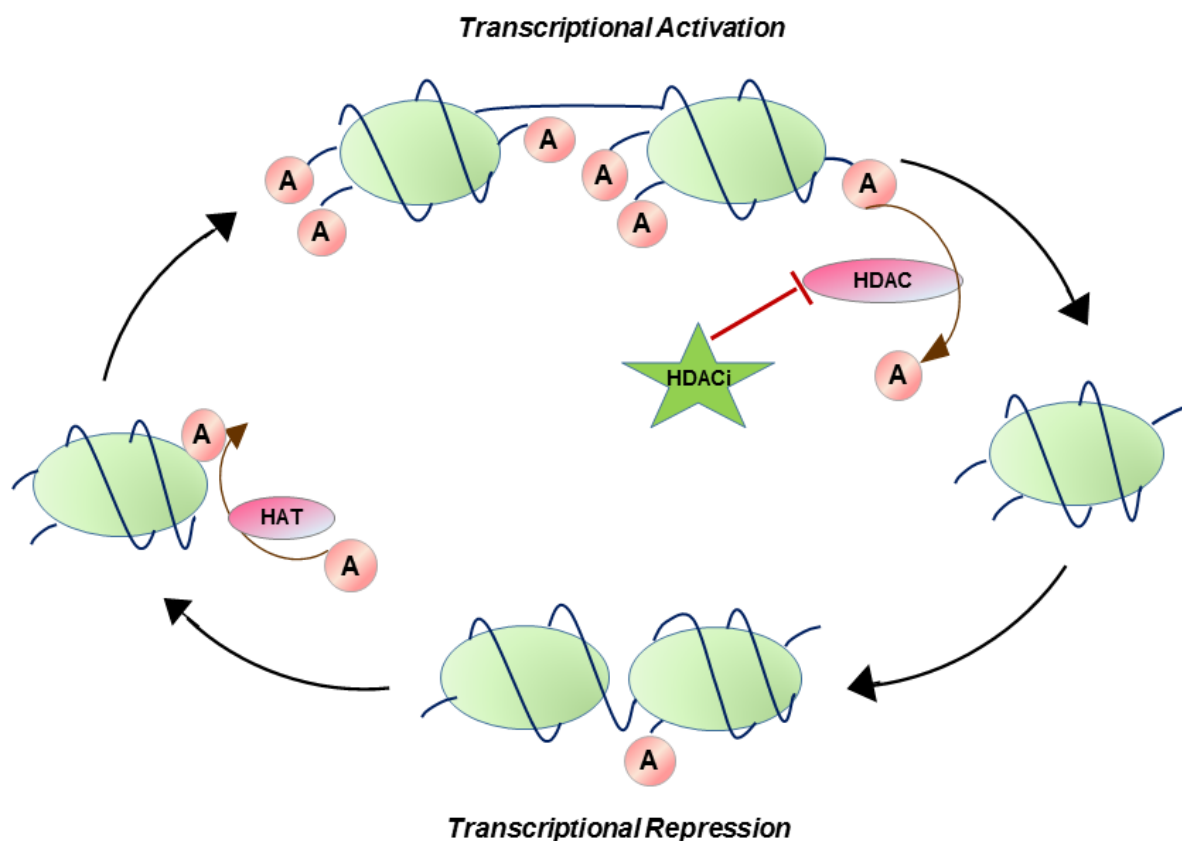


**FIGURE 1.2**: *The schematic representation of histone acetylation and deacetylation effects in transcriptional activation and repression in eukaryotes.*

12

Acetylation - deacetylation is a dynamic reversible process regulated by two crucial enzymes: histone acetyl transferases (HATs) and histone deacetylases (HDACs), respectively. The transfer of acetyl groups by HATs follows acetylation of the amino tails of lysine residues in histones, with a subsequent reduction in affinity to the negatively charged DNA, thus resulting in enhanced transcriptional activity [68].

HATs are broadly divided into two subgroups: type A and type B. Type A HATs are located in the nucleus, where they acetylate nucleosomal histone and non-histone proteins. There are five sub-groups of type A HATs, namely: (a) cyclic-AMP response element binding protein (p300/CBP); (b) GCN-related N-acetyl transferase (GCNT); (c) monocytic leukaemia zinc finger protein (MYST)/Tat interactive protein (TIP60); (d) nuclear receptor co-activators; and (e) general transcription factors. Type B HATs are located in the cytoplasm and acetylate newly synthesized histones [69], [70],[71].

Aberrant acetylation of histones and non-histone proteins (transcription factors, chaperone proteins and nuclear receptors) plays a key role in regulating malignant traits such as proliferation, growth arrest, angiogenesis and apoptosis [72].

In contrast to HATs, HDACs remove the acetyl group from lysine tails, resulting in a highly condensed chromatin and thus altered gene transcription. Eighteen HDAC isoforms are found in humans and are categorized into four classes based on their activity, homology to yeast proteins and cellular localisation [73]. Class 1, 2 and 4 are classical, zinc-dependent enzymes, whereas class 3 enzymes require NAD+ as cofactor [47]. The four classes of HDAC enzymes are summarised in **Table 1.2** [74],[75], [76].

Somatically acquired epigenetic changes in chromatin remodelling events are also identified in many cancers including bladder cancers [77] [78] [20]. Mutations in genes involved in chromatin remodelling process such as UTX (HDMT gene - mutated in 27% of TCC),

CREBBP and EP300 (HAT genes - detected in 20-25% UCC), ARIDIA (SWI/SNF related gene - mutated in 13% of TCC) and aberrant expression of MLL and MLL3 (HMT genes), NCOR1 (HDAT activity), and CHD6 (SNF2/RAD54 complex) were identified from previous studies [79].

| Class | HDACs | Location | Expression |
|---|---|---|---|
| Class 1 | HDAC1, HDAC2, HDAC3, HDAC8 | Nucleus | All tissues (ubiquitous) |
| Class 2a | HDAC4, HDAC5, HDAC7, HDAC9 | Nucleus / Cytoplasm | Skeletal, Cardiac, Bone, Smooth muscles |
| Class 2b | HDAC6, HDAC10 | Cytoplasm | Heart, Liver, Kidney, Placenta, Spleen |
| Class 3 | SIRT1, SIRT2, SIRT3, SIRT4, SIRT5, SIRT6, SIRT7 | Nucleus / Cytosol / Mitochondria | Liver, Pancreas, Fat cells |
| Class 4 | HDAC11 | Cytoplasm | Brain, Testis, Heart, Skeletal muscle |

**TABLE 1.2**: *Summary of the location and expression of 4 classes HDAC enzymes.*

Aberrant acetylation of histones and non-histone proteins (transcription factors, chaperone proteins and nuclear receptors) plays a key role in regulating malignant traits such as proliferation, growth arrest, angiogenesis and apoptosis [72]. Altered expression of different HDACs has been reported in various human diseases, including cancer. Hypoacetylation of histone H4 is a dominant hallmark of human cancer. Hypoacetylation is thought to occur at the early stages of tumour initiation and is thus believed to be critical in

cancer development [80]. Upregulation of HDACs, especially class 1 HDACs, is correlated with poor prognosis in many solid tumours in the advanced stages, including colorectal cancer [81], prostate cancer [82], gastric cancer [83], neuroblastoma [84] and endometrial cancer [85]. HDACs can be aberrantly recruited to target genes through their interaction via fusion proteins. Class 1 HDACs HDAC1 and 2 are found as multi-protein complexes with Sin3, Mi-2/Nur D/CoREST, and HDAC3 is recruited by N-CoR/SMRT complex [86].

In bladder cancer, an overwhelming number of studies have shown that histone modifications and/or aberrant expression of HDACs are associated with urothelial cancer progression. It is evident that trimethylation of lysine 4 on histone 3 (H3K4me3) enrichment and H3K9 acetylation at the promoters are features of transcriptionally active genes, whilst tri-methylation of H3K9 and H3K27 is associated with transcriptionally inactive promoters [87] [88] [89]. Additionally, the expression levels of HDAC1 (both protein and mRNA) were found to be elevated in tumour samples from patients compared to normal samples. Furthermore, treatment with BBN, a chemical known to induce pre-neoplastic lesions in the bladder, has been shown to induce the expression of HDAC1 in mouse models [90]. Previous studies in urothelial carcinoma cells have shown that treatment with different HDAC inhibitors (HDACi) in bladder cancer cells alters the malignant traits of these cells [91] [92] [93] [94]. In bladder cancer, there are reduced levels of global histone modifications compared to normal urothelium. Histone methylation levels decrease with disease severity and are correlated with advanced pathological stages, both in NMIBC and MIBC in a large cohort of clinical samples [95] [96]. Altered histone modifications are also evident in bladder cancer cell lines, and EZH2, a histone methyl transferase, is found to be frequently overexpressed in high-grade aggressive tumours and is associated with transcriptional silencing of tumour suppressor gene E – cadherin [97, 98]. The overwhelming evidence suggesting that altered expression of HDACs and histone modifications are associated with

bladder cancer progression provides the rationale to target HDACs using HDACi in bladder cancer.

## 1.7 HDACi in cancers

At least 15 different HDACi are currently in clinical trials, including representatives from four major classes depending on their chemical structures: hydroxamic acids, cyclic peptides, benzamides and aliphatic acids [99]. In addition to their structures, HDACi also differ in their potency, specificity to inhibit the different classes of HDACs, pharmacokinetic properties and toxicity profile [47]. HDACis from all four classes have been shown to be effective in inhibiting the growth of various cancer cell lines and reducing malignancy in xenograft models [100].

Hydroxamic acids include the majority of the HDACi currently in clinical trials for different types of human malignancies [101]. The HDACi Vorinostat (SAHA) is at the most advanced stage in the clinical trials as a single agent or in combinations; currently completed phase III clinical studies for lung cancer and mesothelioma. Panobinostat (LBH589) is currently in phase III clinical trials for cutaneous T-cell lymphoma (CTCL) after completing phase II trials with promising results (74% tumor reduction)[99]. Givinostat (ITF2357) and Belinostat (PDX101) are in phase II clinical studies for JAK2$^{v617F}$ -expressing myeloproliferative neoplasms and thymoma respectively [99] [47]. Romidepsin (Depsipeptide) is a cyclic peptide completed phase II clinical trials for several solid tumors including ovarian, colorectal, breast, pancreatic cancers. At least two benzamides Entinostat (MS-275) and Mocetinostat (MGCD0103) are also in phase II clinical trials for melanoma and B-cell malignancies [99, 102, 103].

However, many of these agents entered clinical trials with limitations, including low bioavailability, low potency, cardiovascular safety issues and potential drug-drug interactions

through cytochrome P450 isoenzyme [104]. So far, only two of these agents are approved by the FDA: Vorinostat (SAHA – pan HDACi) and Romidepsin (targets class 1 HDACs) were only successful in the clinic for the treatment for refractory, cutaneous and peripheral T-cell lymphoma [105] [106].

### 1.8 Pracinostat (SB939)

Pracinostat (SB939 – *[(2E)-3-[2-butyl-1-[2-(diethylamino) ethyl] H-benzimidazol-5-yl] N-hydroxyarylamide hydrochloride*), the HDACi used for this study is an orally available HDACi. Pracinostat was identified as a potent hydroxamate-based inhibitor of class 1, 2 and 4. In *in vitro* enzyme assays, Pracinostat treatment showed Ki (enzyme inhibitory constant) values 19 - 48 nmol/L for class 1 enzymes, 16 - 247nmol/L for class 2 enzymes and 43nmol/L for class 4 enzyme with no activity against class 3(Sirtuins 1-7) [107, 108]. Pharmacokinetics studies in the mammalian system using Pracinostat indicate that it is highly soluble in aqueous media, with high Caco-2 permeability, and it is metabolized by cytochrome CYP3A4 and CYPIA2 enzymes without producing a metabolite that inhibits the activity of these enzymes, and this leads to high systemic clearance from the liver [109]. The anti- proliferative effect of Pracinostat as measurement of potency was tested *in vitro* using 29 human cancer cell-lines and $IC_{50}$ values were measured. Colon cancer cells ($IC_{50}$ - 0.48µmol/L) and prostate cancer cells ($IC_{50}$ - 0.34µmol/L) were the most sensitive cell lines among all the solid cancer cells. Treatment with Pracinostat did not show anti-proliferative effect on human normal dermal fibroblast.

Pracinostat has been shown to be superior to SAHA (a US FDA-approved HDACi for cancer therapy), with double the potency against HDAC enzymes, without affecting the activity of other zinc-binding enzymes *in vitro*. In *in vivo* studies using colon cancer tumor models, Pracinostat has been shown to accumulate in the tumour bed and provide a sustained

inhibition of colon tumour growth (94%, versus 48% for SAHA). The pharmacological and tumor inhibitory properties of Pracinostat and Vorinostat are summarised in **Table 1.3** [108] [110].

| | Pracinostat (SB939) | Vorinostat (SAHA) |
|---|---|---|
| *in vitro* | Enzyme inhibitory concentration (nmol/L) | |
| | Class 1 19 - 48 | Class 1 33 - 112 |
| | Class 2 16 - 247 | Class 2 30 - 116 |
| | Class 3 43 | Class 3 59 |
| | Anti-proliferative effect- $IC_{50}$ value for the most and less sensitive solid tumor cell-line (nmol/L) | |
| | PC3 (Prostate) - 0.34 | DU145 (Prostate) - 0.96 |
| | BT549 (Breast) - 1.87 | BT549 (Breast) - 4.45 |
| *in vivo* | Plasma concentration after post-dosage | |
| | 2.632ng/ml - 4hrs | 501ng/ml - 4hrs |
| | 2.632ng/ml - 24hrs | Undetectable- 24hrs |
| | Oral bioavailability | |
| | 34% | 8.3% |
| | Tumor growth inhibition | |
| | 94% | 48% |

**TABLE 1.3:** *Effects of Pracinostat and Vorinostat on pharmacological and tumor inhibitory properties.*

Phase 1 studies of dose tolerance of Pracinostat in patients with refractory solid malignancy suggest that the MTD is 80 mg/day with a half-life of $7.2 \pm 6$ h and oral clearance $53.0 \pm 8.8$ l/h, with no significant accumulation in PBMCs on day 15. Pracinostat is well tolerated in these patients, with fewer side effects [111] [112]. A later Phase 2 study in patients with CRPC using Pracinostat as a single agent in chemotherapy-naive patients has shown promising results, with significant reduction in the CTC (64%) with less efficient (6%)

reduction in the PSA response rate [113]. Because of its excellent pharmacological properties, bioavailability, systemic clearance and greater tolerability in humans as shown in Phase 1 clinical trials, Pracinostat is an ideal candidate for HDACi-mediated cancer therapy.

## 1.9 Activating Transcription Factor 3

Activating transcription factor 3 (ATF3) plays an indispensable role in different biological processes, ranging from regulating the immune response and coordinating gene expression responses, to stress signals affecting metabolism and homeostasis. ATF3 has a crucial role in diseases resulting in nerve injury and in cancer [114]. ATF3 has been described as a 'molecular hub' of the adaptive cellular network, because of its context-dependent interaction with numerous signalling pathways and regulators that impact on normal physiological and metabolic processes, inflammatory processes and disease models. ATF3 is an immediate early stress response gene, and in the context of cellular stress, ATF3 has been shown to be induced by TGF-β signalling, specifically interacting via Smad3 signalling in epithelial cells. TGB-β gene expression is upregulated by ATF3 via a positive feedback loop [115] [116]. ATF3 is induced by various ER stress signals, and its functional role is mainly to co-ordinate the transcriptional response induced by eIF2α [117]. ATF3 interacts with various inflammatory regulators, including IL1β, IL6, IL12, TNFα and CCL4, both in immune and non-immune cells [118-120]. In metabolic pathways, ATF3 has been shown to interplay with insulin, glucagon, asparagine synthetase, glucose transferase (Glut4) adiponectin and adiponectin receptor [121] [122] [123] [124] [125].

In the tumour context, ATF3 has been found to be a key determinant in various stages of tumour development to progression. ATF3 has been shown to have an anti- and pro-apoptotic effect in a context-dependent manner in cancers, and similarly it increases the invasive potential of some cells, whilst expression of ATF3 decreases cell motility in other cells [126]

[127] [128]. ATF3 plays a critical role in DNA damage repair and knockdown of ATF3 attenuates this effect, in both a p53-dependent and -independent manner [129]. Previous studies have also found ATF3 to have roles in cell cycle regulation, epithelial-mesenchymal transition, angiogenesis and metastasis [130] [116] [131]. Moreover, there is overwhelming evidence to suggest that ATF3 plays a dichotomous role in various stages of cancer progression. ATF3 has been shown to function as either an oncogenic suppressor or activator, depending on the degree of malignancy, context and cell type [132] [131]. ATF3 has a basic region leucine zipper (bZIP) DNA-binding domain, and by forming homodimers and heterodimers with other bZIP proteins such as c-JUN and Jun B/D, ATF3 can function as either a transcriptional activator or repressor. ATF3 is composed of 181 amino acids, of which 21 serine or threonine, 1 tyrosine and 17 lysine residues are potential sites for post-translational modification, namely phosphorylation, acetylation, methylation or ubiquitination [133, 134]. Studies in breast, squamous skin carcinomas and Hodgkin's lymphoma suggest that ATF3 has an oncogenic role, both in tumour initiation and progression, whilst evidence from colorectal and oesophageal cancers indicates that ATF3 suppresses colon and oesophageal squamous cell tumourigenesis [128, 135-138]. In bladder cancer, we have shown that decreased ATF3 expression in bladder cancer is associated with cancer progression and is correlated with a reduced survival rate of patients with high-grade and metastatic tumours [139]. This study also identified that ATF3 suppresses metastasis in bladder cancer through remodelling of actin filaments and suggested that ATF3 could be utilised as a prognostic marker.

## 1.10    Rationale for this Project

Despite the efforts made to improve the outcome for bladder cancer patients, the recurrence rate of NMIBCs is >70%, for which patients have to undergo regular surgical resections over

the years and need to have lifetime surveillance to monitor recurrence, posing a great economic burden on our healthcare system [9]. The five-year survival rate for high-grade advanced tumours remains <50%, in which case the treatment has not advanced for several decades. Therefore, there is a greater demand for better alternative therapies, accompanied by biomarkers to predict treatment outcomes and improve the therapeutic management of bladder cancer. Many studies in bladder cancer over the past 10 years have suggested that epigenetic changes, mainly histone modifications (acetylation/deacetylation) along with aberrant expression of HDACs, are commonly associated with bladder cancer progression. The evidence strongly indicates that exploration of the epigenetic changes associated with disease progression and targeting HDACs using HDACi would provide better outcomes for patients by delaying or preventing disease recurrence in the early stages (disease-free survival) and may increase survival time in patients with high-grade tumours.

## 1.11    Project Hypothesis and Aims

Previous studies from our laboratory utilising clinical samples and cell lines clearly demonstrated that transcription factor ATF3 expression is gradually decreased or lost as the cancer progresses from low to high grade. The reduced expression of ATF3 may be indicative of possible chromatin remodelling and epigenetic silencing associated with disease progression.

I hypothesise that regulation of ATF3 expression by HDACi Pracinostat in bladder cancer may have potential therapeutic or biomarker utility.

To investigate this alternative therapeutic approach in bladder cancer, I have four specific aims for this study. These aims are:

I) Determine whether treatment with HDACi Pracinostat reactivates the expression of ATF3 *in vitro* and *in vivo* in bladder tumour models.

II) Determine whether reactivation of ATF3 by Pracinostat impairs malignant traits in *in vivo* and *in vitro* bladder cancer models.

III) Define whether ATF3 is integral to determining the treatment response and could serve as a biomarker of response.

IV) Discover other candidate proteins that drive ATF3-dependent non-malignant phenotypes in bladder cancer by polysome-associated RNA sequencing.

### 1.12    Concluding Remarks

Numerous studies have identified epigenetic changes associated with bladder cancer progression, mainly histone acetylation and altered expression of HDACs, as detailed in this chapter. This introduction also summarizes the current treatments available for bladder cancer and the challenges in the field. This thesis will provide an insight into alternative therapeutic approaches for advanced bladder, accompanied by identification of biomarkers to predict treatment outcomes and improve the therapeutic management of bladder cancer.

# CHAPTER -2

*General methods*

## 2.1.    Compound: HDAC inhibitor

Pracinostat (SB939) was synthesised at MEI Pharma (San Diego, - CA, USA) as hydrochloride salt. For *in vitro* studies stock solutions were made by dissolving Pracinostat at a concentration of 10mM in dimethyl sulfoxide and stored in small aliquots at $-20^0$C. For *in vivo* studies Pracinostat was dissolved in 0.5% methylcellulose (w/v) and 0.1% Tween 80 in water for oral dosing.

## 2.2.    Cell Culture

All human cell lines except TSU-Pr1 cells used in this study were obtainable commercially, purchased from ATCC by our institute, The Hudson Institute of Medical Research. The TSU-Pr1 cells were originally obtained from Dr Dan Djakiew (Georgetown University, Washington DC) as previously described [140]. Cell lines used, their origin, description and culture medium is listed in **TABLE 2.1**.

| Cell line | Source | Description | Medium |
|-----------|--------|-------------|--------|
| **SV-HUC1** | ATCC | Immortalized uro-epithelium | F-12K medium |
| **5637** | ATCC | UCC, Grade II | RPMI medium |
| **T24** | ATCC | TCC, Grade III | DMEM medium |
| **TSU-Pr1** | Georgetown University | TCC, Grade III | DMEM medium |
| **J82** | ATCC | TCC, Invasive, Grade III | DMEM medium |
| **TCCSUP** | ATCC | TCC, Grade IV | Earle's BSS with non-essential amino acid |

**TABLE 2.1:** Table summarising the source, grade and culture medium used for the cells

All cell lines were obtained from ATCC (Manassas, VA, USA) and were cultured in the recommended media following ATCC instructions. TSU-Pr1 and HEK293T cell lines were cultured in DMEM (Dulbecco's modified Eagle medium) (Gibco, Life Technologies Cat no.11965-092) supplemented with 10% Foetal Bovine Serum (Gibco, Life Technologies, Cat no.10099-141).

Cancer cell lines used in this study with their status of the commonly found mutations in bladder cancer and origin is listed in the **TABLE 2.2**

| Homozygous | | | | Heterozygous | | Origin |
|---|---|---|---|---|---|---|
| **Cell line** | **FGFR3** | **RB** | **RAS** | **TP53** | **PTEN** | |
| **5637** | WT | WT | WT | R280T | WT | Primary tumor |
| **T24** | WT | WT | G12V | Y126 | R55W | Primary tumour, Untreated |
| **TSU-Pr1** | WT | WT | G12V | Y126 | WT | T24 derived |
| **J82** | K652E | Deleted | WT | E271K | N212fs*1 | Primary tumour, Treated |
| **TCCSUP** | WT | Deleted | WT | E349 | WT | Primary tumour, Untreated |

**TABLE 2.2:** Table summarising the common mutations identified in the cells used.

## 2.3.    Cell Maintenance

All bladder cancer cell lines, normal urothelial cells and HEK293T cells grow as adherent cells in either a T75 or T175 (BD, Cat no. 353112) flasks. When cells reached confluence,

every 3-4 days, media was removed and flasks were washed with 1x PBS (Gibco, Life Technologies, Cat no. 14190 -144). PBS was removed and replaced with 1mL of TrypLE Express (Gibco, Life Technologies, Cat no. 12604-021), cells were left to incubate at 37°C for 5 minutes. Fresh media was added to the plate and cells were seeded into a new flask at 1/6 -1/10 dilution.

## 2.4. Cryopreservation

Cells in the log phase were harvested and resuspended in the appropriate medium with 10% DMSO (Sigma, Cat no. D2650). Cell suspension ~ 1ml was then transferred into NUNC cryotubes (Thermo-scientific, Cat no. 337267) and stored at $-80^0C$ for 24 hours. The next day cells were transferred to liquid nitrogen tank for long-term storage.

## 2.5. Thawing of cells

When media warmed approximately to room temperature, vials of cells were removed from liquid nitrogen and kept on dry ice. To minimize the exposure to DMSO, cells were thawed as quickly as possible at $37^0C$ water bath. To 9ml media at room temperature in a 15ml flacon tube (Corning, Cat no. 430791) the cells from cryotube were transferred and spun downs to remove the DMSO from the freezing medium. The pellets were then mixed with appropriate media and plated into the flask for experiments.

## 2.6. Cell Assays

### 2.6.1. Viability Assay

Cell viability was measured over a period of 6 days using Vialight Plus (Lonza, LT07- 221) high sensitivity cell proliferation kit. The principle of this assay is based on the bioluminescent measurement of ATP that is present in all metabolically active cells. Following the manufacturer's instructions, 1000 cells were seeded onto the 96 well plate in

triplicate in normal growth medium. The treatment with varying concentration of Pracinostat started after an overnight incubation of cells in their normal growth media. Cells were lysed using cell lysis buffer each day for 6 days and ATP monitoring reagent was added to the lysate and luminescence read on FLUOstar Optima (BMG LABTECH, Germany).

### 2.6.2.    Monolayer Wound Healing Assay

Cells were seeded at $1X10^5$ cells/ well in a 24 well plate. Cells were left to grow until a confluent monolayer was obtained. Cells were pre-treated for 24 hours before the scratch wounds were made with a sterile 200ul pipette tips. Photographs were taken immediately following scratching (0hrs) and in regular intervals for 24hours or till the closure of the wounds in the controls wells. The percentage of wound closure was calculated using the formula:

$$\underline{\text{Width at t}n \text{ - Width at t}24} \qquad \text{where 't' is time}$$
$$\text{Width at t}n \text{ - } 100$$

### 2.6.3.    Soft agar Colony Formation Assay

Stock solution of 3% noble agar (BD, Cat no 21220) was made. All colony formation experiments were carried out in 6well plates in triplicates with 0.6% bottom agar layered with 0.3% top agar. In order to make 20ml 0.6% bottom agar, 10ml 2XDMEM (Thermo Fisher scientific, Cat no. 12800-017), 2ml FBS, 4ml 3% agar and 4ml sterile $dH_2O$ were mixed in a 50ml falcon tube (BD, Cat no. 352070) 3ml of the above mixture was added to each 6 well plate and set aside to cool while preparing the cells. Control cells or cells treated with Pracinostat for 3 days were trypsinised and counted to get $3X10^3$ cells. Made 20ml top agar media mixture at 0.3% by mixing 10ml 2XDMEM, 2ml FBS, 2ml agar and 6ml $dH_2O$. 9ml of

top agar mixture was mixed with $3X10^3$ cells avoiding air bubbles and 3mls were plated accordingly. Set to cool for 10 -15 minutes and incubated for 3 weeks before analysing.

### 2.6.4.      Cell Cycle and Apoptosis Analysis

Following treatment with Pracinostat or in DMSO control for 24 hours, cells were harvested, washed twice in ice-cold PBS and fixed in 70% ethanol at -20$^o$C for > 2hours. Fixed cells were centrifuged, and washed with PBS to remove fixative. Cells were stained with 20µg/ml propidium iodide (Life technologies, Cat no. P1304MP) / 0.1% TritonX-100 (Sigma, Cat no X100- 500mL) staining solution with 2.5µg/ml RNase A (Sigma, Cat no. 10109169001) for 30 minutes in the dark at room temperature. Cell cycle distribution was determined using BD Biosciences FACS Canto II analyser (CA, USA) by collecting a minimum of 20,000 cells for each sample. The cell cycle profile was defined by using FlowJo software (version 7.6.3). For apoptosis analysis FITC Annexin V staining was performed according to manufacturer's instructions. Cells were washed twice in PBS and resuspended in 1X binding buffer (BD Pharmingen, Cat no. 556420) at a density of $1X10^6$ cells/ ml. To 100µl of the suspension, 5µl FITC Annexin V (BD Pharmingen, Cat no. 556420) and 10µl PI (50µg/ml) was added and incubated for 15 minutes in the dark. FITC Annexin V positive cells were analysed using the BD Biosciences FACS Canto II analyser within 1 hour.

### 2.6.5.      Transfections and Generation of Stable Cells.

Cells were plated at around 60 -70% confluency and left to attach overnight before doing the transfection. TSU-Pr1 cells were transfected with shRNA targeting human ATF3 to knock-down the expression of ATF3 or vector carrying non-targeting control sequence  to create control cells with Fugene HD (Promega, Cat. no. E2311) transfection reagent. Stable cells were obtained following selection with 2µg/ml puromycin (Invivogen, Cat. no. anti- pr-1) for 10-14 days.

The shRNA target sequences for ATF3 as follows:

ATF3, 5'-TGGAAAGTGTGAATGCTGA-3'

For transient transfections, cells were plated in 24 well plates or 6 well plates at ~60%-70% confluency and let them attached overnight. Transfection itself was carried out according to the manufacturer's instructions. Fugene / DNA ratio was optimized and for TSU-Pr1, J82, and HEK293T cells the ratio was 3:1 (3µl of Fugene: 1µg of DNA). Briefly, the transfection complex was made by mixing required amount of DMEM without serum, DNA and Fugene and this complex then incubated for 15minutes for room temperature. The media from the cells were replaced with fresh media before transfection and the complex is then added to the wells, swirled well and incubated 24-48hrs at $37^0$C and assays were performed.

Bladder cancer cells were plated in 96 well plates for overnight and treated with 4 different concentrations of Pracinostat (control, 50nM, 100nM and 500nM) for 2 days dedicating single concentration per plate. Following Pracinostat treatment, twenty-four concentrations of Carboplatin (Sigma, Cat no C2538) ranging from 0 -200 µg/ml were added to the cells and incubated for 2 days. On day 5, 10µl of Alamar Blue cell viability reagent (Thermo Fisher Scientific, Cat no DAL 1100) was added to each well and incubated for 6 hours measuring the fluorescent intensity using FLUOstar OPTIMA every hour after adding the reagent.

## 2.7.    Molecular Assays

### 2.7.1    Total RNA Extraction and Quantification

Total RNA was extracted from cell lines using Trizol - LS (Invitrogen, Cat. no 10296-028) according to the manufacturer's instructions. Cells at 70% -80% confluency were washed twice with cold PBS. Trizol 1ml / $10cm^2$ flask was added to the cells and mixed gently by pipetting up and down. Cells were centrifuged 12,000g for 10 minutes at $4^0$C. The samples

were incubated for 5minutes at room temperature (RT). Chloroform (Sigma Cat. no 288306 - 1L) 0.2ml/ 1ml of trizol was added to the samples which was shaken for 15seconds by hands. The samples were incubated for 5minutes at RT and centrifuged at 12,000g for 15minutes at $4^0$C. The upper aqueous phase was transferred to fresh 1.5ml eppendorf tubes (Corning, Cat. no MCT-175-C) to which 0.5ml isopropyl alcohol (Sigma Cat. no W292907-1KG-K) was added. The tubes were incubated for 10mins at RT and then centrifuged at 12,000g for 10 minutes at $4^0$C. The supernatant was discarded and the pellet was washed twice in 1ml 75% cold ethanol. The supernatant was discarded and the pellet was air dried for 8-10 mins and then resuspended in sterile RNase free water (Life technologies Cat. no 10977015) and stored at -$80^0$C for longer term.

Quantification of RNA was performed using the Nanodrop spectrophotometer- Nucleic Acids Version 3.7. The quantity was expressed in ng/µl and ratio 260/280 was used as a measure of RNA quality. RNA samples with values only between 1.8 -2.00 were taken for further experiments.

### 2.7.2 Reverse Transcription

RNA was reverse transcribed into cDNA using random primers (Promega, Cat.no C118A) and Superscript III (Thermo Fisher scientific, Cat.no 18080044). Each cDNA reaction contained following; total RNA (1µg) random primers (0.5µl; 250ng) and dNTPs (1µl, 0.3mM). The reaction was initiated when components were mixed and heated on a dry block heater (Ratek instruments, Australia). Samples were then cooled to a $4^0$C for 1minute on ice. 7µl of the following reagents were added to each reactions; 5x first strand buffer (4µl), DTT (1µl), RNase inhibitor (1µl), Superscript III (1µl). Each reaction was incubated at RT for 5mins. on a dry block heater before cooling to $4^0$C on ice, and stored at -$20^0$C.

### 2.7.3      Quantitative Polymerase Chain Reaction (qPCR)

qPCR was performed on an ABI PRISM 700 (Applied Biosystems) using 384 well plate and 10µl reaction. cDNA was diluted to 1/5 and mixed with 3µl sterile water, 1µl (10µM) reverse primer, 1µl (10µM) forward primer and 4µl SYBR green mix. PCR conditions were $95^{0}$C for 10 minutes followed by 40 cycles of reactions at $95^{0}$C for 15 sec and $60^{0}$C for 1min. Relative changes in the level of target genes across cell lines were normalised to housekeeping gene human b-actin, using the delta cycle threshold method as per the ABI PRISM 7000 user manual. For each primer set, cDNA was amplified in triplicate for each sample, in two separate qPCR assays. All qPCR reactions were validated by examining the dissociation curve of the resultant PCR products as per the ABI PRISM 7000user manual. Data from each experiment were combined for statistical analysis. List of primers and their sequences used in qPCR is detailed in Appendix 1.

### 2.8.      Protein Analysis

### 2.8.1      Whole Cell Lysate Extraction

Cells were seeded at sub confluency in clustered tissue culture plates and treated with HDACi for required amount of time. On the day of extraction, media was removed and the cells were washed twice with ice cold PBS. Cells were then lysed in ice-cold RIPA lysis buffer and cells were harvested using a cell scraper (BD falcon, Cat, no 99002). The lysates were transferred to 1.5ml microcentrifuge tubes and was sonicated for 15minutes for complete lysis. The lysate then centrifuged for 20 mins at 13000g at $4^{0}$C. The supernatant which contain soluble proteins was collected and stored at $-80^{0}$C.

### 2.8.2      Protein Quantification

Protein concentrations were determined using Pierece BCA Protein Assay kit (Thermo scientific Cat no 23225) according to manufacturer's instructions. Protein samples were diluted to 1:5 in sterile water. A set of BSA protein standards were prepared concentrations ranging from 0mg/ml – 2mg/ml by serial dilution. Each standards were added to the microplate in duplicates and also the protein samples needed to be tested. The working reagent was prepared (50 parts Reagent A to 1 part Reagent B) and 200µl was added to the standards and test samples. The plate was incubated at $68^0$C for 15mins. Absorbance was measured at 526nm with the reference wave length of 620nm on a FULORO star Optima (BMG Labtech). Standard curve were generated using OPTIMA software (version 2.41) to determine the concentration of the test samples.

### 2.8.3      Western blot

Protein samples were mixed well with 4x samples buffer to get to 1:1 volume for final concentration and heated on a dry block heater for 5-7mins at $100^0$C. After denaturation, the samples are cooled on ice for 5mins, and centrifuged at 14,000g for 30sec. to collect the residual amount of lysate. Samples were then loaded on to precast Bis-Tris Sodium dodecyl sulphate-polyacrylamide gel electrophoresis (SDS-PAGE) gel (varies from 6 -15% depends on the molecular weight of the target protein) with SDS buffer. Separated proteins were then transferred to a PVDF membrane (40um Millipore, Cat.no IPFL00010) using a Sure Lock system (Thermo Fisher Scientific, Cat. no E2311). The membrane was blocked using Odyssey blocking buffer (Millennium science, Cat.no 927-40000) for 1hour at room temperature and incubated overnight with primary antibody at appropriate concentration at $4^0$C. Bots were then washed with 0.1% TBST (3times) and incubated with secondary antibody at room temperature for 1hrs. The targets were detected by scanning the membrane

on the Odyssey Infrared Imaging System (LI-COR Biosciences, USA) and images were analysed with Odyssey Infrared Imaging System version 3.0 software. Loading control was also performed using anti pan-Actin or anti beta-Tubulin antibodies. List of antibodies used in this study is summarised in **TABLE 2.3**

| Protein | Description- catalogue number | MW (KDa) | Working conc. | Source |
|---|---|---|---|---|
| **ATF3 (c-19)** | Rabbit polyclonal # sc188 | 22 | 1:1000 | Santa Cruz Biotechnology |
| **Acetyl Histone-3** | Rabbit polyclonal # 96755 | 14 | 1:2000 | Cell Signalling Technology |
| **Acetyl Histone-4** | Rabbit polyclonal # 2591 | 16 | 1:2000 | Cell Signalling Technology |
| **Acetyl α -tubulin** | Rabbit monoclonal # 5335 | 52 | 1:1000 | Cell Signalling Technology |
| **Actin** | Mouse monoclonal # ab8226 | 42 | 1:10000 | Abcam |
| **α- Tubulin** | Mouse monoclonal # | 50 | 1:5000 | Abcam |
| **VEGF  A (20)** | Rabbit polyclonal # sc152 | 21 | 1:1800 | Santa Cruz Biotechnology |
| **pRB1** | Rabbit polyclonal # 9307 | 106, 110 | 1:1000 | Cell Signalling Technology |
| **PARP** | Rabbit polyclonal # 9542 | 89, 116 | 1:1000 | Cell Signalling Technology |
| **HDAC1** | Rabbit polyclonal # 17-10199 | 65 | 1:1000 | Millipore |
| **HDAC3** | Rabbit polyclonal # 06-890 | 49 | 1:1000 | Millipore |

**TABLE 2.3** List of antibodies used in western blot for this study

### 2.9. Xenotransplantation Assays

#### 2.9.1 Injection of Cancer Cells

Cell lines were passaged according to the methods described above. Aliquots of one million cells were centrifuged, washed and re-suspended in 50µl of DMEM complete media. The cell suspensions were mixed with 50µl Matrigel (Corning, Cat. no. 354234) to make 1:1 suspension and tubes were gently mixed and kept on ice. This suspension was then injected subcutaneously into the right flank of Balb/C nude mice.

#### 2.9.2 Tumor Measurements

Measurements of weight of mice and tumor sizes were taken daily. Tumors were measured along the longest axis (length - *l*) first and the second measurement was perpendicular (width -*w*) to initial measurement. Tumor volumes ($mm^3$) were then calculated using the following formula:

Tumor volume ($mm^3$) = ($width^2$ x length)/2

The percent tumor growth inhibition (%TGI) was calculated according to the following formula: $\%TGI = (C_{day\ a} - T_{day\ a}) / (C_{day\ a} - C_{day\ 1}) \times 100$ in which $C_{day\ a}$ is the median tumor volume for vehicle control group on day a, $T_{day\ a}$ is the median tumor volume for treatment group on day a, and $C_{day\ 1}$ is the median tumor volume for the vehicle control group for on day 1.

#### 2.9.3 Dosing Drug

Once tumor volume reached ~200$mm^3$, the mice were randomized to receive Pracinostat (100mg/ kg, 50mg/ kg) as a single agent or vehicle (0.5% methyl cellulose and 1% Tween ) as oral suspension. The dosing was scheduled in such a way that the maximum tolerated

dosage (MTD) of 100mg/Kg was orally given in 5 days on and 2 days off schedule [108], whereas lower dosages were given daily.

### 2.9.4    Collection and Preservation of Xenograft Tumors for Analysis

When tumor volume reached 800mm$^3$, mice were culled and the tumors dissected from the skin and underlying tissue and were then cut into two pieces. First piece was kept in a cassette and placed into buffered formalin (Orion Laboratories, Cat. no. BUFO1536F) for fixing 24 - 48hrs at room temperature on a rocker and processed further for staining. The second piece was snap frozen using liquid nitrogen in a 1.7ml Eppendorf tubes.

### 2.10.    Immunohistochemistry and immunofluorescence analysis

For Immunohistochemistry, sections of 4μm were made, from processed xenograft tumor samples. Representative sections from both Pracinostat treated mice xenografts and vehicle control mice xenografts were analyzed for each marker.

**De-parafinization and rehydration:** The slides were dewaxed in histosolve for 5 minutes twice and transferred into gradient concentrations of ethanol (100%, 75% and 50%) for 3 minutes each. The slides were washed under running tap water for 30 seconds, before incubation with 1x Citrate buffer (pH -7.8) for 5 minutes at room temperature.

**Antigen retrieval:** The slides were immersed in citrate buffer in a pressure cooker and epitope unmasking was performed boiling the slides using a microwave with high power (100$^0$C). When the slides were cooled they were placed in dH2O for 5 minutes and continued with the staining.

**Staining slides:** After washes in PBS-Tween (0.05%), excess liquid was removed and marked around the tissue using a wax pen (Thermo Fisher scientific, Cat .no 00-8877). Endo-peroxidase blocking (Dako, Cat. no. S2001-30) was added on the sections for 10minutes at

room temperature and followed protein serum block (Dako, Cat.no. X0909) for 15 minutes for blocking the non-specific tissue proteins. Primary antibodies or concentration-matched isotype controls were applied and incubated overnight at $4^0$C. The sections were washed with PBS or PBST (PBS with 0.5% TritonX-100) and incubated with universal biotinylated secondary antibody (LSAB+ Link, Dako, Cat.no. K0690-11) and streptavidin-peroxidase (LSAB+System-HRP, Dako, Cat. no. K0690-11) for 30 minutes at room temperature. Finally DAB - chromogen (Dako, Cat. no. K3468-11) was used to develop the signal from tissue sections.

**Counter staining slides:** The slides were placed in Mayer's haematoxylin for 5 minutes to counter stain the nucleus. After washes in dH2O the slides were dehydrated in 70% -100% ethanol and histosolve twice for 5 minutes. The slides were then mounted using DePex mounting medium (Merck, Cat. no. BDH361254D) and air-dried before analysis and images were taken for analysis using a Leica bright-field microscope for analysis.

For immune-fluorescence, the epitope unmasking and the primary antibody or its matched isotype controls were performed as described above. Followed by overnight incubation with the primary antibody, labelled secondary antibody was applied on the sections for 1hr. at room temperature in the dark. Mounting medium containing DAPI (Thermo Fisher scientific, Cat. no D1306) was applied for mounting and slides were dried in the dark for 24hrs. Images were captured using Nikon C1 confocal microscope (Nikon Eclipse Digital sigh 50i camera) for analysis.

## 2.11. Statistical analysis

Statistical analysis was performed using GraphPad Prism software version (version 6.0c) and displayed as the mean and SEM. Significant difference between two groups were analysed using unpaired Student's *t* test and one-way Anova with Turkey posttest was conducted for

multiple comparison and P< 0.05 was considered as statistically significant. Correlation between variables was evaluated by Pearson rank correlation coefficient. Survival analysis was performed using Kaplan-Meier method and log-rank test.

# CHAPTER -3

---

*HDAC inhibitor Pracinostat reactivates ATF3 expression in bladder cancer cells and alters malignant phenotypes in vitro*

---

## 3.1. Introduction

Activating Transcription Factor 3 (ATF3) has diverse roles in normal physiological and cellular process, including homeostasis, metabolism, and co-ordinating gene expression for cellular stress signalling. ATF3 is also been shown to play a crucial role in disease models such as inflammation, nerve injury and in cancer [114]. Evidence in tumor models suggesting that ATF3 can act as a tumor inducer and a suppressor, depends on cellular context, and degree of malignancy [133, 134, 141]. Evidence from breast, prostate, squamous skin and Hodgkin's lymphoma indicates that ATF3 is an oncogenic factor whilst in colon and esophageal cancers, ATF3 acts an oncogenic suppressor [135] [136] [137] [128, 138]. In bladder cancer, our previous study has shown that expression of ATF3 is inversely associated with cancer progression and loss of ATF3 expression is correlated with a reduced survival rate in patients with high-grade and metastatic tumors [139]. This study also confirmed that the loss of ATF3 expression is associated with an aggressive cancerous phenotype in bladder cancer cells.

ATF3 is a transcription factor with basic region leucine zipper (bZIP) DNA-binding domain and by forming homodimers and heterodimers with other bZIP proteins such as c-JUN and Jun B/D, ATF3 can function as either a transcriptional activator or repressor. ATF3 is composed of 181 amino acids, of which 21 serine or threonine, 1 tyrosine and 17 lysine residues are potential sites for post-translational modification, namely phosphorylation, acetylation, methylation or ubiquitination[142]. The activating or repressing activity is mostly to be determined by many factors such as post-translational modifications, chromatin structure, the identity of collaborating transcription factor, and other interacting proteins in the complex and the cellular context.

Acetylation and deacetylation of the lysine residue in the amino terminal of histones is a key post-translational modification and is controlled by enzymes HATs and HDACs in eukaryotes. Acetylation and deacetylation of histones play a crucial role in transcription regulation through alteration of chromatin structure which is critical in determining a particular gene is expressed. Hypo-acetylation of H4 which is thought to be an early crucial event in the cancer initiation.

Modulating acetylation pattern of histones has been investigated in different cancer models both by using compounds inhibiting activity of HATs and HDACs for the past 10 years. The first compound studied in the HDACi category was Trichostatin A, which was found to inhibit activity of HDACs cell proliferation [143]. Vorinostat (SAHA) was the first HDACi to get approval from the United States FDA for clinical application as a cancer therapeutic agent [144] [145]. Currently, there is a great demand for better HDACi, which can tolerated well by patients, with better pharmacokinetics properties and good bioavailability. In this study, I am using an orally available pan-HDAC inhibitor (class I, II and IV) Pracinostat to modulate the epigenome, which has demonstrated superior pharmacological properties than SAHA, accumulates in the tumor tissue and provides a sustained inhibition [108] [110] of colon tumors. Pracinostat is metabolized by cytochrome CYP3A4 and CYPIA2 enzymes without producing a metabolite that inhibits the activity of these enzymes, and this leads to high systemic clearance from the liver and it does not interact with any other zinc binding enzymes, such as matrix metalloproteinases and hence having a low potential for off-target side effects [109].

The cause of loss of expression of ATF3 in bladder cancer progression has not been explored, and our previous study indicating a possible chromatin remodelling and epigenetic silencing of this gene may be a major event as cancer progress. That reactivation of ATF3 by using an

epigenetic modulator such as an HDACi has any potential therapeutic benefit remains to be investigated to improve the clinical management of bladder cancer.

This chapter will demonstrate that the treatment with HDACi Pracinostat restores the expression of ATF3 in bladder cancer cells and the reactivation of ATF3 has functional significance in altering the malignant properties of these cells.

## 3.2. Results

### 3.2.1 HDACi Pracinostat reactivates the expression of ATF3 in bladder cancer cell lines

Decreased expression of ATF3 is associated with bladder cancer progression and reduced patient survival rates [139]. Loss of ATF3 expression as cancer progresses suggests that chromatin remodelling and the concomitant loss of histone acetylation may lead to epigenetic silencing of ATF3. To re-establish the normal acetylation pattern and thus to reactivate ATF3 expression, we treated a series of bladder cancer cell lines of different tumor grade with the HDACi Pracinostat. The results show that Pracinostat treatment reactivated ATF3 expression in a concentration- and time-dependent manner in bladder cell lines (Figures 3.1, 3.2 and Appendix 2). This was observed in all five cell lines tested (5637 - (grade II), T24 (grade III), TSU-Pr1 (grade III), J82 (grade III), TCC-SUP (grade IV). As shown in Figure 3.1, cell lines (5637, TSU-P1, and J82) tested for changes in ATF3 mRNA expression associated with Pracinostat, there observed significant fold increases in ATF3 expression in 5637 (P<0.001) and TSU-Pr1 cells (P<0.01), as early as 6 hours after Pracinostat treatment, whilst significant changes were observed in J82 after 12 hours. In parallel, re-expression of ATF3 protein was also observed in the above five cell lines (Figure 3.2 and Appendix 2). This coincided with progressive increases in the acetylation of the histone proteins H3 and H4. Densitometric analysis (Figure 3.2 (ii)) confirmed the effect of concentration- and time-dependent activation

of ATF3 in bladder cancer cell lines tested. As this trend was observed in all five lines tested, it appears that tumor grade is not associated with the changes in reactivation. Additionally, although we observed an increase in the acetylation of the non-histone protein α-Tubulin at 500 nM Pracinostat (Figure 3.3), no cell death was observed at this concentration of Pracinostat treatment that restored ATF3 expression (as shown by absence of cleaved PARP in all three cell lines tested, Appendix 3). Analysis of apoptosis in TSU-Pr1 cells by Annexin V staining supported this finding, revealing that a similar proportion of cells (7-9%) stained for early and late apoptosis, both in the control cells and in cells treated with 500 nM Pracinostat for 24 hours (Figure 3.4). Together, these results demonstrate that Pracinostat treatment re-establishes the acetylation pattern of histone proteins and restores the expression of ATF3, without inducing cellular death in these bladder cancer cells.
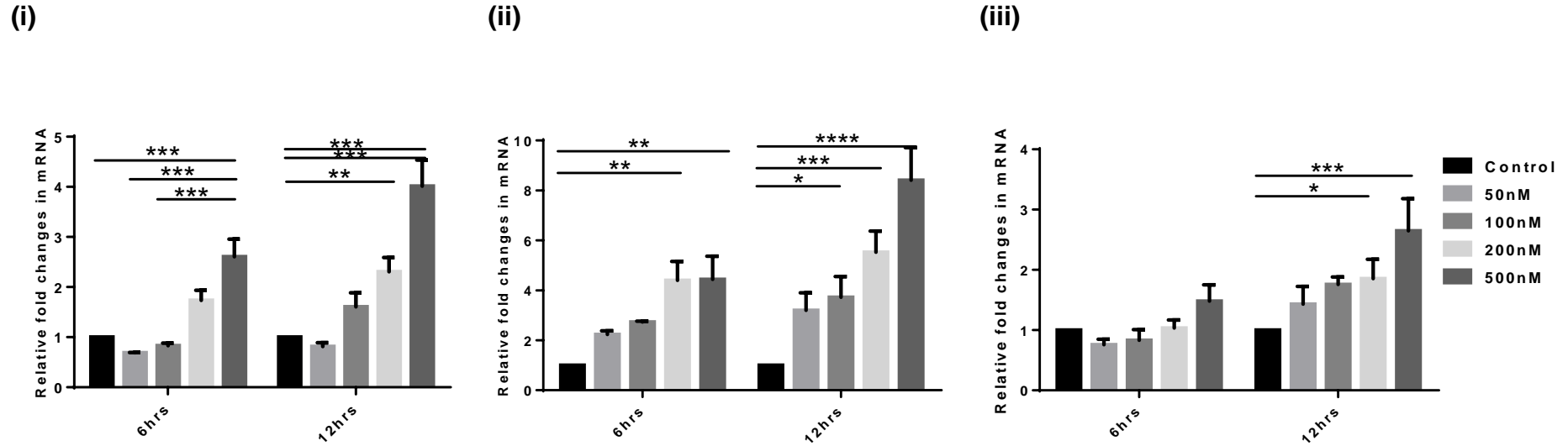
**Figure 3.1:** *Pracinostat reactivates ATF3 mRNA expression in vitro in a dose- and time-dependent manner.* Quantitative real-time PCR for detecting ATF3 reactivation in bladder cancer cell lines of different tumor grades: (i) 5637, (ii) TSU-Pr1, (iii) J82 at 6 hours and 12 hours of treatment with Pracinostat. Pracinostat treatment significantly increased the relative expression of ATF3 in 5637 (***P≤0.001) for ≥100 nM and in TSU-Pr1 (**P≤0.01) for ≥200 nM Pracinostat cells by 6 hours of treatment and by 12 hours in J82 cells (*P≤0.05). Data shown is the mean ± SEM. n = 3 replicate per cell lines.

**(i)**

Pracinostat (nM)

Tumor Grade

5637
ATF3
Acetyl -H3
Acetyl -H4
Actin

TSU-Pr1
ATF3
Acetyl -H3
Acetyl -H4
Actin

J82
ATF3
Acetyl -H3
Acetyl -H4
Actin

0  20  50  100  200  500  20  50  100  200  500

12Hrs        24Hrs

**(ii)**

ATF3 protein relative expression

Control
20nM
50nM
100nM
200nM
500nM

12hrs    24hrs

44
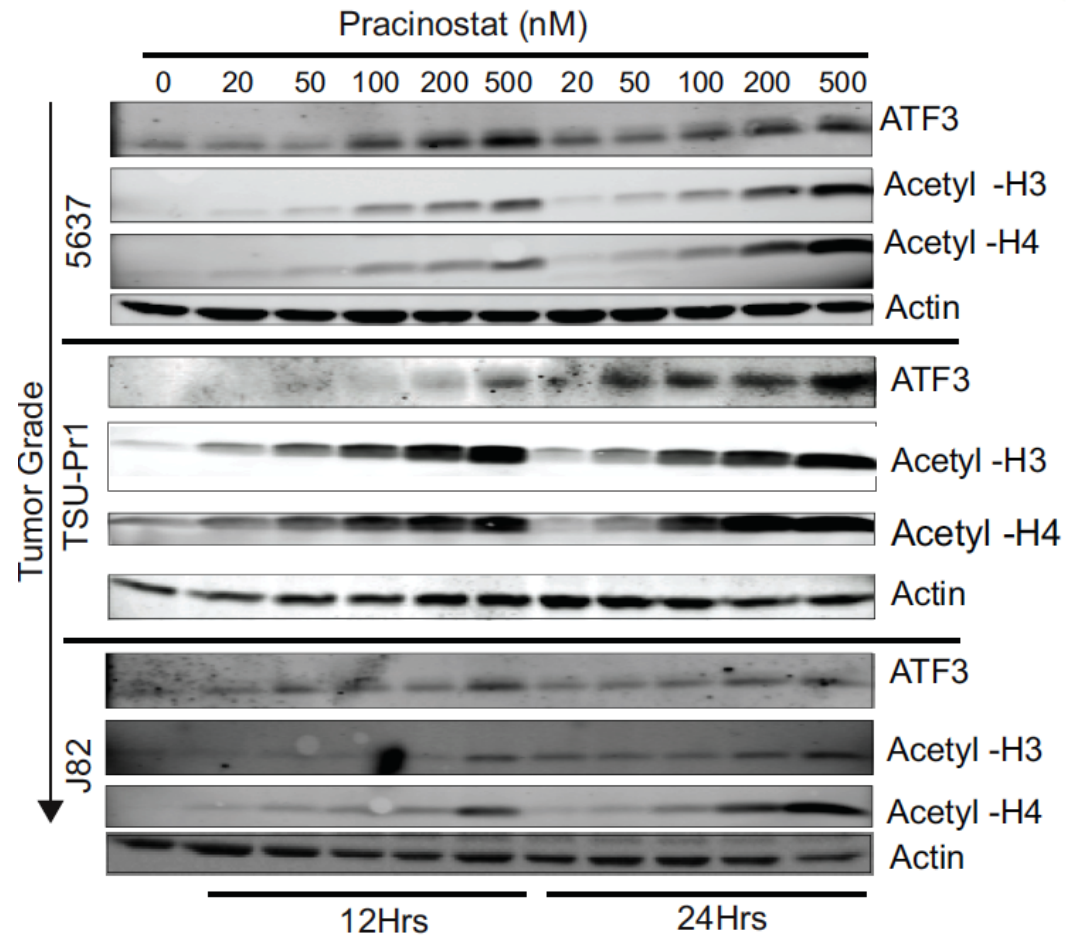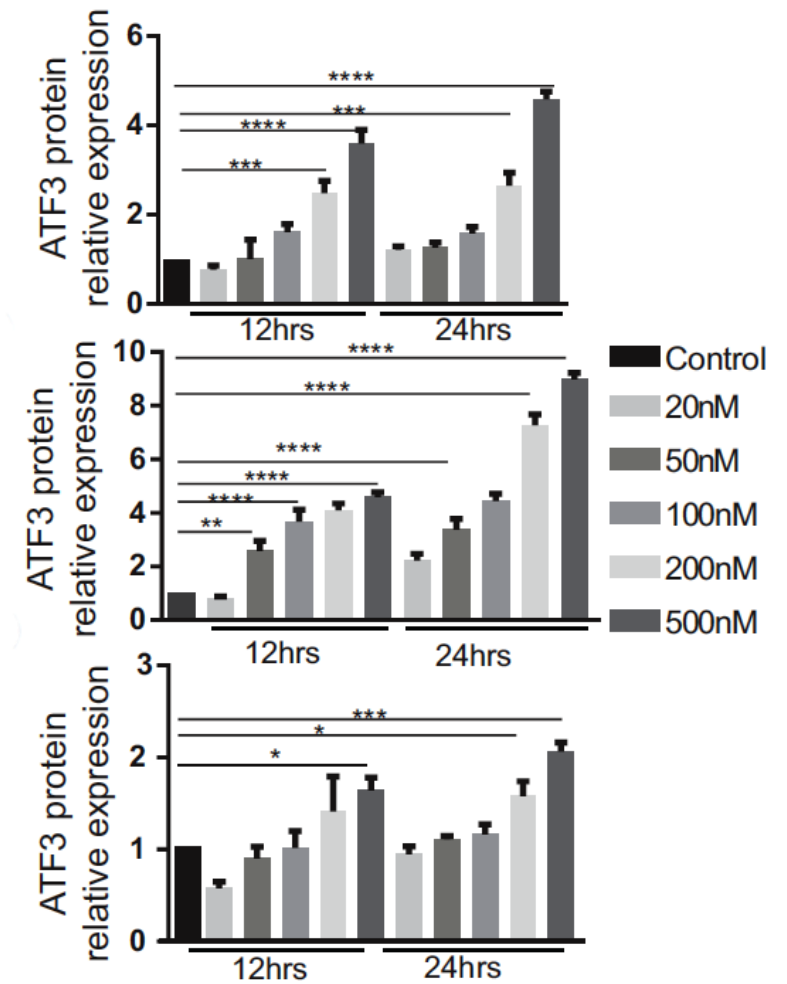
**Figure 3.2: Pracinostat reactivates ATF3 protein expression *in vitro* in a dose- and time-dependent manner.** (i) Western blot analysis of three cell lines (5637, TSU-Pr1, J82) treated with increasing concentrations (20-500 nM) of Pracinostat for 12 hours and 24 hours. Reactivation of ATF3 in a dose- and time-dependent manner also coincides with progressive increase in acetylation of H3 and H4. Actin was used as an internal control to standardize the relative expression of ATF3 at the protein level. Data shown are representative of 3 separate experiments. (ii) Densitometric analysis showing a dose- and time-dependent ATF3 reactivation in the three bladder cancer cell lines upon treatment with Pracinostat (n = 3).
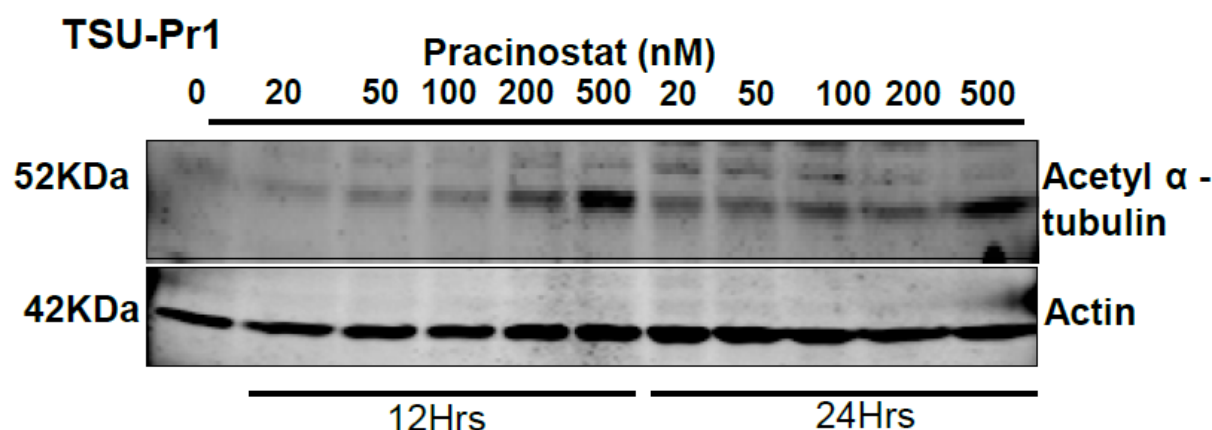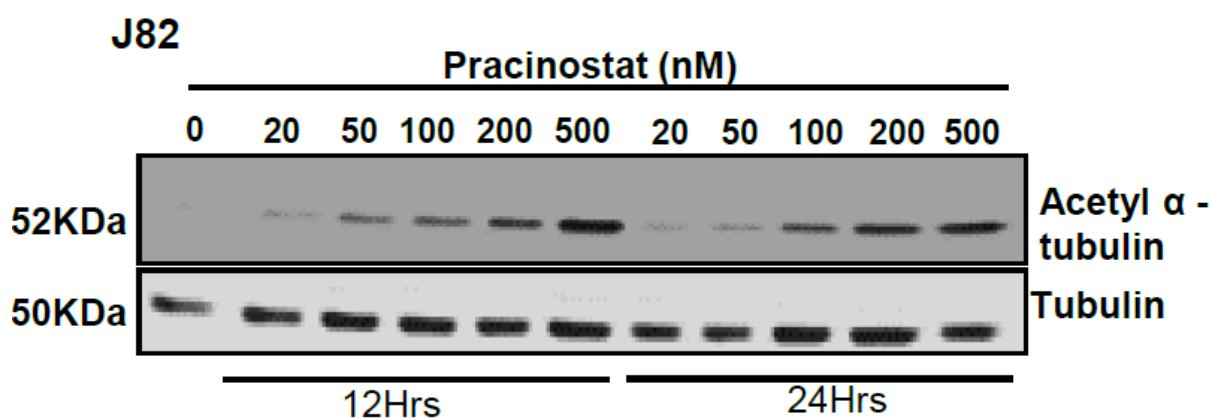
**Figure 3.3:** *Pracinostat increases acetylation of non-histone protein tubulin at higher doses.* Immunoblot analysis of acetylated alpha-tubulin in (i) TSU-Pr1 cells and (ii) J82 cells. Increased acetylation of alpha-tubulin was observed at 500 nM Pracinostat in TSU-Pr1 cells, whilst a gradual increase in the acetylation pattern was observed from 100 nM Pracinostat in J82 cell lines. Actin served as the loading control for TSU-Pr1 cells, while tubulin for J82 cells. Data shown are representative of two separate experiments.

**(i)** Control

**(ii)** 500nM Pracinostat
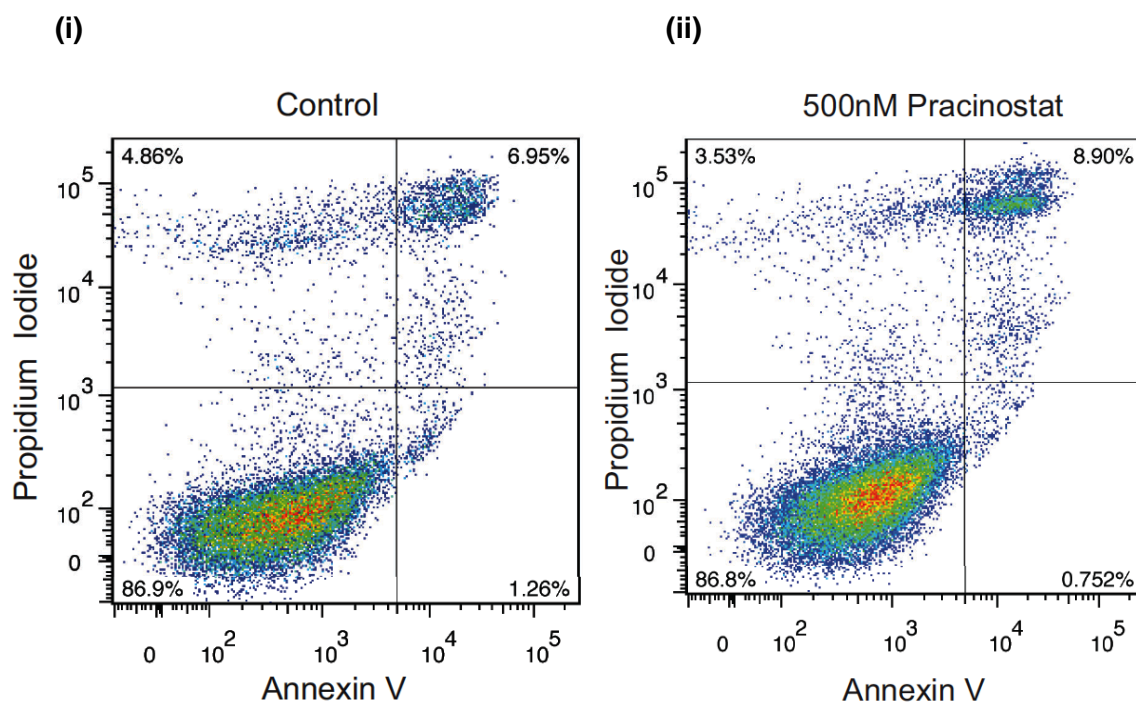
**Figure 3.4:** *Apoptosis analysis on TSU-Pr1cells treated with 500nM Pracinostat for 24 hours compared to untreated control cells*. Scatter plot showing the apoptotic rate in TSU-Pr1 cells by double staining with AnnexinV and Propidium Iodide (PI). The top two quadrants, which accounts for dead and late apoptosis cells, showed the percentage of cells were similar in (i) untreated control and at (ii) 500nM of Pracinostat. The percentage of live cells in the Annexin (-ve) and PI (-ve) remained the same in both cases (~86.9%; n = 2).

### 3.2.2 Pracinostat treatment and reactivation of ATF3 alters phenotypic behaviour *in vitro*

Next we explored the functional significance of reactivation of ATF3 and re-establishment of histone acetylation in bladder cancer cell lines. To test phenotypic changes associated with the Pracinostat treatment and reactivation of ATF3, different functional assays were performed. To analyze the viability of bladder cancer cell lines under Pracinostat treatment, the cells were cultured with Pracinostat (50, 100 or 500 nM) for 6 days, and cell viability assessed. Pracinostat significantly reduced the *in vitro* proliferation rate of all five bladder cancer cell lines tested in a dose-dependent manner (Figure 3.5 (i) and (ii)). At a concentration as low as 100 nM, Pracinostat demonstrated a significant effect on the viability of three (T24, TCC-SUP, TSU-Pr1; $P<0.05$) of the five cell lines we tested, whilst 500 nM Pracinostat resulted in a significant growth reduction in all five cell lines.

Since anchorage-independent growth on a soft agar surface to produce colonies is characteristic of malignant transformation, we investigated whether treatment with Pracinostat had any impact on this capacity of bladder cancer cells. Not all bladder cancer cells were able to make colonies on soft agar; only two cell lines T24 and TSU-Pr1 were tested. Accordingly, T24 and TSU-Pr1 cells were treated with Pracinostat for 3 days, plated on agar at a low density and incubated at 37°C for 21 days to allow the formation of spheres (Figure 3.6). The number of spheres formed at both 200 nM and 500 nM of Pracinostat was significantly reduced in TSU-Pr1 cells to 75% ($P=0.008$) and 85% ($P=0.005$) respectively when compared to the DMSO control (Figure 3.6 (i) and (iii). The colony formation in T24 cells is also significantly reduced at 500nM Pracinostat treatment ($P\leq 0.05$) (Figure 3.6 (ii) and (iv).

We also tested the nature of the cell-to-cell interaction in 2D cultures of the cell lines, with and without Pracinostat treatment, by measuring their scratch wound closure capacity. Wounds made in cells treated with 50 – 500 nM Pracinostat for 24 hours remained open at the time point when a wound made in DMSO control cells was closed (Figure 3.7 (i) and (ii)). There was a significant delay in the wound closure process in T24 cells treated with Pracinostat at a concentration of 200 nM (Figure 3.7(i)) from 6 hours (P<0.001, percentage of wound closure), and 40% of the wound remained open. Similarly, for 5637 cells, 25% of the wound remained open after treatment with 200 nM Pracinostat compared to the control (Figure 3.7(ii)). Taken together, the data suggest that Pracinostat treatment in these bladder cancer cell lines restores a more non-malignant phenotype.

**(i)**
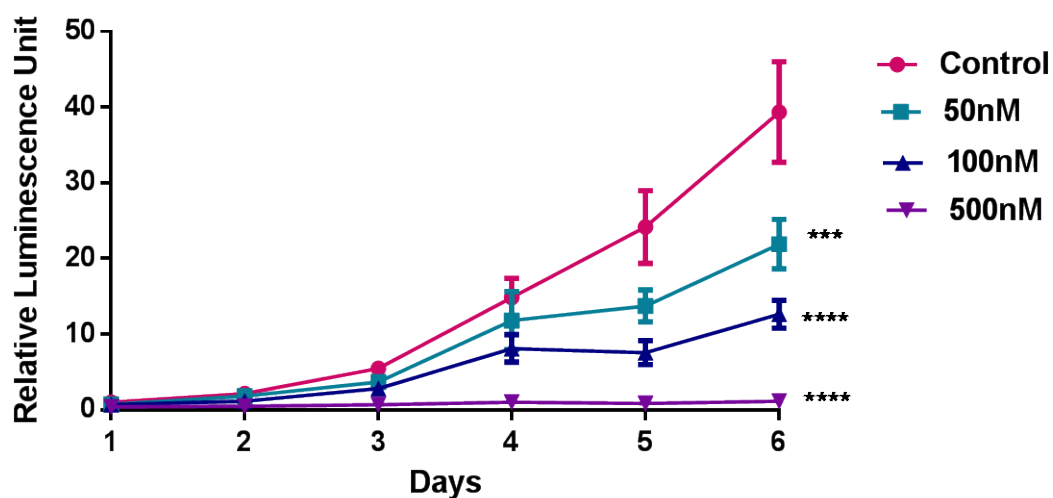


**(ii)**

|         | Control | 50nM    | 100nM   | 500nM   |
|---------|---------|---------|---------|---------|
| 5637    | 100     | 87 ± 4.4| 84 ± 6.6| 23 ± 1.9|
| T24     | 100     | 81 ± 9.8| 61 ± 6.1| 7 ± 2.1 |
| TCC-SUP | 100     | 64 ± 5.1| 44 ± 7.3| 4 ± 1.9 |
| J82     | 100     | 95 ± 3.6| 87 ± 7.1| 45 ± 4.3|

**Figure 3.5:** *Proliferation analysis of bladder cancer cells treated with Pracinostat.* (i) Assessment of viability by Vialight assay on TSU-Pr1 cells treated with Pracinostat demonstrated a dose-dependent growth inhibition of these cells over a period of 6 days, and fold changes in relative luminescence unit was plotted in the graph. All three doses tested showed a significant reduction in proliferation rate in these cells ($P < 0.05$; n = 4). (ii) Table summarizing the percentage of viable cells after 6 days of Pracinostat treatment with different concentrations (50 nM, 100 nM and 500 nM) in other four bladder cancer cell lines. Data represent mean ± SEM; n = 4 per cell line.

**(i)**



Control                200nM                500nM

**(ii)**
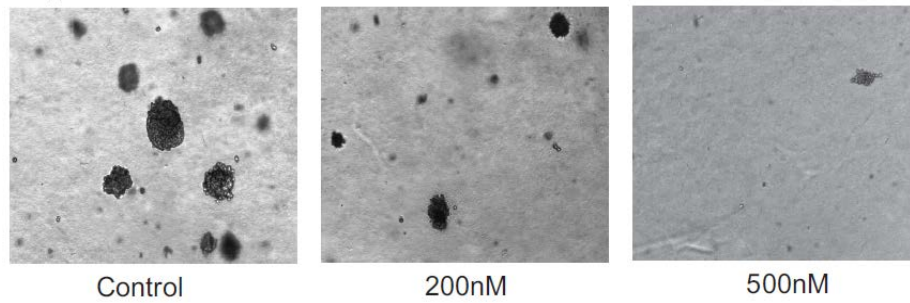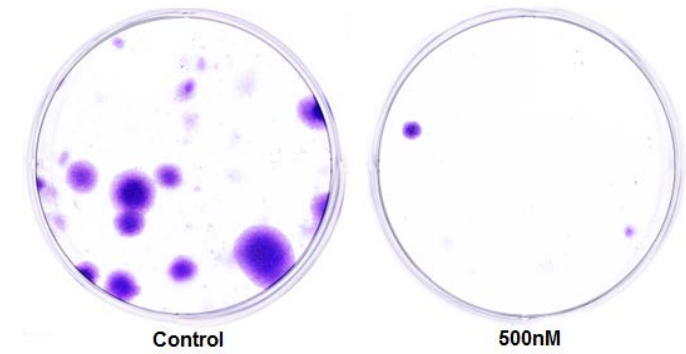


Control                500nM

**(iii)**
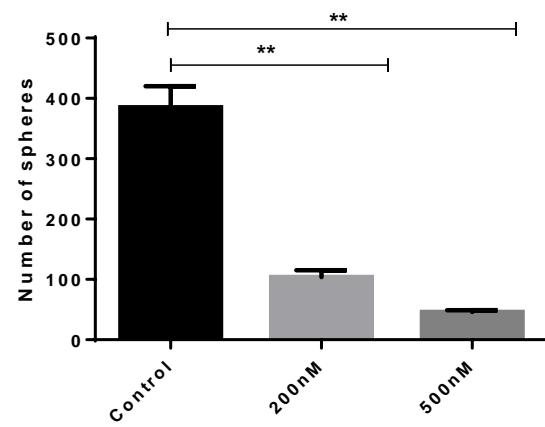


**(iv)**
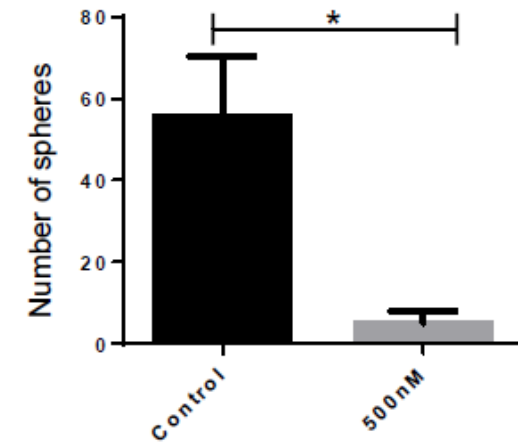
**Figure 3.6:** *Soft agar colony formation assay.* (i) Representative images of triplicate experiments of soft agar colony formation assay on TSU-Pr1 cells treated with Pracinostat (200 nM, 500 nM) for 3 days compared to the control cells. (ii) Representative images of colony formation assay on T24 control cells or cells treated with Pracinostat for 3 days (iii) Quantification of spheres from soft agar assay. Colony number was reduced by ~75% (P=0.008) in cells treated with 200 nM Pracinostat and ~ 85% (P=0.005) in cells treated with 500 nM Pracinostat. (iv) Quantification of colonies; colony number was significantly reduced in cells treated with 500 nM Pracinostat (*P≤0.05) compared to the control cells. Data shown are representative of three independent experiments and represents mean $\pm$ SEM.

**(i)**
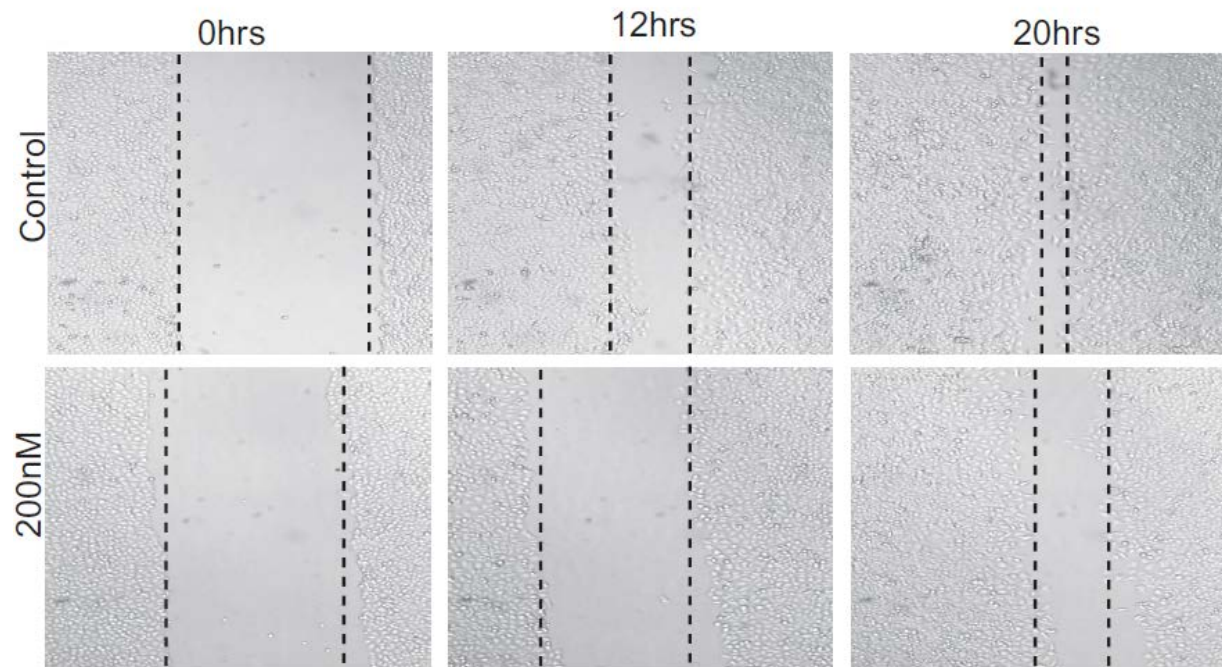


**(ii)**
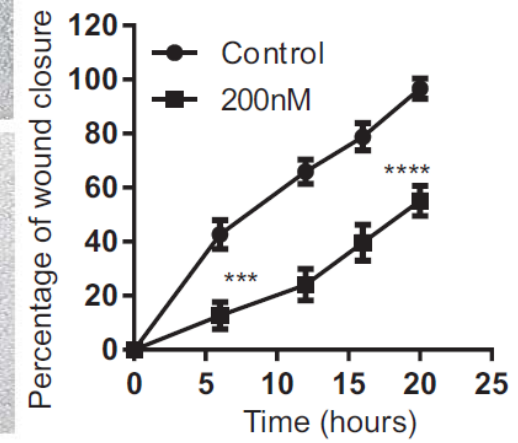
Scratch wound assay in T24 bladder cancer cells
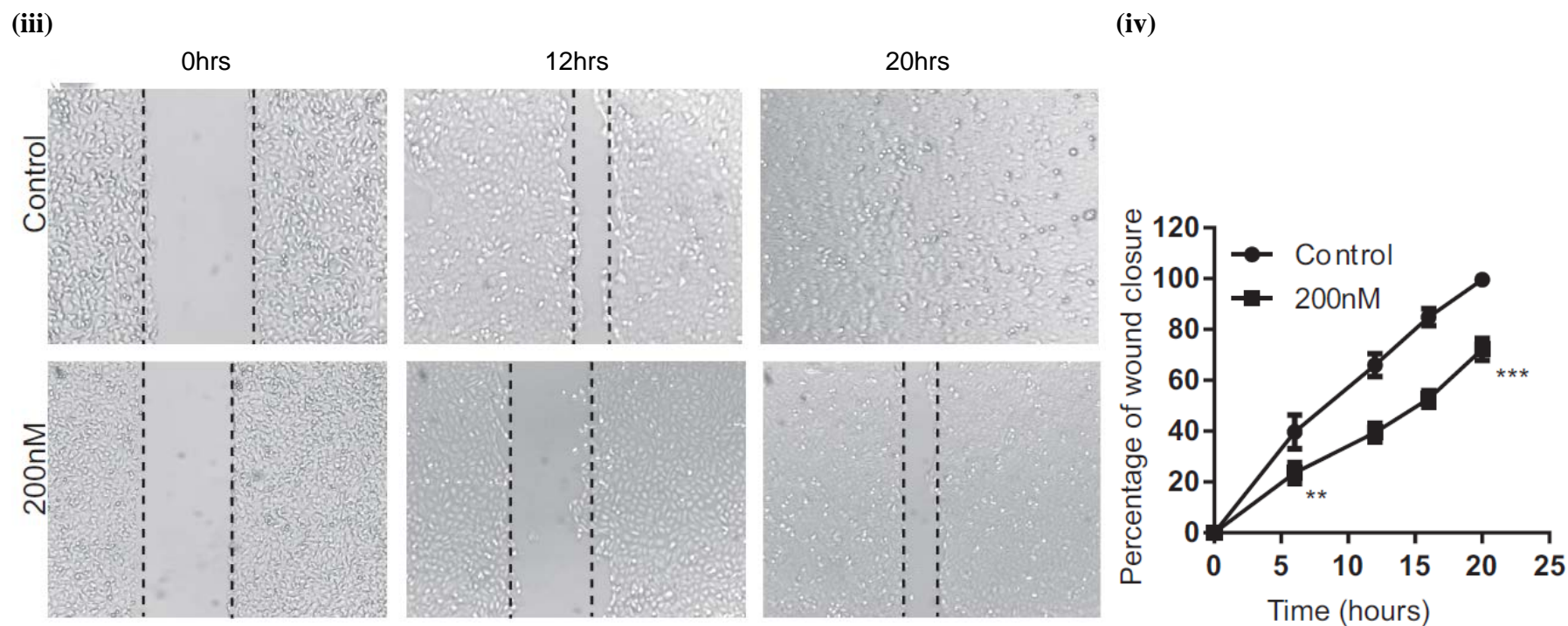
**(iii)**                                            **(iv)**

**Scratch wound assay in 5637 bladder cancer cells**

**Figure 3.7:** *Wound healing assay on T24 (i), (ii) cells and 5637 (iii), (iv) cells treated with Pracinostat.* Representative images of 3 different experiments for each cell line at different time points (0, 12 and 20 hours) are shown. **C** (ii) and (iv) Cell migration was assessed by measuring the relative wound closure. Data represent mean ± SEM (n=3; **$P \leq 0.05$; ***$P \leq 0.001$; ****$P \leq 0.0001$).

### 3.2.3    Pracinostat treatment induces cell cycle arrest at G0/G1 phase and activates tumor suppressor genes in bladder cancer cells, but not in normal urothelial cells

The earlier results shown that Pracinostat treatment over a period of 6 days in culture affects the viability of bladder cancer cell lines. To investigate whether this effect is due to impairment in their cycling capacity, we compared the cell cycle pattern of bladder cancer cells, with and without Pracinostat treatment. Treatment with Pracinostat induced G0/G1 phase arrest in all bladder cancer cells tested (Figure 3.8 (A) and (B)). The percentage of cells entering into the S phase is strikingly reduced, with a subsequent accumulation of cells in G0/G1 phase in all cancer lines (Figure 3.8). In contrast, in normal urothelial cells SV-HUC1 (Figure 3.8A (ii)), the percentage of cells in the S phase remained similar to the untreated controls even at the highest concentration (500 nM) of Pracinostat, with an increase in G2/M phase suggesting that the normal cells are relatively resistant to Pracinostat-mediated treatment. This is consistent with previously published observations indicating that the proliferation inhibitory concentration of Pracinostat is >100 µmol/L in normal human dermal fibroblast, and ≤1 µmol/L in another 29 cancer cell lines [108].

We further investigated the changes in the expression of tumor suppressor genes implicated in bladder cancer, such as retinoblastoma (RB1) and p21. RB1 has been identified as a predominant growth and tumor suppressor in bladder cancer [146]. Hyper-phosphorylated RB1 is inactive, with phosphorylated serine residues, and is unable to bind E2F and control the cell cycle. When RB1 is hypo-phosphorylated (active RB1), it binds to E2F and prevents transcription of target genes. Treatment with Pracinostat resulted in an increase in the hypo-phosphorylated (active) RB1 in a dose-dependent manner in three of the bladder cancer cell lines we tested (Figure 3.9 (i), suggesting that an increase in expression of hypo-

phosphorylated RB1 may have an impact on cell cycle arrest in bladder cancer cells. In J82, a grade 3 tumor cell line, RB1 expression is lost in control cells but Pracinostat treatment restored hypo-phosphorylated RB1 (active form) expression. Consistent with that observation, immuno-cytochemistry on TSU-Pr1 cells also demonstrate the increased nuclear expression of active (green) in dose depended manner compared to the control cells (hyper-phosphorylated RB, yellow) (Figure 3.9(ii). The tumor suppressor gene, cyclin-dependent kinase inhibitor p21 $^{Cip/WAF}$, was also reactivated in cell lines treated with 500 nM Pracinostat (Figure 3.9(i)).
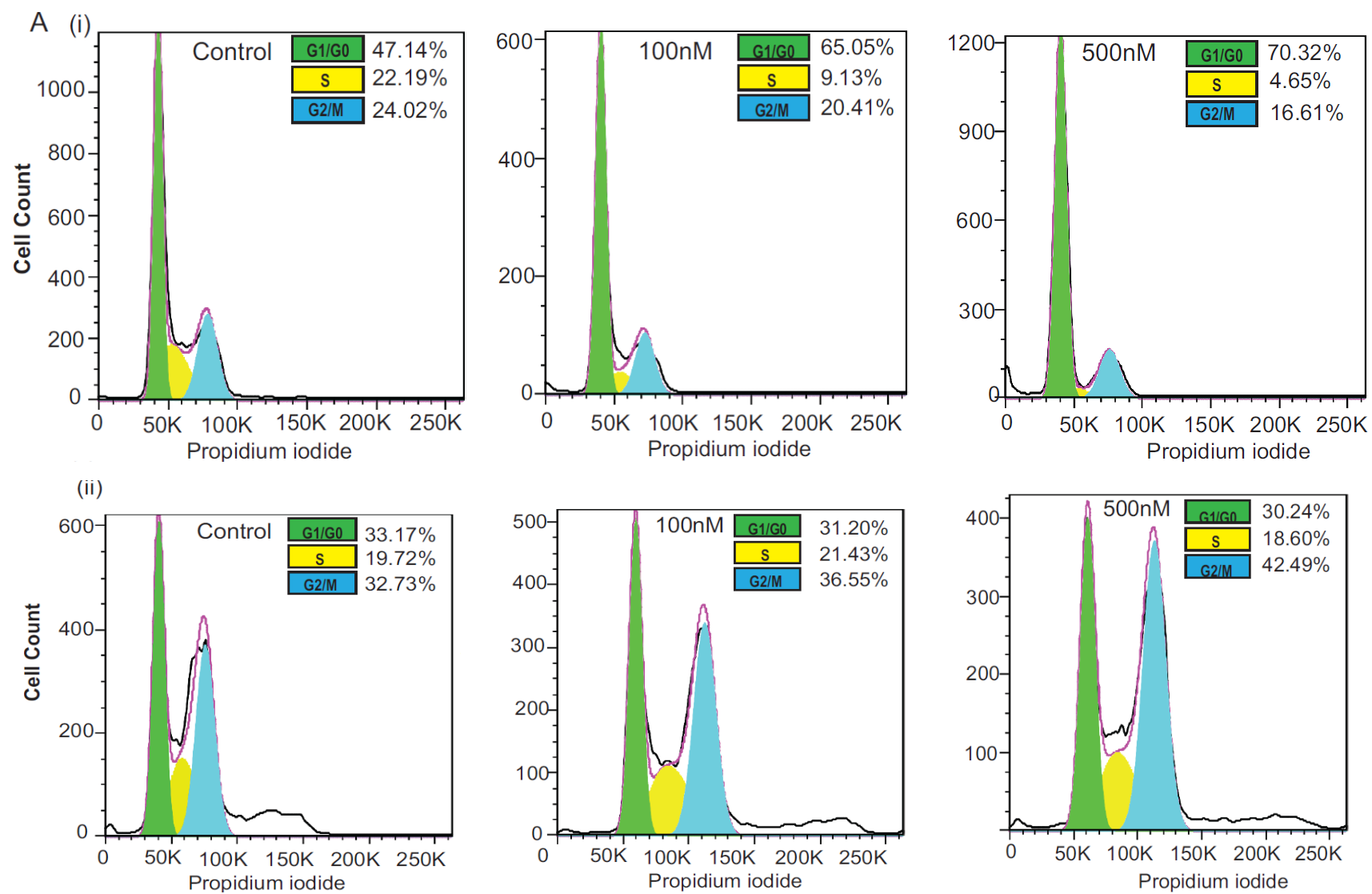
**B**
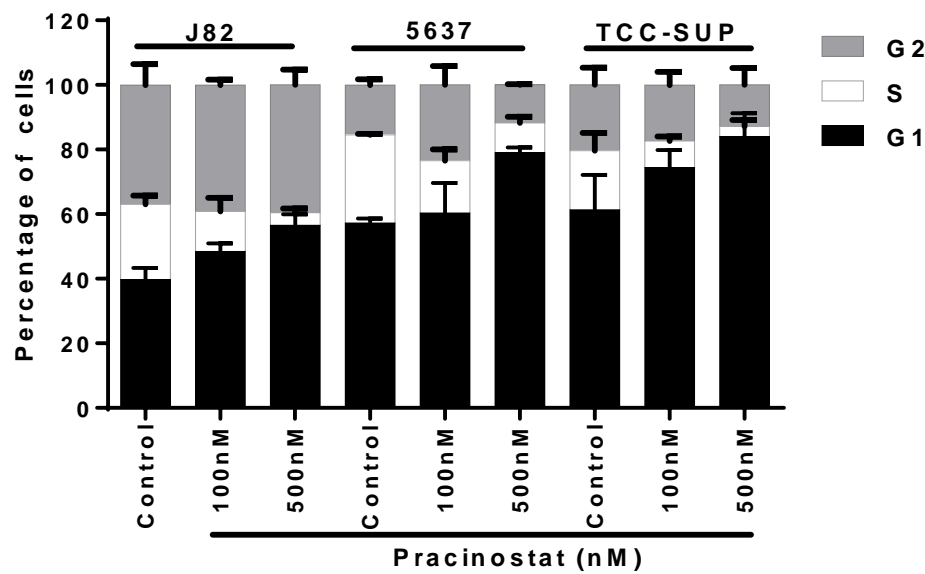


**Figure 3.8:** *Pracinostat treatment accelerates cell cycle arrest in cancer cells; normal urothelial cells demonstrate resistance.* **(A)** (i) Representative images of cell cycle analysis by flow cytometry in T24 bladder cancer cells treated with 100 nM and 500 nM Pracinostat for 24 hours compared to the untreated control. The cells in S phase were significantly reduced with the increased concentration of Pracinostat. The percentage of cells in S phase in untreated T24 control cells were 22.19%, which was gradually reduced to 9.13% and 4.65% with 100 nM and 500 nM Pracinostat with a gradual increase in G0-G1 phase. **(A)** (ii) Representative images of cell cycle distribution of normal urothelial cells, SV-HUC1 untreated, compared to 100 nM and 500 nM Pracinostat treated for 24 hours. The percentage of cells in S phase remained similar in untreated and Pracinostat-treated normal cells (~20%). **(B)** Cell cycle distribution of three different bladder cancer cells; the quantitation is presented as mean ± SEM (n =3).

**(i)**



**(ii)**



| Control | 100nM | 500nM |
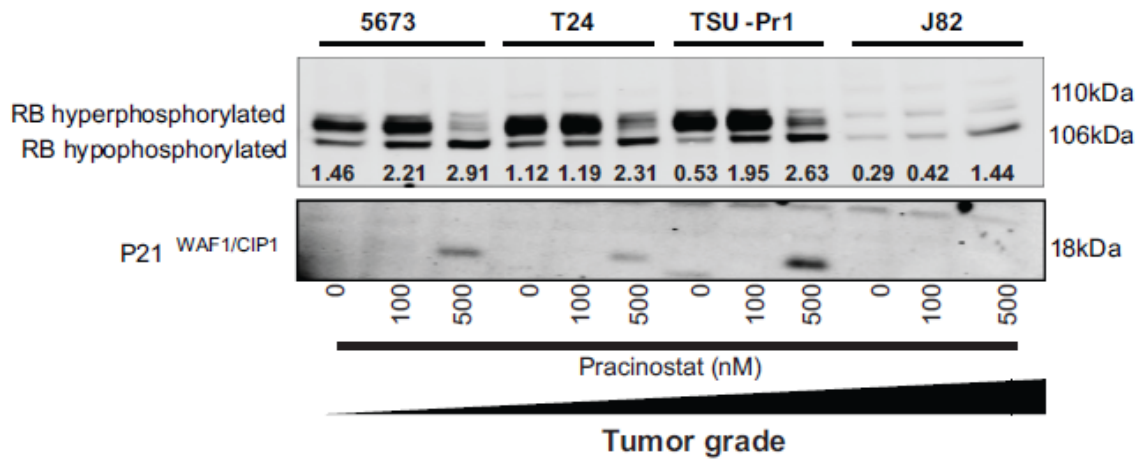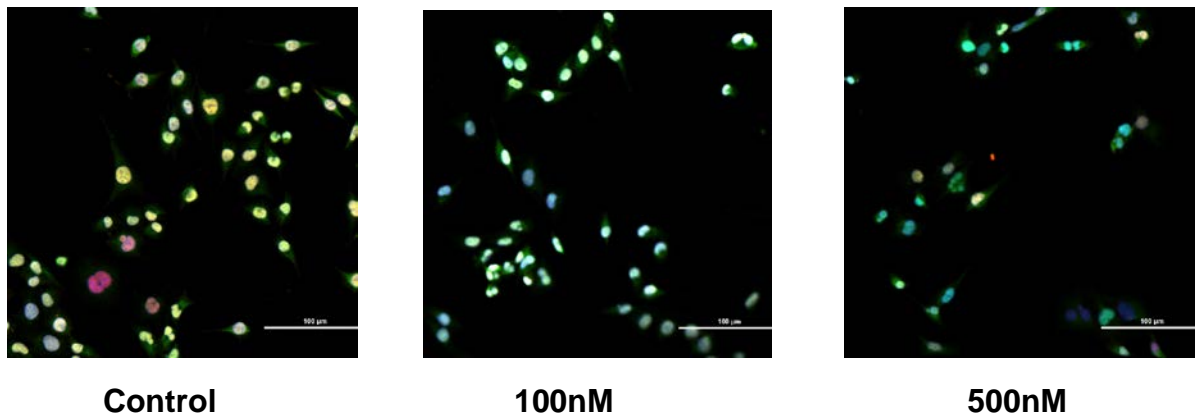
**Figure 3.9:** *Pracinostat treatment activates tumor suppressor genes*. Immunoblot analysis of tumor suppressor genes associated with bladder cancer (RB1 and p21). Expression analysis in four different bladder cell lines indicated a dose-dependent transition from hyper-phosphorylated (inactive) to hypo-phosphorylated (active; 106 KDa) form of RB1. Representative of replicated experiment (n = 2). (B) Immuno-cytochemistry on TSU-Pr1 cells also demonstrated that Pracinostat treatment altered the nuclear expression of hyper-phosphorylated inactive (*pRB - red*) to hypo-phosphorylated active RB (*RB1-Green*) (n = 3).

### 3.2.4        Pracinostat treatment increases sensitivity to platinum

Chemotherapy using platinum based compounds is the standard of care in advanced bladder cancer. Chemotherapeutic agents such as cisplatin and carboplatin bind to DNA and form adducts which results in impairment in cell repair mechanism and finally leads to cell death. Most human DNA is tightly compacted around histones, limiting the access of drugs targeting DNA such as platinum resulting in declined anti-tumor efficacy. Since both the functional significance of DNA and structure of chromatin has an important role in cancer development, intervening on alteration in DNA and in chromatin together could provide a better therapeutic outcome, although the targets of HDACi and chemotherapy are different [147]. Although, the actual molecular mechanism underpinning the combination treatment largely unknown, the proposed mechanism suggest HDACi releases the chromatin and subsequently resulting in greater access to DNA and finally results increased cytotoxicity[148]. Accordingly, I explored the efficacy of Pracinostat in sensitising cells to chemotherapy in a combination treatment regime. My study utilized Carboplatin (an analogue of cisplatin, $2^{nd}$ generation platinum), a less toxic platinum compound for the gastro-intestinal tract and less neurotoxic, to test in combination with HDACi Pracinostat in bladder cancer cell lines. Pracinostat with varying concentration was used to pre-treat both the platinum sensitive cell lines (TSU-Pr1, J82 and TCC-SUP) and resistant cells (T24 - platinum resistant variant). A dose dependent increased sensitivity was observed at all three concentrations of Pracinostat in TSU-Pr1 cells (Figure 3.10(i)) (representing all 3 sensitive cell lines). Pre-treatment with 500nM Pracinostat lowered the half maximal inhibitory concentration ($IC_{50}$) value for platinum from 27µg/ml to 10µg/ml in TSU-Pr1 cells. Pre-treatment with 500nM Pracinostat in platinum resistant T24 cells demonstrated a significant increase ( at~10µg/ml) in sensitivity to platinum compared to Carboplatin only (control cells - 70µg/ml) treated cells

(P$\leq$0.001) (Figure 3.10 (ii)). The IC$_{50}$ value of Carboplatin was 65 $\pm$ 0.06 µg/ml when platinum resistant T24 cells were pre-treated with 500nM Pracinostat.
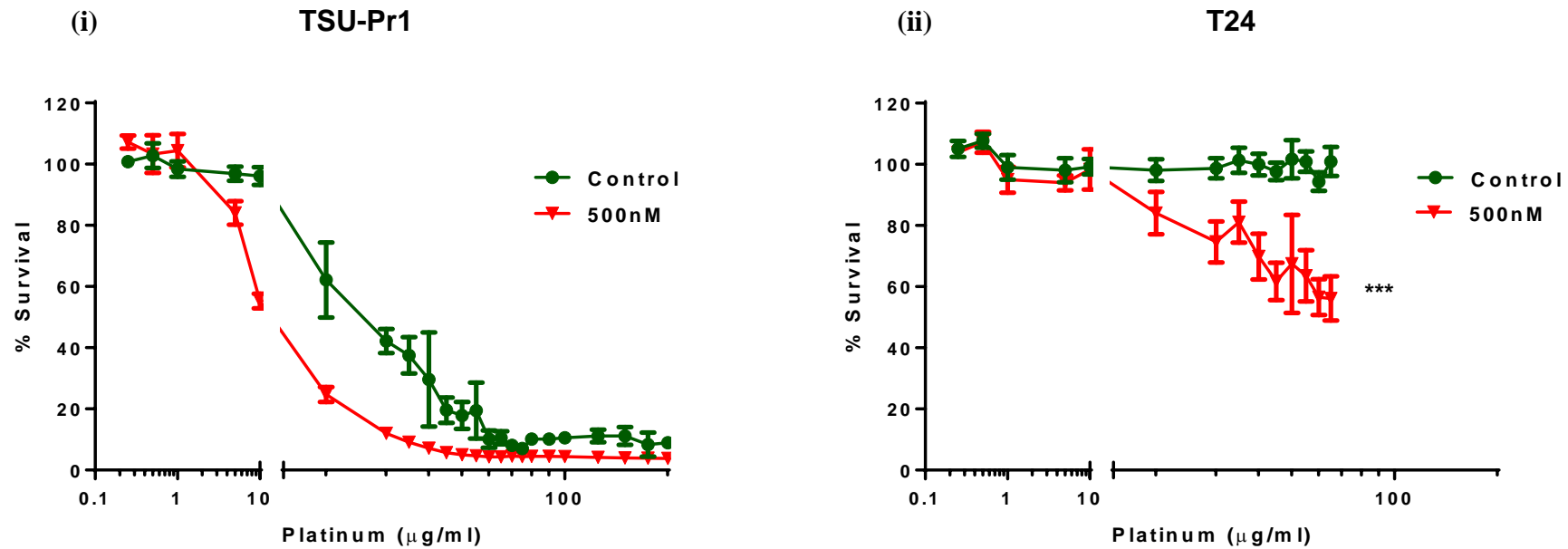
**Figure 3.10:** *Pracinostat treatment increases the sensitivity to platinum treatment in bladder cancer cells.* Sensitivity to platinum was tested in (i) TSU- Pr1, platinum sensitive cell and in (ii) T24, platinum resistant cells by pre-treating the cells with Pracinostat for 48hrs prior cisplatin treatment. (i) TSU-Pr1 cells displayed a dose depended increased sensitivity to platinum treatment: data showing only for 500nM Pracinostat (ii) 500nM Pracinostat pre-treatment in resistant T24 cells significantly increased the sensitivity to platinum in these cells (***P≤0.001).

### 3.2.5 The level of expression of HDAC enzymes may dictate the degree of sensitivity in different cell lines *in vitro*.

*In vitro* functional assays with Pracinostat in our panel of bladder cancer cells, including viability, 2D migration, cell cycle analysis, and platinum treatment showed that there was a concentration-dependent sensitivity in every cell line tested. However, the degree of sensitivity to Pracinostat varied in different cell lines and was independent of the tumor grades from which the lines were derived. In viability assay (Figure 3.5) three of the five lines showed significantly reduced viability when Pracinostat was used at a concentration of 100nM, whereas the other two cell lines were less sensitive to Pracinostat treatment. In scratch wound assay (Figure 3.7) T24 cells showed a significant delay in wound closure at 6 hours with 40% of the wound remaining open whilst 5637 showed 25% of the wound remaining open after the same time. Previous studies have proposed differing levels of HDAC enzymes in different cells as a mechanism of resistance to HDACi-mediated therapy [149, 150]. Thus I compared the level of expression of HDAC enzymes between the resistant cell lines (5637 and J82) and sensitive cell lines (TCC-SUP). Quantitative real-time PCR targeting different classes of HDAC enzymes demonstrated a relatively increased level of expression of class 1,2B and class 4 HDAC enzymes in the resistant cell lines compared to the sensitive cell line (Figure 3.11(A)). Elevated expression of HDAC1 and HDAC3 enzymes in less sensitive cells (Figure 3.11 B) compared to the sensitive cells was also observed using Western blot. Together, these results indicate that the increased expression of these target molecules may contribute towards different degrees of sensitivity to Pracinostat treatment.

**A    (i)**
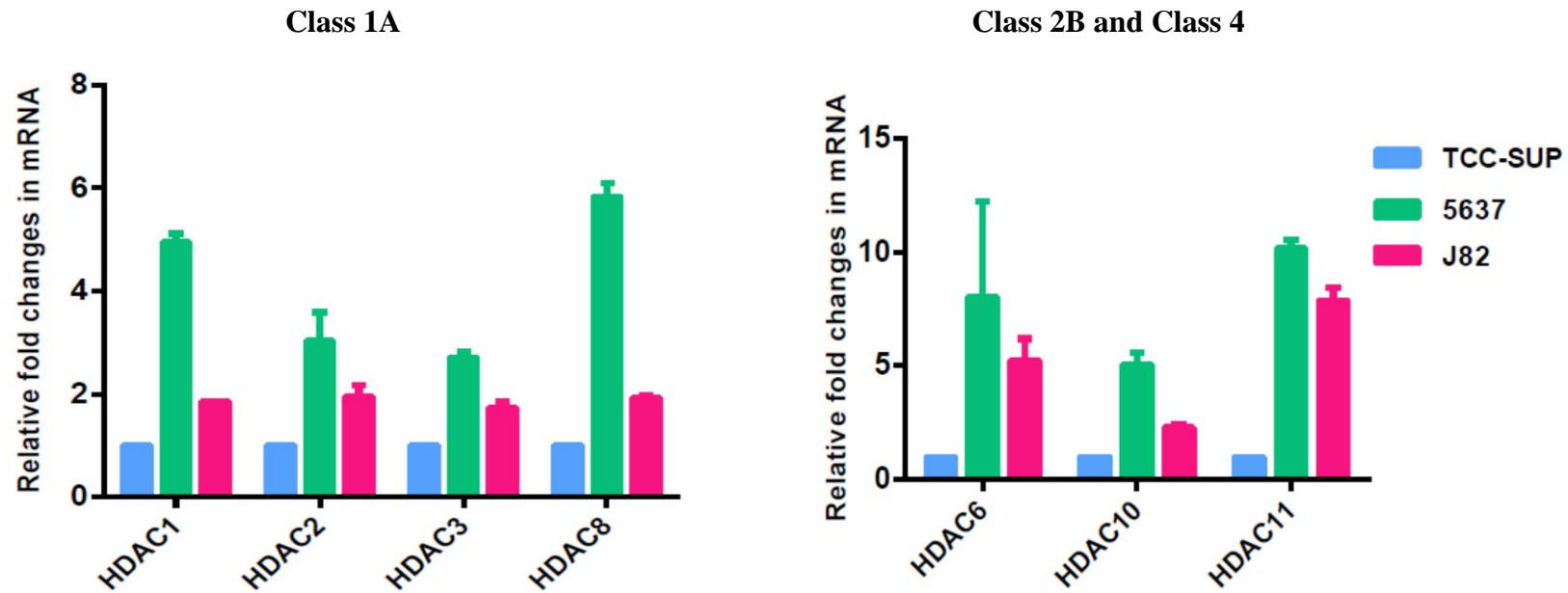


**Figure 3.11(A): The level of expression of HDAC enzymes may dictate the degree of sensitivity in different cell lines *in vitro*.** (i) Quantitative real-time PCR for class 1, 2B and class 4 HDAC enzymes demonstrated a relatively increased level of expression in resistant cell lines (5637, J82) compared to the most sensitive cell line (TCC-SUP) (n=3).
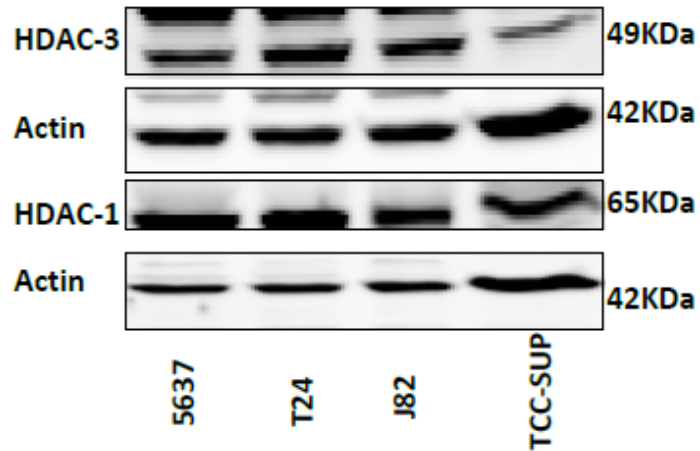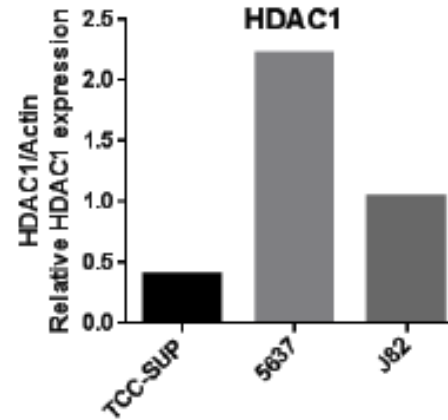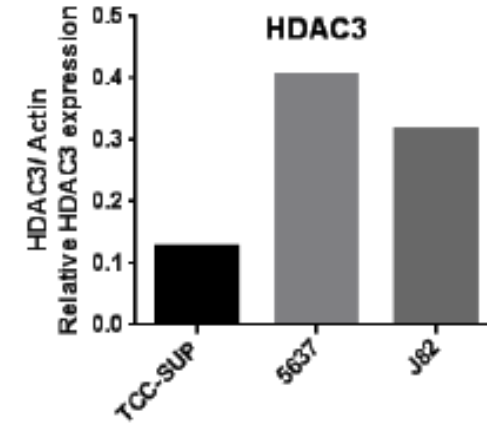
**Figure 3.11 (B): The level of expression of HDAC enzymes may dictate the degree of sensitivity in different cell lines *in vitro*.** Immunoblot analysis of class 1 HDAC enzymes confirming that expression of HDAC1 and HDAC3 enzymes are lower in the highly sensitive cell line (TCC-SUP) in the panel compared to the less sensitive cell-lines (5637, T24 and J82). (iii) Densitometric analysis showing a dose- and time-dependent ATF3 reactivation in the bladder cancer cell lines upon treatment with Pracinostat (n = 1).

### 3.3. Discussion

In this chapter, I was able to demonstrate that, using the pan-HDACi Pracinostat, ATF3 expression was reactivated *in vitro* in a series of bladder cancer cells of different grade and origin, and subsequently results in alteration of their malignant traits. My study showed that the range of concentration of Pracinostat I have used was adequate to reactivate the expression of ATF3 at mRNA (6 hours and 12 hours) and protein levels after (12hrs and 24hrs) of treatment in all five bladder cancer cell lines tested in a concentration- and time-dependent manner (Figure 1, 2 and Appendix 2). At the same time, the highest dosage of Pracinostat I have tested, 500nM, did not induce cellular death in bladder cancer cells while restoring ATF3 expression. Annexin V staining indicates the percentage of live cells after 24 hrs of 500nM Pracinostat treatment remains the same as in control. Absence of cleaved PARP in all three cell lines tested (Appendix 3) also corroborated the absence of cellular death under these conditions. It is important to note that the dosages I have used in this study do not induce cellular death, but rather re-establish the global acetylation pattern of cells (H3 and H4 acetylation), which may subsequently result in the formation of euchromatin and the activation of transcription factors, including ATF3.

*In vitro* functional assays with Pracinostat in bladder cancer cells demonstrated that there was a concentration-dependent sensitivity in every cell line tested. However, the degree of sensitivity to Pracinostat varied in the different cell lines. Three of the five lines showed significantly reduced viability at a concentration of 100nM Pracinostat, whereas the other two cell lines were less sensitive, independent of their tumor grades from which they derived (Figure 3.5). T24 cells showed a significant delay in wound closure at 6hours with 40% of the wound remained open whilst 5637 showed a lesser 25% of the wound remained open after the same time (Figure 3.7). Heterogeneity within cancer cell populations is a common

survival advantage against anti-cancer therapy, including HDACi. Additionally, previous studies have proposed different mechanisms of resistance to HDACi-mediated therapy including differing levels of HDAC enzymes in different cells [149], HDACi efflux mechanism and the level of P-glycoprotein [151] [152]and changes in signaling pathways, including anti-apoptotic factors such as BCL-2 and NF-κB [153, 154]. While the detailed mechanisms underlying differences in sensitivity were not explored, an increase in the expression of class 1 and 2B HDAC enzyme RNA and an elevated protein expression of HDAC1 and 3 in less sensitive cells (Figure 3.11 A and B) may contribute towards cell line resistance to Pracinostat.

HDACi have been shown to impose G1 phase arrest and subsequent activation of P21 in malignant cells [91] [155]. In accord with this, cell cycle analysis of Pracinostat-treated cells indicates G0/G1 phase arrest and restricted entry into S phase, coincident with de-phosphorylation of RB1 and induction of p21 (Figure 3.9). The percentage of normal cells (HUC1 – normal urothelial cells) in S phase remains unaffected by Pracinostat treatment; normal cells progress through the cell cycle and there was an increase of cells in G2/M phase. G2/M arrest and the resistance of non-cancerous cells to HDACi have been previously described [156] and reflect the presence of a G2 checkpoint in normal cells, which is absent in the majority of cancer cells; abolishing the G2 checkpoint using checkpoint kinase-1 abrogates this resistance [157]. Reactive Oxidative Species (ROS) and the redox pathway have also been implicated in the resistance of normal cells to HDACi. [158]. SAHA (Vorinostat) increases the level of thioredoxin ( TRX- a scavenger of ROS) in normal cells that prevents the accumulation of ROS and increased resistance whare as transformed cells, SAHA induces TRX binding protein ( a negative regulator of TRX), accumulation of ROS and subsequent cell death.

Platinum based compounds such as cisplatin are the first-line standard treatment for advanced bladder cancer. Platinum based compounds form covalent platinum - DNA adducts that lead to double strand breaks, DNA damage and cell death [159]. Acquisition of platinum resistance is found to be common in advanced bladder cancers [160]. Combining HDACi with chemotherapeutic drugs that specifically target DNA, such as cisplatin and its derivative carboplatin enhances the efficacy of these drugs [161]. Treatment with HDACi results in a transcriptionally active chromatin structure, which possibly enhances the anti-tumor effect of DNA binding agents. In my study, all platinum sensitive cell lines tested showed an increase in sensitivity to platinum, a synergistic effect with pre-treatment with Pracinostat. More importantly, in the resistant variant T24 cells pre-treatment with Pracinostat significantly increased the sensitivity to platinum. A number of HDAC inhibitors have been explored in combination with platinum-based chemotherapy including TSA, SAHA, and VPA in solid tumors [147, 162]. Clinical studies in advanced non-small-cell lung cancer (NSCLC) showed that treatment with SAHA improved the efficacy of carboplatin and paclitaxel by improving the response rate from 12.5% to 34% [163]. Synergistic induction in cytotoxic effect of platinum in combination with SAHA was also been shown in cervical cancer cells, oral squamous cell carcinoma and head and neck cancers [148, 164]. Similarly, *in vitro* studies using valproic acid (VPA) in combination with cisplatin have demonstrated amplified anti-cancer activity over cisplatin alone in many cancer cell lines, such as melanoma, ovarian cancer, head and squamous cell carcinoma [147, 165, 166]. TSA mediated enhanced induction of cell death by cisplatin has been previously shown in platinum resistant variant of ovarian and bladder cancer cells[167]. Previous studies using platinum resistant bladder cancer cell line T24R2, demonstrated a significantly improved rate of growth inhibition (~ 87%) when combined with TSA after 72 hours of cisplatin treatment [168]. Previous studies in ovarian cancers suggested that increased expression of class 1 HDACs; HDAC 4 (regulates

the activation of STAT1 activation leads to chemo-resistance) and HDAC 3 leads to a defective response to DNA damage and aberrant histone positioning on chromatin [169, 170] and recommended a combination treatment for overcoming resistance. My results demonstrated that prior treatment with Pracinostat resulted in significant improvement in sensitising bladder cancer cells (both sensitive and resistant) to platinum therapy. Similar to the previous studies, my results provide further rationale for the use of platinum and the HDACi Pracinostat as a combination therapy in advanced bladder cancer, and indicates combination of these agents may synergistically increase the treatment efficacy with improved outcome.

# CHAPTER - 4

*ATF3 re-expression correlates with tumor response
to Pracinostat in vivo*

## 4.1 Introduction

In the previous chapter, HDACi Pracinostat shown to activate the re-expression of ATF3 *in vitro*, resulting in significant alteration of malignant properties in series of bladder cancer cell lines of different origins and grades I have tested. It is important to investigate if the observation my study made *in vitro* using Pracinostat can be translated to *in vivo* xenograft models using bladder cancer cells. Xenograft models, where human cells are injected into the flank of BALB/C nude mice are consistently and successfully used as a next immediate step to screen the efficacy of new cancer therapeutic strategies in pre-clinical settings. Pre-clinical studies in colorectal cancer xenografts demonstrated that Pracinostat accumulates in the tumor tissue and selectively inhibits cancer cells but not normal cells with excellent pharmacokinetic properties when compared to SAHA [108, 110]. In Phase I clinical studies, dose tolerance tests in patients with advanced solid tumors, Pracinostat has been well tolerated at 60mg for 5 days for 2 weeks with pharmacokinetic (PK) properties similar to a pre-clinical study and with less side-effects [171]. A very recent Phase II study demonstrated a promising response by Pracinostat treatment with a significant reduction in the level of circulating tumor cells (CTC) (~60%) in advanced prostate cancer patients although PSA responses did not support single agent activity [113]. From these studies, it is clear that Pracinostat is a superior HDACi, with greater tolerability and improved PK properties making it an ideal anti-cancer drug for treating solid malignancies potentially in combination with other agents.

To investigate the *in vivo* properties, I sought to perform xenotransplantation assays as detailed in the methods sections. Though subcutaneous xenograft models using immune-deficient mice requires a caution that the stromal system from mouse models may not

necessarily replicate the results in human systems, these models are widely used for studying the efficacy of anti-cancer drugs and provide clinically relevant pharmacokinetic parameters[172, 173]. In the case of Pracinostat, the pharmacokinetic properties have been studied both in pre-clinical systems using mouse models and also in Phase I clinical studies using patients with advanced malignancies. Thus, in my study, the xenograft model would validate the findings I made *in vitro* and would represent a natural circulatory and neo-vascularization system to investigate how the tumor establishes and responds for orally administrated Pracinostat.

This chapter will demonstrate that the oral administration of HDACi Pracinostat restores the expression of ATF3 in xenograft tumor samples and subsequently influences the angiogenesis and apoptosis in tumor tissues *in vivo*.

## 4.2 Methods

Detailed method for xenotransplantation assays, immuno-histochemistry, and immuno-florescent are described in general methods - chapter 2.

### 4.2.1    Image Analysis

Representative sections from both Pracinostat treated and vehicle control mice xenografts for immuno-histochemistry and immune-fluorescent images were taken for analysis using a Leica bright-filed microscope. For correlation studies between ATF3 and Ki67, cells were identified as ATF3 positive via immune-histochemistry on Pracinostat treated xenograft samples by nuclear localization of ATF3 on the next immediately adjacent serial section and measured for Ki67 staining. Minimum staining thresholds used to categorize positive from negative staining were established using matching isotype control samples of the Pracinostat-

treated xenografts. Image J (version 1.49k) was utilized to measure and assess the staining intensities.

For dual immunofluorescence analysis of CD31 and α-SMA, the specimens were digitized via whole-slide scanning with Nikon C1 confocal microscope. Image analysis was performed using Imaris software (Bitplane AG). Fluorescent images were thresholded and masked for fluorescence intensity to remove auto fluorescence and non-specific signal. The total number of green or red positive blood vessels per image was counted as number of connected areas in the respective masked images. Subsequently, the red channel mask was applied to the green channel to obtain the total number of red fluorescent vessels also showing green fluorescence and vice versa.

## 4.3 Results

### 4.3.1 Oral administration of Pracinostat resulting in regression of tumor *in vivo*

To investigate the biomarker potential of measuring the reactivation of ATF3 expression by Pracinostat *in vivo*, bladder cancer cell lines TSU-Pr1 and T24 (Figure 4.1) were injected into the flanks of nude mice. Full engraftment of TSU-Pr1 cells was observed 2-3 weeks after injection. Mice were initially randomized to receive vehicle control or 100 mg/kg Pracinostat in a cycle of 5 days on 2 days off, orally for 21 days. The dosage was chosen based on published observations where 97% of tumor growth inhibition was recorded for colon cancer xenografts with a maximum of 16.6% body weight loss [108]. The results (Figure 4.1 (ii)) show tumor volumes in Pracinostat-treated mice were significantly smaller when compared to the vehicle control group, exhibiting greater tolerability to the drug over 20 days (Figure 4.1 (i)). In Pracinostat-treated mice, the median tumor volume was 190.04 mm$^3$ on day 20 of treatment, compared to 529.08 mm$^3$ for the vehicle control group (Figure 4.1 (ii). This is

equivalent to 98% (P<0.0001) TGI in Pracinostat-treated mice (100 mg/kg) compared to the vehicle control group.

Histological changes between the vehicle control and Pracinostat-treated mice were analyzed by hematoxylin and eosin staining on paraffin embedded tissue sections (Figure 4.2A). Control tumors exhibited a uniform distribution of viable cells stained with hematoxylin, whereas the sections from Pracinostat-treated samples demonstrated large areas of necrotic or late apoptotic cells characteristically stained by eosin only.
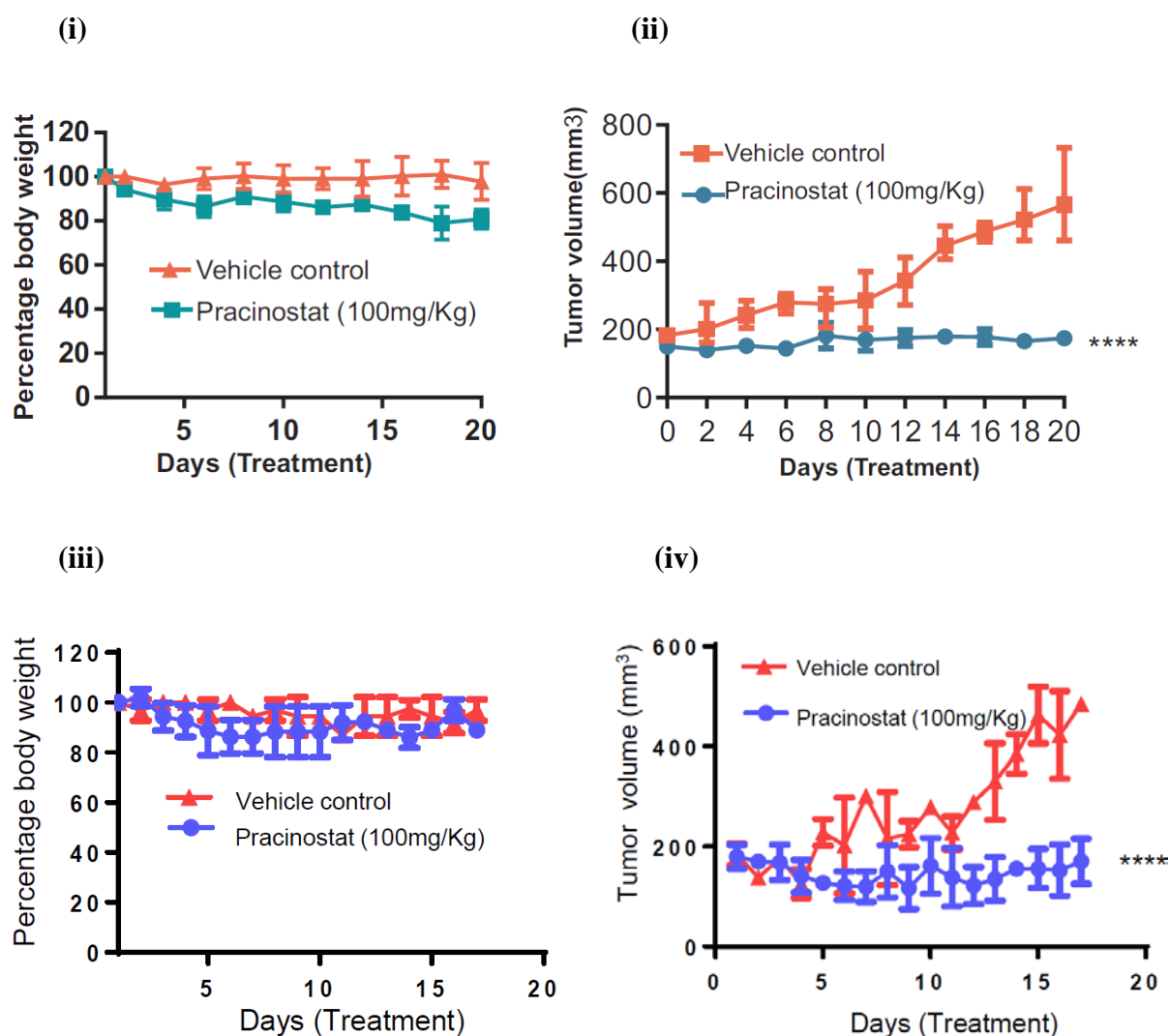
**Figures 4.1:** Efficacy of Pracinostat (100 mg/kg) as a single agent for treatment of mice bearing TSU-Pr1 bladder xenografts: (i) percentage body weight and (ii) tumor volume. The tumor volumes were significantly different in Pracinostat-treated groups compared to the vehicle groups (****$P \leq 0.0001$). Efficacy of Pracinostat (100 mg/kg) as a single agent for treatment of mice bearing T24 bladder xenografts. (iii) Tumor volume and (iv) percentage body weight. The tumor volumes were significantly different in Pracinostat-treated groups compared to the vehicle groups (****$P \leq 0.0001$).

**A**

Vehicle                    Pracinostat 100mg/Kg



**B**

Vehicle    Pracinostat100mg/Kg
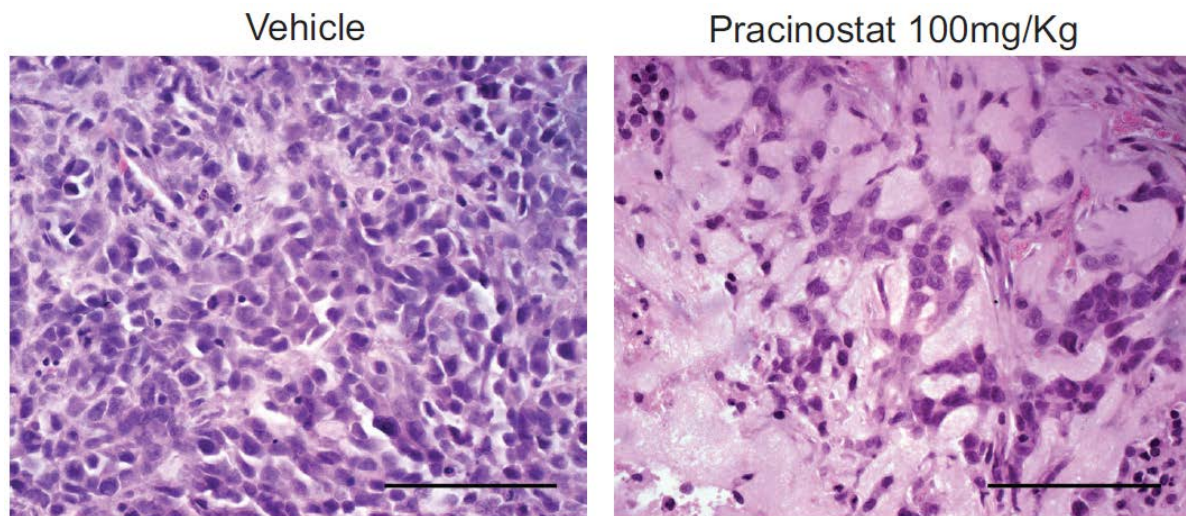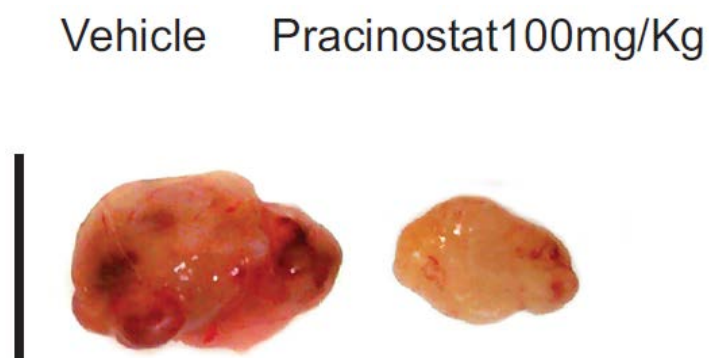


**Figure 4.2:** Representative images demonstrating histological changes in vehicle control mice compared to Pracinostat (100 mg/kg) treated mice for 3 weeks; hematoxylin and eosin staining, image magnification x40, scale bar 100 µM (n=8 mice per group). (ii) Representative macroscopic images of tumors from vehicle-treated mice and Pracinostat-treated mice.

### 4.3.2 Pracinostat re-establishes the acetylation in xenografts

Re-establishment of acetylation pattern of histone proteins is an indicator of Pracinostat accumulation in the xenografts. Similar to the *in vitro* observation of increase in acetylation of histone3 and histone 4 with the Pracinostat treatment, oral administration of Pracinostat in mice increased the acetylation in *in vivo* xenografts. Immuno-histochemistry on representative sections from Pracinostat treated xenograft samples exhibited the nuclear localization of Acetyl H3 compared to the control samples (Figure 4.3).
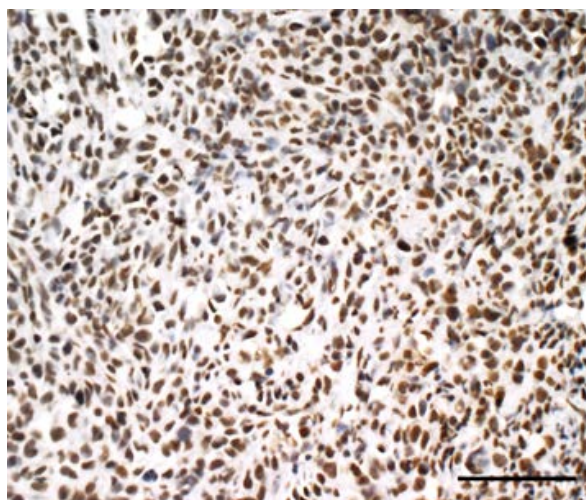
**Vehicle**  **Pracinostat**
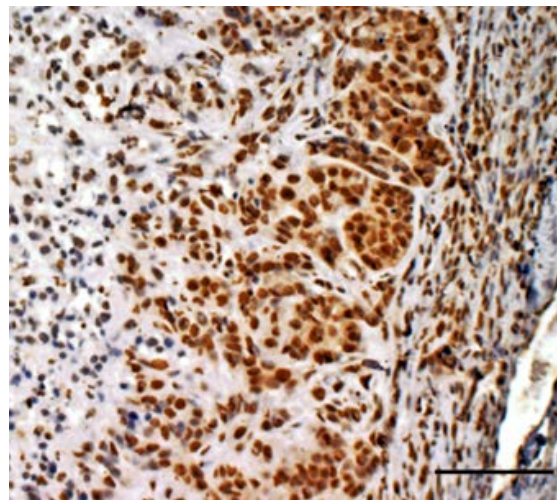


**Figure 4.3:** Immunohistochemistry analysis of Acetyl Histone-3 in mouse xenograft vehicle control and Pracinostat treated samples. Representative sections from Pracinostat treated mice shows an increased intensity in the nuclear marker - Acetyl Histone 3 compared to vehicle control (n=8 mice per group).

### 4.3.3    ATF3 re-expression correlates with the tumor response *in vivo*

Consistent with the observation made *in vitro*, oral administration of Pracinostat reactivated ATF3 expression in xenograft samples. Immunohistochemistry analysis on tissue samples collected from early to late stage of therapy clearly demonstrated nuclear re-expression of ATF3 in the treatment-responding core of the tumor tissue in Pracinostat-treated samples (Figure 4.4(i)). Intriguingly, the majority of cells expressing ATF3 were in a non-proliferative state, indicated by loss of expression of the proliferative nuclear marker Ki67. Cells expressing ATF3 were detected only in the treatment-responding core of the tumor, which is largely devoid of Ki67 expression, and actively proliferating cells (Ki67-positive cells) were mainly located towards the outer edge of the xenograft sample. The staining intensity of the cells expressing ATF3 in the treatment-responding edge of the tumor samples was scored and data analyzed to evaluate whether ATF3-expressing cells were in a non-proliferating state (Figure 4.4 (ii). The mean intensity of cells expressing ATF3 was negatively correlated to Ki67 expression (Figure 4.4 (ii); r = - 0.66, P<0.0001). As expected, tissue samples from the vehicle control group stained negatively for ATF3 and demonstrated abundant expression of Ki67.

**(i)**
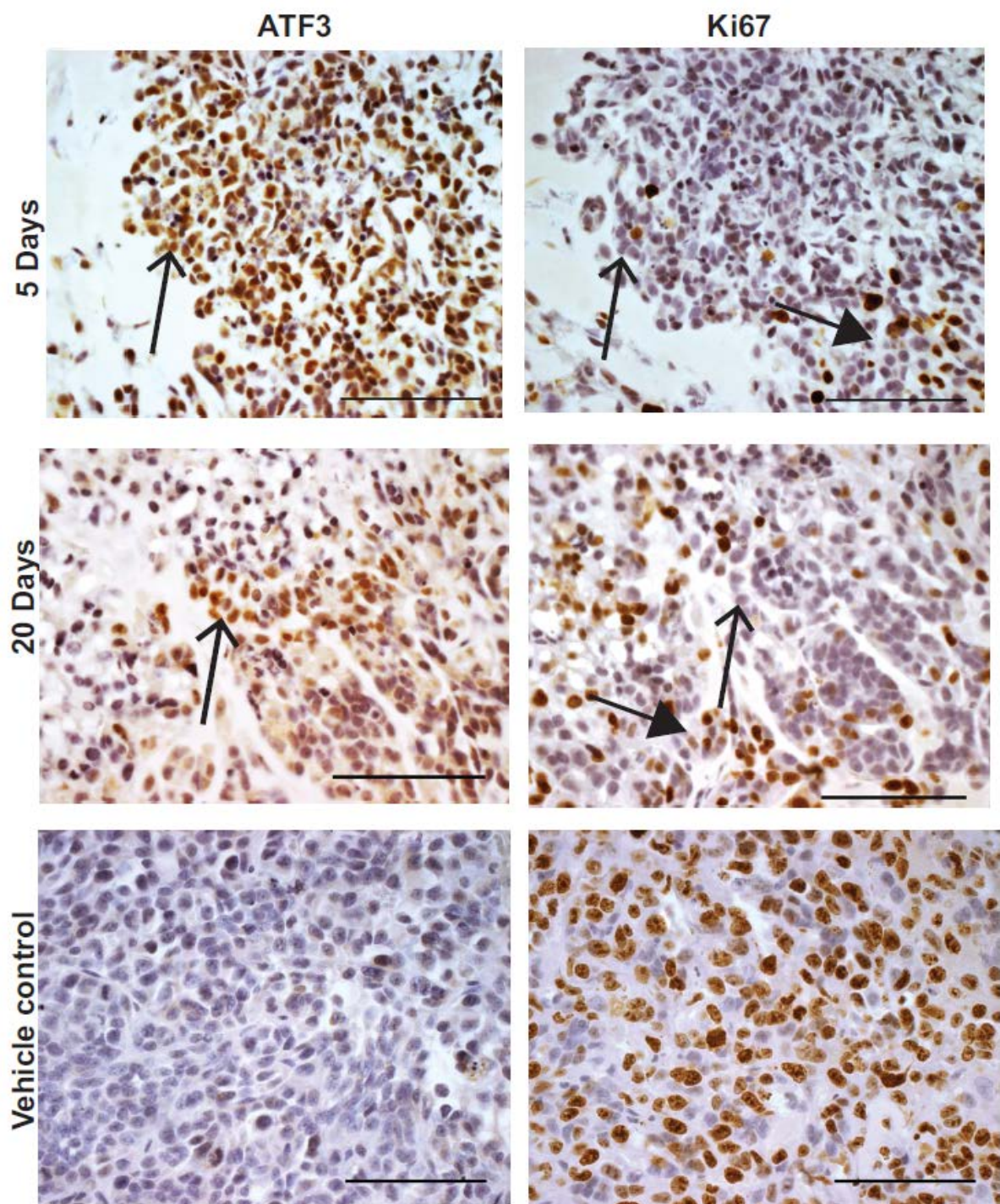
**(ii)**
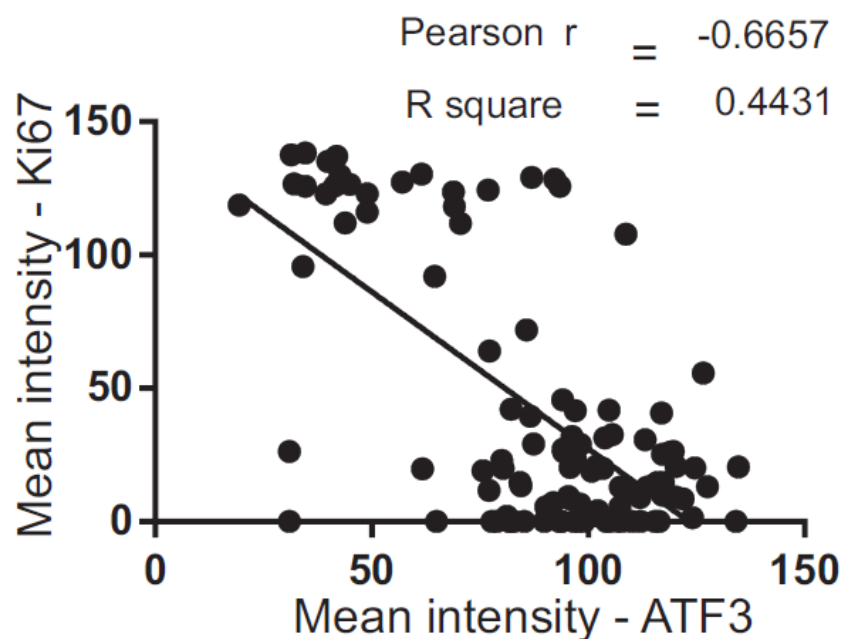


**Figure 4.4:** Immunohistochemistry analysis of ATF3 and Ki67 in mouse xenograft samples after treatment. Serial sections were stained for ATF3 and Ki67 respectively after 5 days (top panel) and 20 days (middle panel) of Pracinostat treatment. Cells expressing ATF3 (thin arrow head) are mainly in the treatment responding edge of the tumor, and cells expressing Ki67 (proliferating) (thick arrow head) are away from the responding edge. Representative images for vehicle control xenograft samples for ATF3 and Ki67. Image magnification x40, scale bar 100 µM. (ii) Scatter plot and linear regression analysis of staining intensity of the cells in the treatment-responding edge of the xenograft samples (n=10). Cells identified as ATF3 positive were located and mean intensity was determined using image J and measured for Ki67 staining.

### 4.3.4    **Pracinostat treatment induces apoptosis** *in vivo*

To extend our findings on tumor response to treatment with Pracinostat, we examined markers of apoptosis in xenograft samples. Caspase-3 has been reported to play an important role in apoptosis, especially the active form of the enzyme, cleaved caspase-3 [174] [175]. Immunohistochemistry analysis of xenograft samples demonstrated that both cytoplasmic and perinuclear cleaved caspase-3 were expressed by the remaining tumor cells of Pracinostat-treated samples treated for 20days compared to the vehicle control, suggesting that there is a marked induction of apoptosis signals in the treatment group (Figure 4.5).
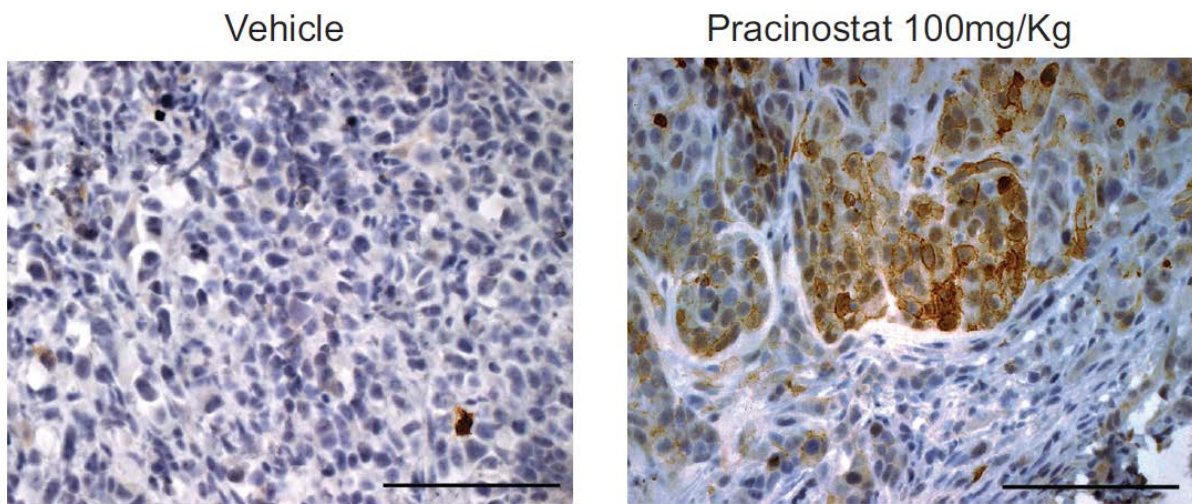
**Figure 4.5:** Representative images of immunohistochemistry sections of cleaved caspase-3 staining in vehicle- and Pracinostat-treated mice (n=8 mice per group). Peri-nuclear and cytoplasmic staining of cleaved caspase -3 indicates the activation of apoptosis in the treated samples. Image magnification x40, scale bar 100 µM.

### 4.3.5    Pracinostat treatment inhibit angiogenesis in *in vivo* xenografts

Neovascularization is vital for *in vivo* tumor growth, and reduction of micro-vessel density is a measure of anti-angiogenic activity. Endothelial cell marker CD31 or platelet endothelial cell adhesion molecule-1 (PECAM-1) is commonly used to quantify angiogenesis in xenograft models [176]. Immunohistochemistry analysis of CD31 in xenograft samples indicated a profound increase in the number of blood vessels in the vehicle control group compared to the Pracinostat-treated samples (Figure 4.6 (i)). Quantification of micro- vessel density confirmed that there was a significant reduction in the number of micro-vessels in Pracinostat-treated mice compared to the vehicle control mice (Figure 4. 6(ii); P<0.0012). To further support the finding of an anti-angiogenic effect for Pracinostat, we examined xenograft samples using dual-immunofluorescence staining for CD31 (red) and α-SMA (green), thereby depicting vascular integrity in these samples (Figure 4.7 (i)). Association of α-Smooth Muscle Actin (SMA)-expressing pericytes with vascular endothelial cells indicates vascular maturation [177]. Immunofluorescence analysis of tumor samples demonstrated that numbers of newly formed blood vessels without pericytes and vessels with pericytes are significantly higher in the vehicle control group (P<0.0001), indicating actively growing tumors in the untreated group (Figure 4.7 (i) and (ii)). In the Pracinostat-treated group, the endothelial cells and pericytes were strikingly reduced, indicating a treatment-associated reduction in angiogenic activity. Interestingly, the number of pericytes was slightly higher than the number of endothelial cells in Pracinostat-treated tumor samples, suggesting the presence of collapsed vessels following treatment, although this was not significant (Figure 4.7 (i)).

**(i)**
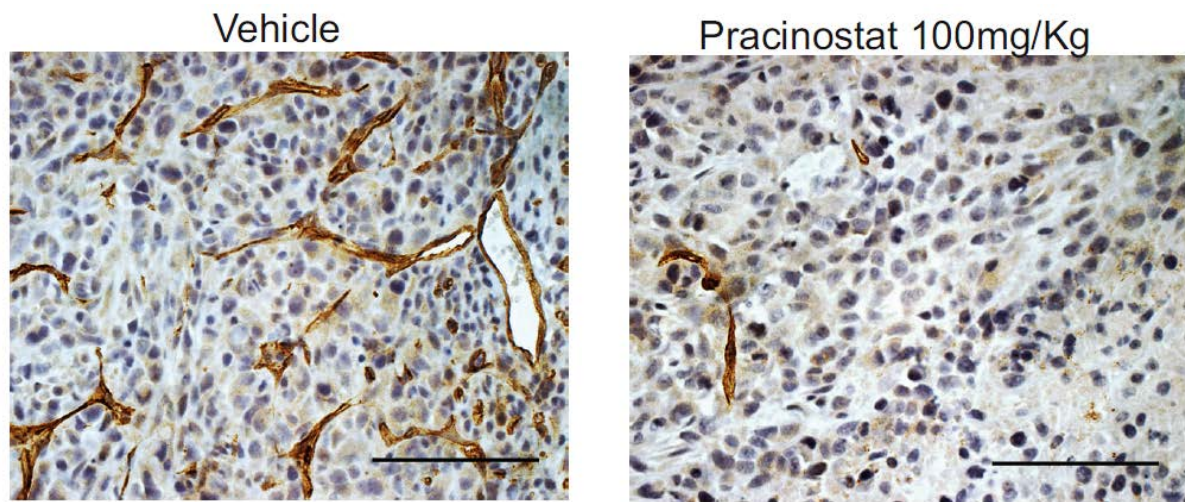


**(ii)**
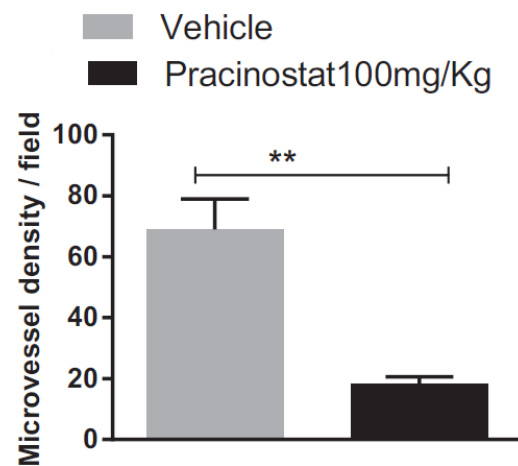


**Figure 4.6:** Representative images of immunohistochemistry analysis of endothelial cell marker CD31 on vehicle-treated and Pracinostat-treated mice tumor samples. (ii) Microvessel density was quantified by identifying neovascular 'hot spots' and unbiased scoring of the number of vessels stained for CD31 in representative sections of vehicle control and Pracinostat-treated mice (**P≤0.01). Quantification of data from n=8 mice per group, error bars ± SEM.

**(i)**



Overlay                         CD31                        SMA
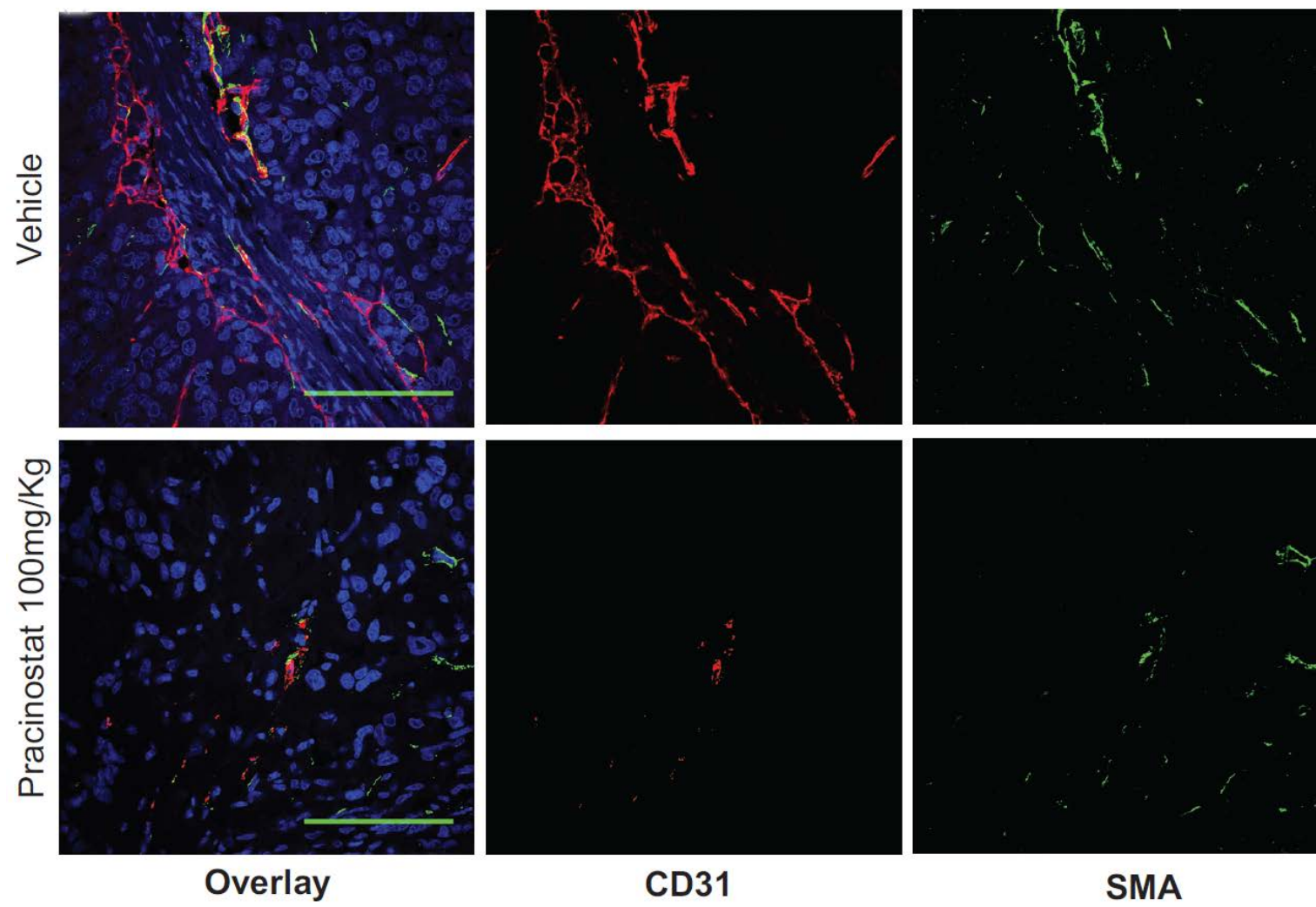
**(ii)**
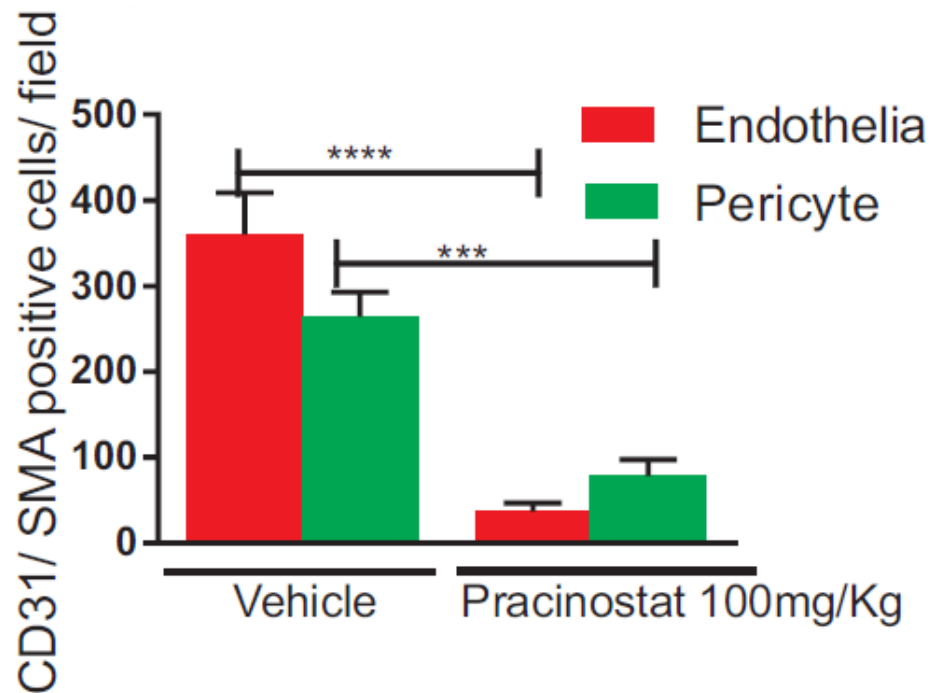


**Figure 4.7:** (i) Dual immunofluorescence detection of CD31 (red) and α-SMA (green) in vehicle- and Pracinostat-treated mouse xenograft samples for vascular integrity. (ii) Quantification of CD31 and SMA scoring was determined as described in Materials and Methods (***P≤0.001; ****P≤0.0001).

The expression of VEGF-A, a potent angiogenic agent that stimulates the full cascade of events required for angiogenesis, was also analysed [178]. *In vitro* Pracinostat treatment for 24 hours significantly reduced the expression of VEGF-A expression in all three cell lines tested (Figure 4.8(ii)). Histology analysis of xenograft tumor samples demonstrated areas with abundant expression of VEGF-A in controls, which was undetectable in Pracinostat-treated samples (Figure 4.8(i)).

**(i)**
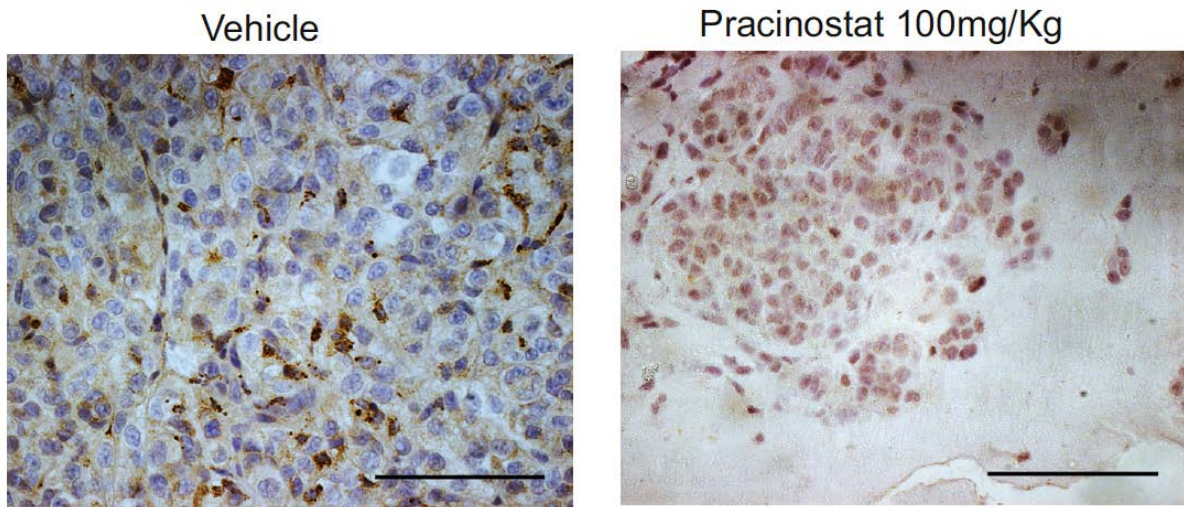


**(ii)**
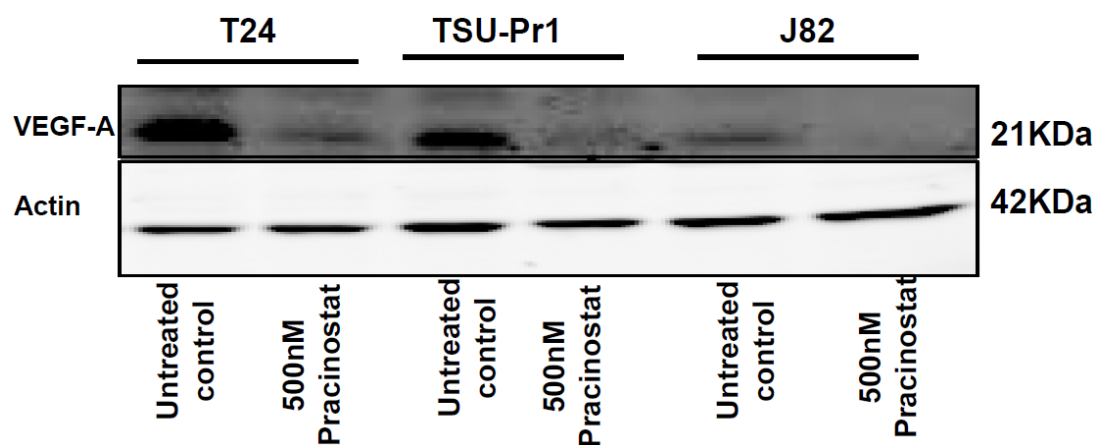


**Figure 4.8:** **Pracinostat treatment inhibits the production of proangiogenic factor VEGF-A *in vivo* and *in vitro*.** Representative images of immunohistochemistry sections of VEGF-A staining in vehicle- and Pracinostat-treated mice. Image magnification x40, scale bar 100 µM. Western blot analysis showing that the treatment with 500 nM Pracinostat for 24 hours completely inhibited the production of proangiogenic factor VEGF-A in three different bladder cancer cell lines.

## 4.4 Discussion

In this chapter I demonstrated that consistent with the observation made *in vitro,* the oral administration of HDACi Pracinostat treatment restores the expression of ATF3 in mouse xenograft samples with a subsequent tumor regression after 20 days of treatment. Histology data from *in vivo* mouse model also reaffirmed the re-expression of ATF3 in the responding core of the tumor from early- to late-stage therapy. The *in vivo* data clearly displayed re-expression of ATF3 in xenograft samples in the responding core of the tumor is inversely correlated with expression of Ki67- proliferation marker, cells away from the treatment responding core. From these observations, my study clearly demonstrates that restoration of ATF3 during Pracinostat treatment is essential for predicting treatment outcome. Moreover, these results are the first observations of the reactivation of ATF3 in real time with HDACi treatment in non-proliferating cells in the responding core of the tumor.

Parallel to this reactivation of ATF3, Pracinostat treatment triggers a cascade of events including anti-angiogenesis and apoptosis (Figure 4.5, 4.6, and 4.7). Angiogenesis describe the formation of new blood vessels from the existing vasculature, and this is the fundamental physiological process in tissue repair, wound healing and in development [179]. In xenotransplantation, new blood vessels formation in tumor cells can occur by sprouting from pre-exciting vasculature from host with the aid of fibroblasts, macrophages and endothelial cell progenitor cells. The malignant cells secrete pro-angiogenic factors including VEGF to induce the new vasculature formation, and subsequent growth and survival of tumor.

Previous studies have identified the anti-angiogenic properties of other HDACi, including trichostatin A, SAHA and valproic acid [180] [181] [182]. The *in vitro* data we present in cancer cell lines and *in vivo* results in mouse xenograft samples show that the pro-angiogenic factor VEGF-A (one of the essential factors shown to facilitate angiogenesis) secreted by

tumor cells is inhibited by Pracinostat treatment (Figure 4.8). Furthermore, staining for blood vessels and pericytes was also significantly reduced with Pracinostat treatment *in vivo*, compared to controls. Perivascular smooth muscle cells are essential for vascular integrity, by providing physiological and mechanical support for blood vessels [183]. Untreated bladder xenografts showed a significantly higher number of blood vessels and pericytes than Pracinostat-treated tumor samples (Figure 4.7). A combination of blood vessels with and without a lining of pericytes suggests the presence of an actively growing tumor aided by a reactive stroma in control xenografts. Interestingly, we observed that Pracinostat treatment induced damage to the structure of blood vessels, with a slight increase in the number of pericytes, which may have formed to support the endothelial lining before the start of treatment. Although we clearly demonstrate inhibition of angiogenesis associated with Pracinostat treatment, this anti-angiogenesis effect could be a consequence of ATF3 reactivation or independent of ATF3 – mediated by Pracinostat.

In this chapter, I have demonstrated the efficacy of Pracinostat as a single agent for treating subcutaneous bladder xenograft tumors. Oral administration of Pracinostat resulted in 98% reduction in tumor volume compared to the control with greater tolerability, and this was comparable to the observation made in colorectal cancers [108]. Similar to *in vitro* observation, Pracinostat treatment resulted in nuclear re-expression of ATF3 in the treatment responding core of the xenograft tumors, which subsequently resulted in anti-angiogenesis and apoptosis. My observations in pre-clinical xenografts models provide a striking rationale for clinical trials with Pracinostat in bladder cancer.

# CHAPTER -5

*Reactivation of ATF3 is integral to the Pracinostat mediated tumor response in vivo and in vitro*

## 5.1.　　　Introduction

Activating Transcription Factor 3 (ATF 3) has diverse roles in normal biological and cellular functions. In cancer scenarios, depending on the context and degree of malignancy, ATF3 plays as an oncogenic activator or suppressor in different cancers as previously described. In bladder cancer, previous studies from our laboratory have shown that expression of ATF3 is inversely associated with cancer progression and loss of ATF3 expression is correlated with a reduced survival rate in patients with high-grade and metastatic tumors [139]. Further, my study thus far established that treatment with the pan-HDACi Pracinostat re-establishes a normal acetylation pattern and thus reactivates the expression of ATF3 in bladder cancer *in vitro* and *in vivo* and alters the malignant phenotypes.

In this chapter I explored whether re-expression of ATF3 is central to determining tumor response in HDACi-mediated anti-cancer therapy. To that extent, my first aim was to generate stable ATF3 knockdown cells and compare the behaviour of these cells with the control cells in the presence of Pracinostat. This chapter will describe the observations from a number of *in vitro* functional assays to demonstrate the pivotal role of ATF3 in restoring the anti-malignant behaviour of bladder cancer cells. Further, I went on to show the *in vivo* anti-tumor efficacy in the stable knockdown versus control cells in a xenograft models with the oral administration of Pracinostat. Together, the results from *in vitro* and *in vivo* data strongly suggests that re-expression of ATF3 by Pracinostat treatment has a decisive role in determining the tumor response in Pracinostat mediated anti-cancer therapy. Finally, my study has identified a possible down-stream target of ATF3, the *Retinoblastoma* protein (RB1), a key tumor suppressor. Regulation of the expression of RB1 provides a potential mechanism by which ATF3 may induce non-malignant behaviour in bladder cancer cells.

## 5.2. Results

To investigate whether re-expression of ATF3 is central to determining tumor response in HDACi-mediated anti-cancer therapy, the first step was generating stable knockdown TSU-Pr1 cell lines (with low basal level expression of ATF3) by transfecting these cells with short hairpin RNA (shRNA) targeting human ATF3 or a non-targeting control sequence to generate a control cell line (Figure 5.1). The stable cells from both the ATF3 depleted (~40%) shATF3 and the non-targeted shcontrol cells were pooled and selected using 2ug/ml puromycin.
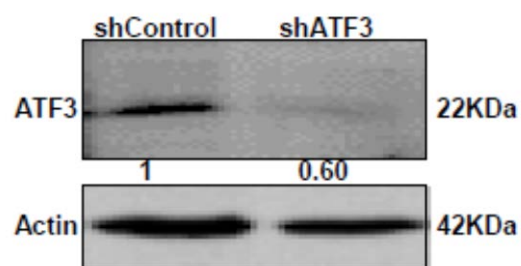
**Figure 5.1:** Immunoblot analysis of stable cell lysates from TSU-Pr1 knockdown cells confirming the short hairpin RNA sequences targeting ATF3 knocked down the expression of ATF3 compared to the non-targeting control. Actin was used as the loading control. Data shown is representative of three independent experiments.

### 5.2.1. ATF3 expression defines the sensitivity to Pracinostat treatment *in vitro* and *in vivo*

To understand the significance of the treatment with Pracinostat in the presence and absence of ATF3, I performed *in vitro* functional assays including viability, colony formation and wound healing assay on the stable cell lines (Figure 5.2, 5.3, 5.4 and Appendix 4, 5, 6). To compare the viability of ATF3-depleted cells and control cells in the presence of Pracinostat, the cells were cultured in varying concentrations of Pracinostat (50, 100, 200 and 500 nM) for a period of 6 days and analyzed. Although Pracinostat treatment had an anti-proliferative effect on both lines, the proliferation rate of ATF3-depleted cells was significantly higher than control cells over time (Figure 5.2(i)) and Appendix 4), particularly at lower concentrations of the drug (50, 100 and 200 nM). Pracinostat-treated (100 nM) ATF3 knockdown cells exhibited a significantly higher proliferation rate from day 4 compared to the shcontrol cells ($P<0.004$ for Day 4, $P<0.0001$ for Days 5 and 6). Protein lysates were analyzed by Western blot to monitor the reactivation of ATF3 in these cells over 6 days with Pracinostat (100nM) treatment and clearly showed less reactivation of ATF3 in the knockdown cells compared to the control (Figure 5.2(ii)). Next, the difference in colony forming capacity of the stable knockdown (shATF3) vs control (shCtrl) cells was compared. Accordingly, cells pre-treated with 200nM Pracinostat for three days and matching untreated cells were seeded at low density to form colonies and incubated for 18 days. The treatment with 200nM Pracinostat for three days had a significant impact on the shcontrol cells, where the number of colonies was strikingly reduced ($P< 0.001$), whilst the stable ATF3 knockdown cells treated with Pracinostat had no significant reduction in colony number ($P = 0.1031$) (Figure 5.3 and Appendix 5). Two-dimensional cell migration and cell–cell interaction was

also analyzed by measuring wound closure in control and knockdown cells (Figure 5.4 and Appendix 6). The rate of wound closure was faster in untreated and Pracinostat-treated knockdown cells compared to the control cells. The cells in which ATF3 expression was silenced underwent wound closure at a much earlier time point (12 hours), compared to control cells in the presence of Pracinostat. In control cells, 50% of the wound remained open at the time it was closed in knockdown cells (P<0.001). Together, the *in vitro* data strongly suggest that the cells in which the expression of ATF3 was silenced fail to respond to Pracinostat treatment.

**(i)**

**(ii)**
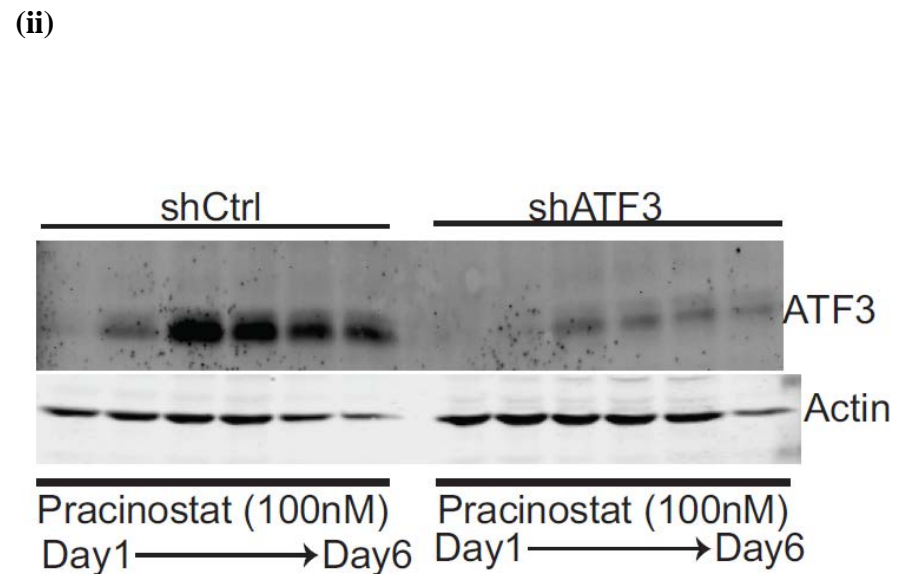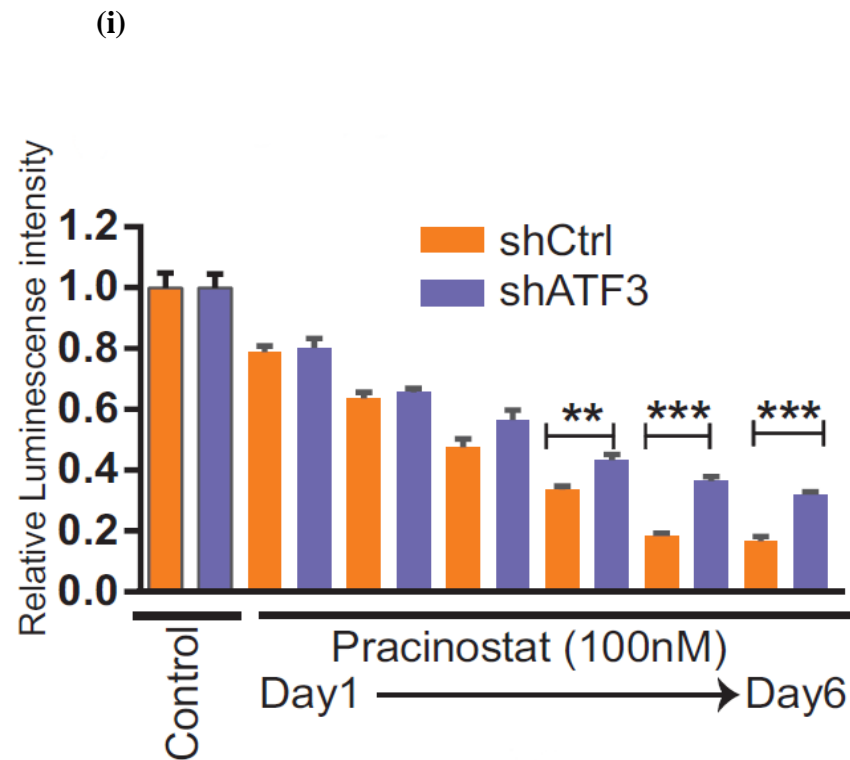
**Figure 5.2:** Assessment of viability by Vialight assay on stable control cells and ATF3-depleted cells treated with Pracinostat over a period of 6 days at a concentration of 100 nM. From day 4 the proliferation rate was significantly higher in knockdown cells compared to control cells (**$P \leq 0.01$, ***$P \leq 0.001$). (ii) Immunoblot analysis confirmed the re-activation of ATF3 in control cells compared to knockdown cells over 6 days in treatment with Pracinostat. Actin was used as the loading control; Data shown is the representative two replicative experiments.
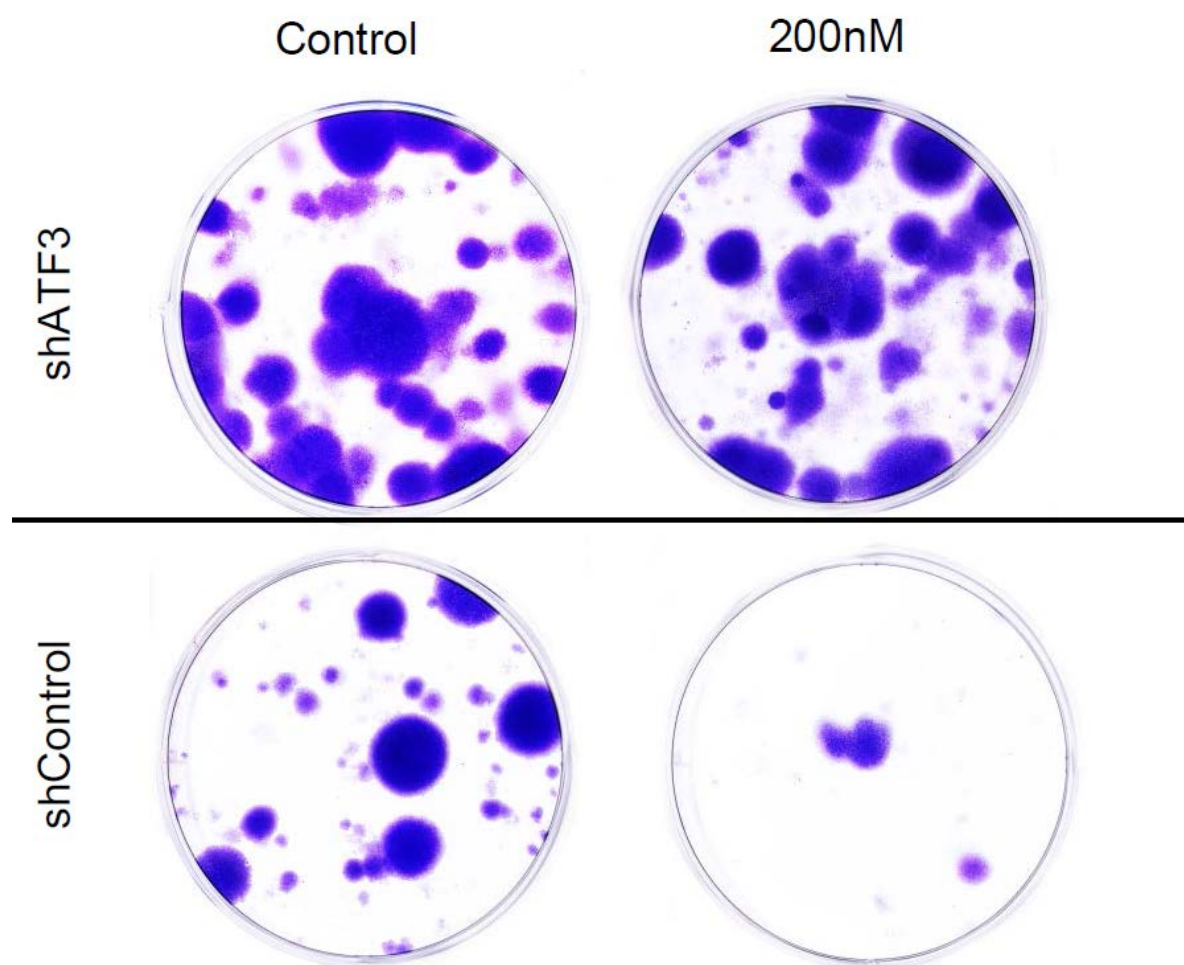
**Figure 5.3:** Representative images of colony formation assay on shATF3 and shcontrol cells treated with Pracinostat compared to their matched untreated controls (n=2). Upper panel, colonies formed in the untreated and Pracinostat treated ATF3 depleted cells (shATF3) showing Pracinostat treatment has no effect in the absence of ATF3. Lower panel, Shcontrol cells, upon treatment with Pracinostat has significant reduction in the number of colonies.
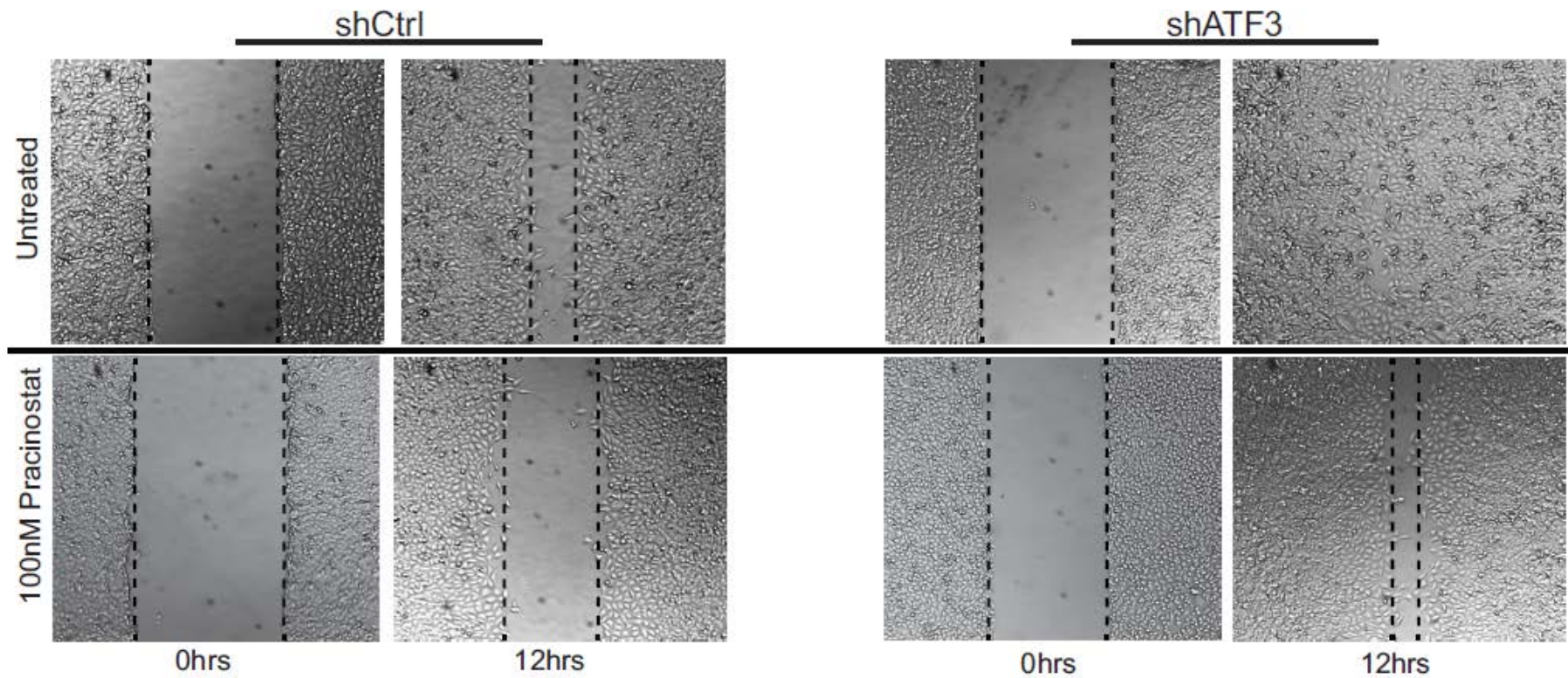
**Figure 5.4:** Representative pictures of scratch wound assay on cells – stable control and ATF3 knockdown cells treated with 100nM Pracinostat or untreated. Scratches were made on the confluent cells and wound closure was monitored over 16 hours (n = 3).

To extend our findings, we explored the functional significance of the loss of ATF3 expression with Pracinostat treatment *in vivo*. Control cells and ATF3 knockdown cells were injected into the flank of the nude mice and Pracinostat administrated orally daily for up to 30 days at 50 mg/kg, a dose that did not result in body weight loss (Figure 5.5(i)). In Pracinostat treatment groups, the tumor volumes of ATF3-depleted xenografts were significantly larger than in the shcontrol group (<400 mm$^3$ at the end of the experiment; P<0.0001) and reached the endpoint volume (≥800 mm$^3$) earlier, at 25 days after treatment (Figure 5.5(ii)). The tumor volume data showed that Pracinostat treatment delayed the rate of tumor growth in mice with ATF3-depleted xenografts compared to matching vehicle controls (although this was not significant; P=0.6470). In the shcontrol xenografts, tumor volumes were significantly different between Pracinostat-treated mice with the vehicle control (P<0.0001). Importantly, the overall tumor growth rates in ATF3-depleted xenografts were higher than in the shcontrol xenografts. The association between ATF3 expression and survival rate was also evaluated in the Pracinostat-treated groups (Figure 5.6). Pracinostat treatment induced ATF3 expression in control xenografts, which responded well to treatment with 100% of mice in this group surviving to the end of the experiment, whereas the median survival in the ATF3-depleted group was 22.5 days. Kaplan-Meier survival analysis showed a significant difference in the survival curves for these two groups (Figure 5.6: P<0.0001).

**(i)**
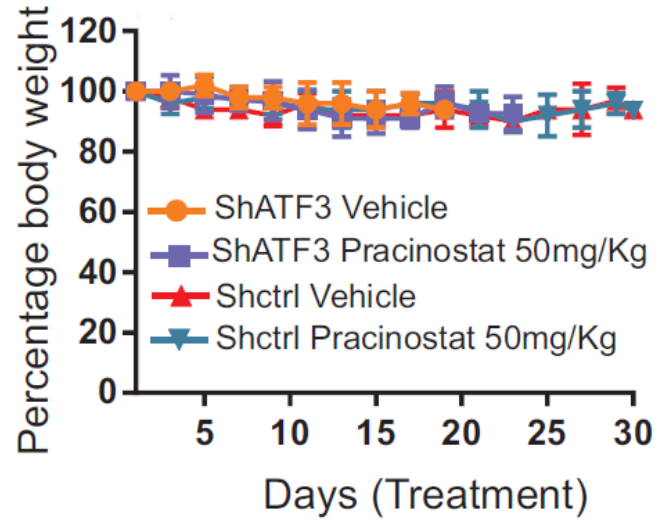
**(ii)**
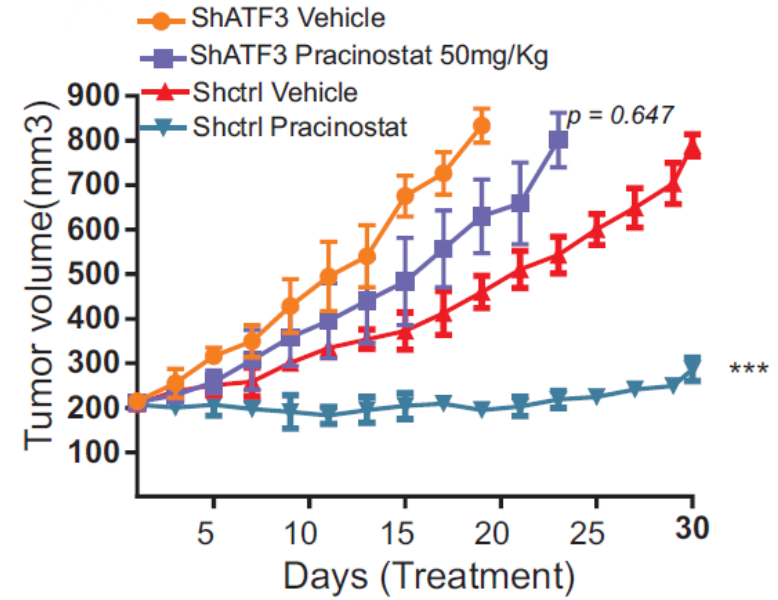
**Figure 5.5:** *In vivo* tumor growth and survival in mice with bladder xenografts with control cells and knockdown cells and treated with Pracinostat administrated orally daily up to 30 days at 50 mg/kg or vehicle control. (**i**) Percentage body weight, showing no significance difference in the weights between treatment and control groups. (**ii**) Tumor volume was significantly smaller in Pracinostat-treated shcontrol cells (shCtrl) (***P≤0.001) compared to the non-treated shCtrl. Though there was a delay in tumor progression in shATF3 xenografts treated

with Pracinostat, the change was insignificant (P=0.6470) compared to the untreated control (ShATF3) mice. Data points represent the mean tumor volume for each group (n=8 mice/group; error bars $\pm$ SD).
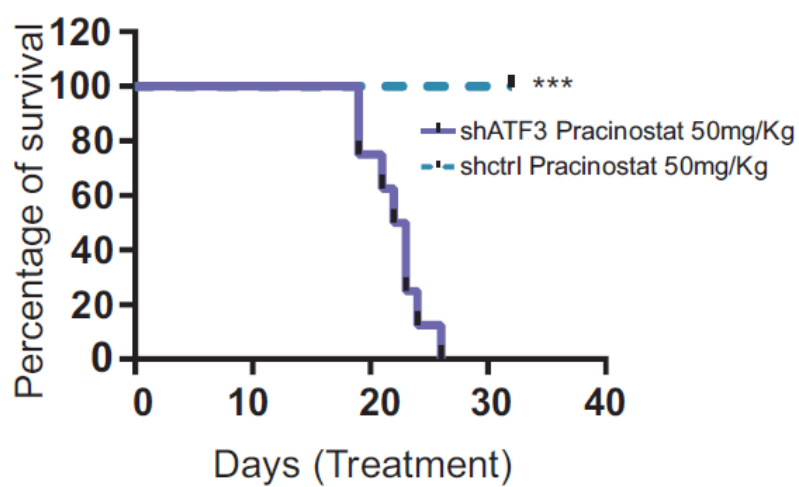
**Figure 5.6:** Kaplan-Meier survival curves showing a significance difference in the survival between the shcontrol and shATF3 treated with Pracinostat (\*\*\*P ≤ 0.001; n= 8 mice per group).

The activity of Pracinostat in delaying the rate of tumor growth in the treatment group was further examined by assessing the acetylation pattern of H3 in the xenograft samples. Immunohistochemistry analysis of ATF3 knockdown xenograft samples demonstrated increased expression of acetylated H3 in Pracinostat-treated samples compared to matching vehicle control samples (Figure 5.7(i). We then tested whether the increased acetylation pattern was reflected in the proliferation status of Pracinostat-treated ATF3-depleted xenografts samples. However, immunohistochemistry analysis of proliferation marker Ki67 demonstrated that the number of cells in actively proliferating status is similar in vehicle control and the Pracinostat-treated ATF3-depleted group (Figure 5.7(ii)). As expected the expression of Ki67 is far less in Shcontrol xenografts treated orally daily up to 30 days with 50 mg/ Kg Pracinostat.

shATF3     shcontrol

(i) Vehicle     Pracinostat 50mg/Kg     Pracinostat 50mg/Kg

Acetyl H3

(ii)

Ki67
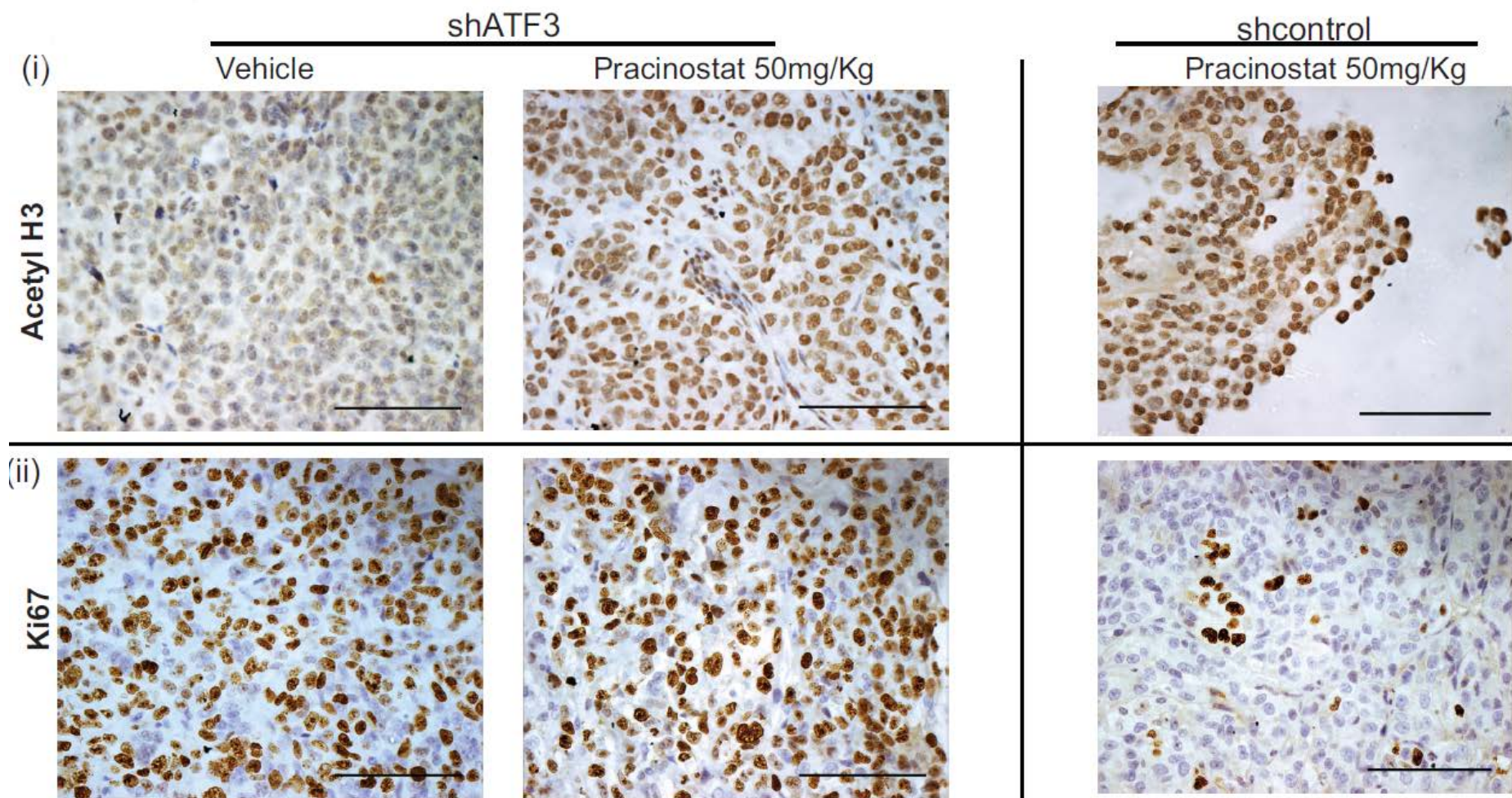
**Figure 5.7:** Representative images of immunohistochemistry analysis of xenografts samples of shATF3 (+/ - 50mg/ Kg Pracinostat orally daily for up to 30 days) and shcontrol (treated with 50mg/Kg Pracinostat orally daily for up to 30 days) for acetyl-histone 3 (i) and Ki67 (ii). Image magnification x40, scale bar 100 µM (n = 8 mice per group).

### 5.2.2.    ATF3 regulates the expression of tumor suppressor gene Retinoblastoma (RB1)

Retinoblastoma (RB1) is the first tumor suppressor gene was identified by the studies of retinoblastoma- a rare childhood cancer [184]. Inactivation of RB1 is implicated in many cancers beyond retinoblastoma including lung, bladder and breast to name a few [185]. RB1 gene is a principal cell growth and tumor suppressor in bladder cancer and is lost or inactivated as the tumor progress into advanced stages [146, 186]. Mutations in RB1 gene have also been identified in low and high grade urothelial cell carcinomas [187].

Uncontrolled cell proliferation is a key feature of malignancy, and RB protein is solely responsible in regulating the cell cycle machinery through the restriction point within the G1 phase of the cell cycle [188]. RB inactivation and subsequent cell cycle progression is initiated when RB is phosphorylated by cyclin D and cyclin-depended kinases 4 or 6 which results in inhibiting RB binding with its target E2F transcription factors and ultimately in uncontrolled proliferation[189, 190]. Recruitment of class 1 HDACs to RB1 promoter is also implicated in epigenetic silencing of RB and failure in regulating the cell cycle [191].

As described in chapter 3, my study clearly demonstrated that the treatment with Pracinostat restored the expression of ATF3, and subsequently resulted in induction of cell cycle arrest and re-expression of hypo-phosphorylated (active) RB1 *in vitro.*  Further, as described in chapter 4, *in vivo* xenograft results confirmed that the re-activation of ATF3 is only in non-proliferating, treatment responding cells in the tumor core, during the oral administration of Pracinostat. All these data collectively indicating that ATF3 may be a key regulator of a downstream target gene which has a central role in regulating cell proliferation and subsequently in tumor suppression. Therefore, I next sought to explore the regulatory effect of ATF3 on RB1 expression in bladder cancer cells.

To investigate the role of ATF3 in regulating the transcription of RB1, I decided to analyse the promoter region of the RB1 gene to identify any possible ATF DNA binding sites. This led to the identification of an ATF binding site, TGACGTT, ⁻186 - ⁻192 relative to the transcription initiation site in the promoter region of RB1 (Figure 5.8(iii). Further, I performed transient over-expression of ATF3 in J82 cell lines (Grade -3 bladder cancer cells that have lost RB1 expression) using an ATF3-pcDNA expression or control vector. The immunoblot analysis showed that over-expression of ATF3 is sufficient to restore the expression of the RB1 protein in these cell lines (Figure 5.8 (i)). To further examine the potential functional activity of this ATF binding site on RB1 promoter, I performed a cell cycle analysis on ATF3 over expressing bladder cancer cells J82 cells. Cell cycle pattern of ATF3 over-expressing J82 cells showed a reduction in the percentage (~7%) of cells in the synthetic phase of the cell cycle compared to pcDNA control cells (Figure 5.8 (ii)) indicating the prospect of a functionally active ATF binding site on the RB1 promoter.

**(i)**



| | | |
|---|---|---|
| RB1 | | 106kDa |
| ATF3 | | 22kDa |
| α-tubulin | | 55kDa |

pcDNA     ATF3-pcDNA

**(ii)**



G1/G0 - 37.3%
S - 13.5%
G2/M - 32.9%

G1/G0 - 43.4%
S - 5.88%
G2/M - 38.28%

**(ii)**



RB1 Promoter

RB1 Gene

5'  ATF  3'

-192  -TGACGTT-  -186

110
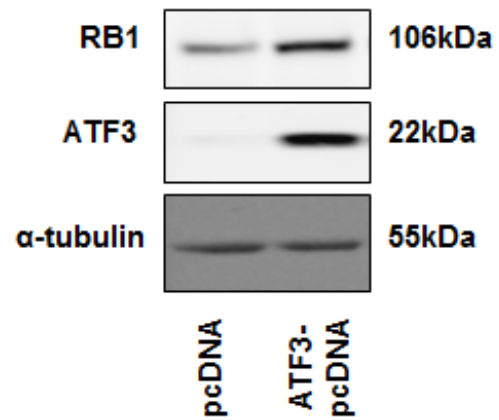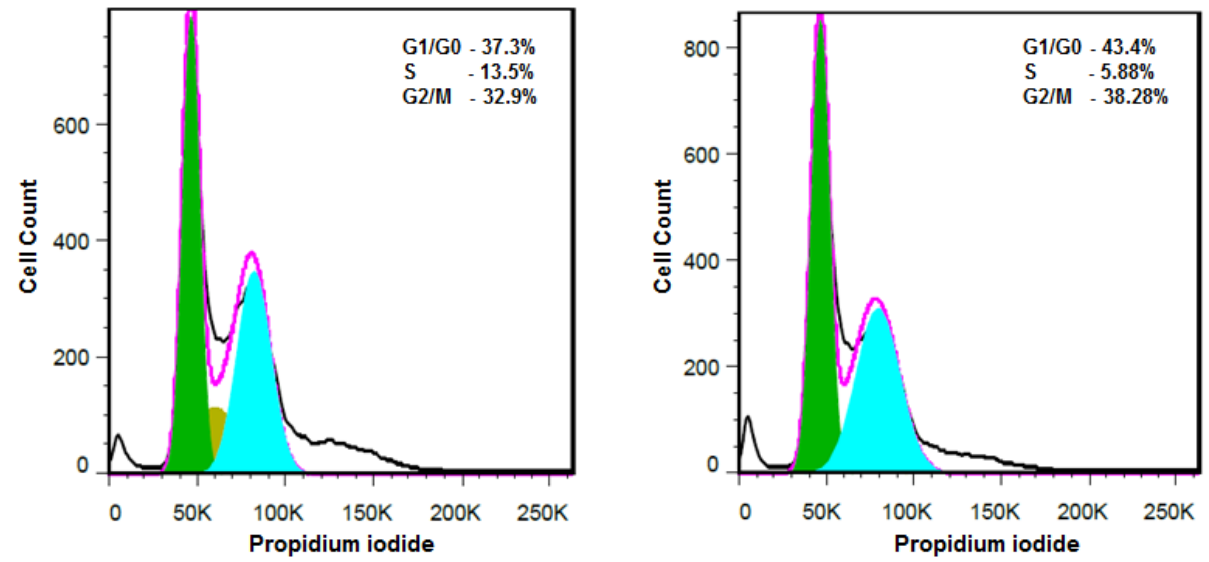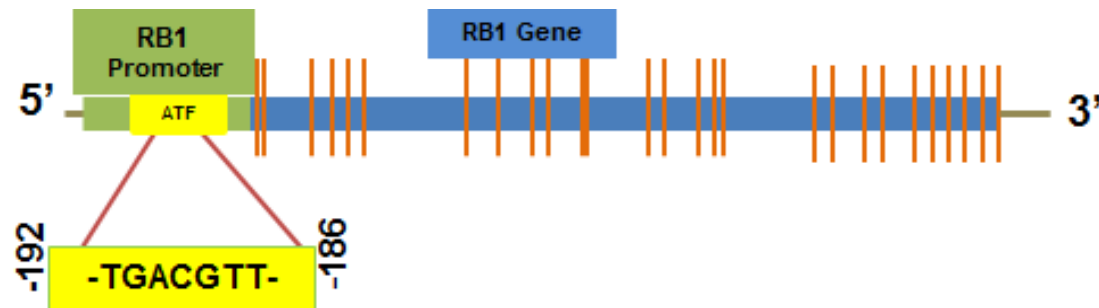
**Figure 5.8: ATF3 regulates the transcriptional activation of RB1.** (i) Western blot analysis J82 cell lines over-expressing ATF3 displayed an increase in expression of RB1 in those cells. α-tubulin serves as a loading control for both the control cells and over-expressing cells (n=3) (ii) Expression of ATF3 accelerates cell cycle arrest in ATF3 over-expressing J82 cancer cells compared to the control cells**.** Representative images of cell cycle analysis by flow cytometry in J82-ATF3 cells compared to the control and the percentage of cells in S phase were reduced compared to the control cells (n=2). (iii) ATF3 DNA binding site is associated with RB regulatory elements- diagram showing that the RB promoter region containing an ATF binding site, 186 bases from transcription start site.

## 5.3. Discussion

Here I demonstrated that the reactivation of ATF3 is critical in determining the tumor response to Pracinostat by employing a series of *in vitro* functional assays and an *in vivo* tumor model comparing cells expressing ATF3 to controls upon treatment with Pracinostat. It is important to note that the knockdown of ATF3 protein expression in stable knockdown cells was ~40% compared to that of the control from repetitive experiments and so determining the correct dosage of Pracinostat is highly crucial for all the functional assays *in vitro* and in the *in vivo* treatment regime to demonstrate a difference. In the cell viability assay, 100nM Pracinostat treatment has an anti-proliferative effect both on shATF3 cells and on shcontrol cells, however, as the days progress, the proliferation rate of shATF3 cells was significantly higher compared to the control (Figure 5.2(i)). The reactivation of ATF3 Pracinostat treatment of the shcontrol cells compared to the shATF3 cells was demonstrated in parallel with protein blotting (Figure 5.2(ii)). Similarly, in the *in vivo* tumor models, the oral administration of 50mg/Kg daily reduced the tumor volume in shATF3 xenograft compared to the untreated shATF3 xenografts, but this was not significant (Figure 5.5(ii)). Increased acetylation of the H3 marker in the nucleus of Pracinostat treated shATF3 mouse xenograft tumor samples clearly indicates Pracinostat is effectively re-establishing the acetylation pattern in tumor samples. But the effect of Pracinostat in re-establishing the acetylation pattern and chromatin re-structuring is not sufficient to stop the tumor growth in absence of ATF3 re-expression. The expression of proliferative marker Ki67 in these xenografts clearly demonstrated that there is no significance difference in actively dividing cells between these two groups (Figure 5.7).

Reactivation of ATF3 upon treatment with Pracinostat is providing a significant survival advantage in xenografts with shcontrol cells. Kaplan-Meier survival curve confirms that 50%

of the shATF3 xenograft bearing mice reached the endpoint in 22 days and the remaining 50% succumbed after 30 days of Pracinostat treatment (Figure 5.6).In contrast, all the shcontrol xenograft bearing mice treated with 50mg/Kg Pracinostat survived till the end of the experiment clearly demonstrating that, re-expression of AFT3 is a key defining factor of survival when treating advanced bladder cancers with Pracinostat. Accordingly, I conclude from the data presented that the transcription factor ATF3 could be utilized as a potential marker of the response to HDACi-mediated therapy in advanced bladder cancer, where ATF3 expression is lost.

Previous reports [118] have identified a direct association of ATF3 with HDAC1 in regulating acetylation patterns and chromatin structures in innate immune systems. In inflammation associated with acute kidney injury it has been shown that the epigenetic modulation regulated by ATF3 has a potential to protect against chronic inflammation [192]. During inflammation, ATF3 recruits HDAC1 to the ATF/NF-kB sites in the IL-6 and IL-12 gene promoters resulting in euchromatin and inhibition of inflammatory genes. Earlier studies in colorectal cancer using HDACi as cytotoxic agents showed that ATF3 contributes to enhancing the synergistic effect of HDACi, in combination with cisplatin [193]. Although there is earlier evidence of epigenetic modification and HDAC association of ATF3 in cancer and inflammation models, mine is the first study depicting a crucial role in cancer for ATF3 re-expression using HDACi in bladder cancer as a model to determine the treatment response or outcome in HDACi mediated cancer therapy.

It is possible that some key target molecules are involved through which ATF3 is regulating the phenotypic changes observed in this study *in vivo* and *in vitro* after re-expression by Pracinostat in these models. My study clearly demonstrated that the treatment with Pracinostat and re-storation of ATF3 subsequently resulted in cell-cycle arrest, induction of

one of the major tumor suppressor genes implicated in advanced bladder cancer, RB1 *in vitro*. More importantly, *in vivo* xenografts exhibited reactivation of ATF3 occurs mainly in the tumor responding core, away from actively proliferating cells. A previous study identified that naturally occurring point mutations in the RB1 promoter region that bind RBF-1, SP1, and ATF results in decreased expression of the RB1 gene and suggested that this may result in developing retinoblastoma [194]. Another publication demonstrated that over-expression of Rb stimulates Rb promoter activity through the ATF binding site, that the carboxyl-terminal domain of Rb is responsible for the RB1 auto-induction through ATF2 (one of the CREB family transcription factor), and that loss of this regulation may contribute to retinoblastoma [195]. These two studies suggest the significance of the ATF binding site in the promoter region in regulating the expression of RB1 with the second study identifying ATF2 (one of the ATFs) as having a main role in this regulation. As described previously, ATF3 has been shown to be a tumor suppressor in previous studies in cancers such as colon and oesophageal squamous cell carcinomas and this suppression activity was identified as promoted through regulating the expression of p53 [138, 196, 197]. My results demonstrated that the expression and functionality of tumor suppressor RB1 is also regulated by ATF3 and this is the first study identifying RB1 as a putative target of ATF3 in cancer models and therefore provides possible mechanism for ATF3 mediated restoration of non-malignant phenotype both *in vivo* and *in vitro*.

# CHAPTER - 6

*Analysis of ATF3-dependent gene expression in Pracinostat treated bladder cancer cells*

## 6.1.    Introduction

My study thus far demonstrated that epigenetically silenced ATF3 expression in advanced bladder cancers can be restored by treating with the HDACi inhibitor Pracinostat. Pracinostat treatment resulted in re-establishment of the heterochromatin structure in the cancer cells, which ultimately may have reactivated the expression of ATF3. The reactivation of ATF3 was evident both *in vivo* and *in vitro* bladder tumor models which consequently resulted in a number of significant functional and phenotypic changes in tumor models. In *in vitro*, the Pracinostat treatment and reactivation of ATF3 resulted in reduced viability, migration, clonogenecity, increased sensitivity to platinum, and induction of cell cycle arrest. In *in vivo* xenografts, oral administration of Pracinostat restored ATF3 expression in treatment responding core of the tumor concomitant reduction of angiogenesis and induction of apoptosis. As described in chapter 5, I now established the fact that re-expression of ATF3 is crucial in regulating this phenotypic changes and ultimately determining the treatment response to Pracinostat mediated anti-cancer therapy. Orchestrating these phenotypic changes associated with ATF3 may involve several other molecules, in some cases the direct target of ATF3. Chapter 5 also described the identification a new ATF3 target, the Retinoblastoma (RB1) tumor suppressor gene, and described regulating the expression of RB1 by ATF3 likely induces cell cycle arrest in bladder cancer.

In order to identify other key translated proteins that will drive any ATF3 dependent phenotype, I sought to explore the translating transcriptome (translatomes) by adopting a novel technique - translating ribosome affinity purification (TRAP) of mRNA [198, 199]. The measurement of entire set of transcriptomes became very popular with the development of high-throughput RNA sequencing (RNA-seq) and global quantification with DNA

microarray analyses[200]. Although transcriptome analyses gives a good indication of changes in gene expression associated with disease and treatment, the level of mRNA do not necessarily correlate with the level of proteins they encode and thus the functional significance is ambiguous [201]. Thus the analysis of translatomes - mRNAs recruited to ribosome for protein synthesis, can be applied to associate the functional significance and regulatory effect of genes expression changes in the above situations. The method of TRAP was first described by Heiman et al, where they utilised the affinity purification of cell type specific polysomal mRNA from brain and is based on the theory that all mRNA translated to protein are at one point attached to the ribosomes or poly-ribosome complex and affinity tag fused to a ribosomal protein would allow isolation of bound mRNA [198].

Protein synthesis in a eukaryotic cell is mediated by ribosomes – a large ribonucleoprotein complex and a typical eukaryotic cell contain millions of ribosomes and a single ribosome add about two amino acids to a polypeptide chain in one second [202]. The ribosome is composed of 4 ribosomal RNA (rRNA) and 79 ribosomal proteins (RPs) are shared by two subunits named large (60S) and small (40S) to make the completely assembled 80S complex [203]. These subunits are assembled at the nucleolus by the association of newly transcribed and modified rRNA with ribosomal proteins. These subunits are then exported to the cytoplasm where it regulate the translation machinery [202].

The process of translation process involve three different steps; initiation, elongation and termination [204]. Translation is initiated by translation initiation factors (eIFs) recruiting mRNA to the 40S unit of the ribosome. This newly formed initiation complex then scan the mRNA from 5' to 3' for the initiation codon. At this stage larger subunit joins with the complex and lead to the formation of the complete 80S complex. During elongation, elongation factor (accessory proteins) and ribosomes travel along the coding region of mRNA

and synthesis polypeptide. During protein synthesis, multiple initiation occurs on each mRNA molecule being translated. The soonest the preceding ribosome has translated enough of the nucleotide sequence to move out of the way, 5' end of the mRNA threaded into a new ribosome. The mRNA molecule being translated are therefore are usually found in the form of polyribosomes (polysomes) (Figure 6.1). Final termination step is characterised by the release of budding polypeptide and dissociation of ribosomes from mRNA [204].
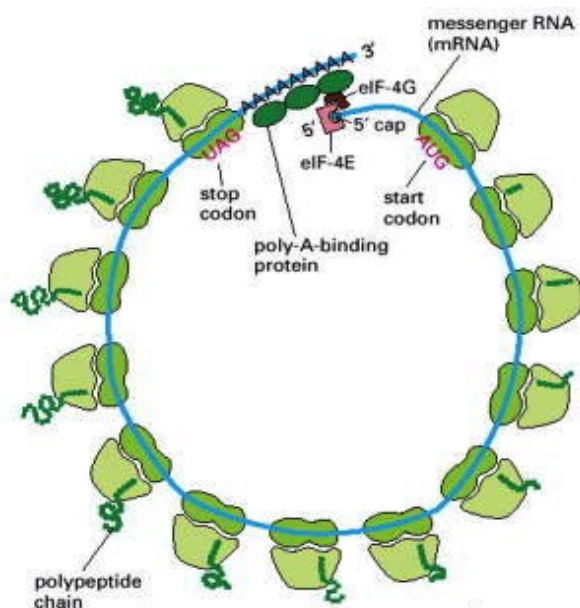


**Figure 6.1:** *A Polyribosome.* Schematic showing a eukaryotic polyribosome and multiple translation of an mRNA. (Adapted from Alberts, B et al, RNA to Protein -2002)

### 6.2.    Principle - TRAP Methodology

The TRAP methodology and RNA sequencing in mammalian cell system was pioneered by Heiman at al, where they used it to characterise the molecular expression of specific cells types from complex central nervous system by tagging polysomes in defined cell population of CNS system. The technique is based on the theory that all mRNAs translated into protein at one point are attached to ribosomes (polysomes) for the synthesis of polypeptides corresponding to the coding mRNA sequence, and an immuno-affinity tag fused to ribosomal

118

protein would allow the isolation of bound translating mRNA (Figure 6.2). For tagging the polysomes, GFP fused to the N-terminus of 60S (larger subunit) of the ribosomal protein. The tagged polyribosomes (polysomes) are captured by anti-GFP antibody coated with magnetic beads. mRNA bound to the tagged polysomes are isolated and subsequently analysed for target expression.
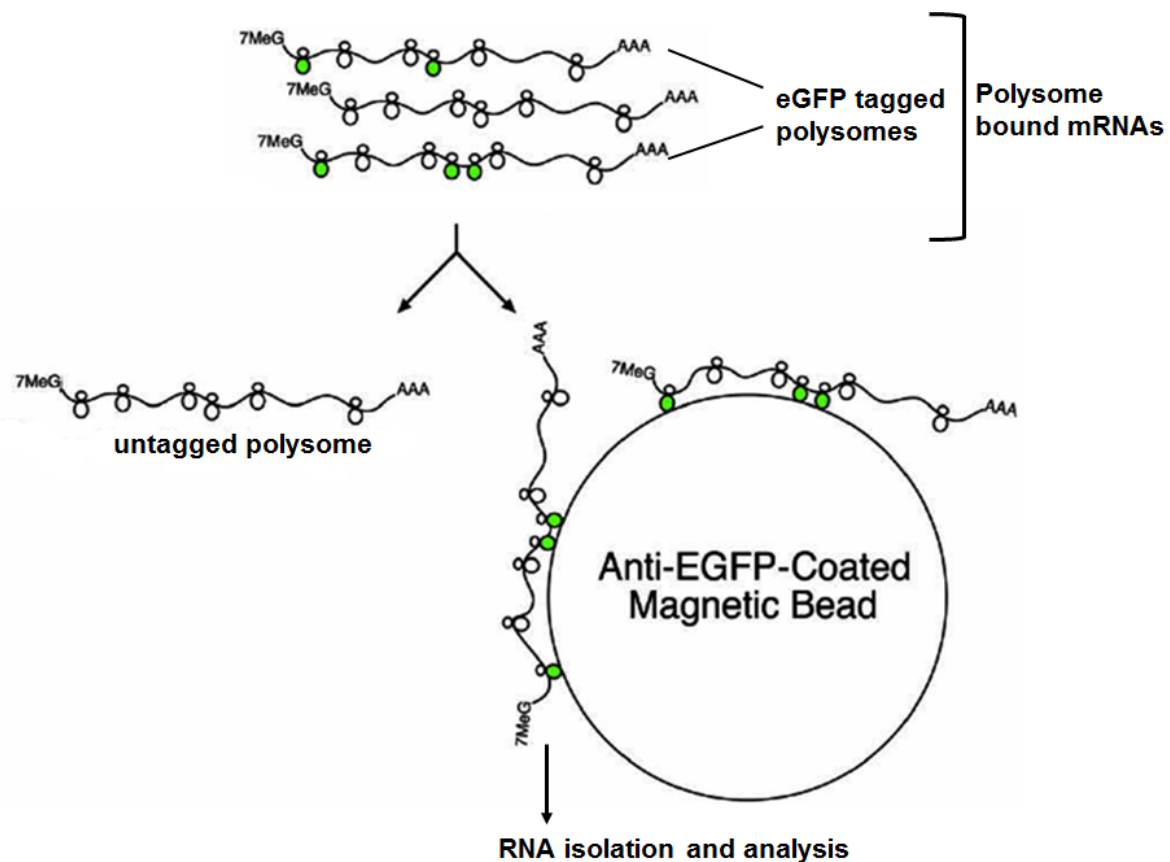


**Figure 6.2**: *Schematic of TRAP methodology*; Immuno-affinity purification of eGFP-tagged polysomes with anti-GFP beads coated antibody and subsequent isolation of mRNA (translatomes) and analysis. (Adapted and modified from *Heiman at al, Cell -2008*)

### 6.3. Materials and Methods

The methods of stable and transient expression in cell lines, Immunofluorescence, and qRT-PCR are detailed in the general method chapter.

#### 6.3.1. Construction of protein expression vector

Monomeric green fluorescent protein (mGFP) tagging 'N' terminus of Ribosomal Protein L-10 transcript variant-a (RPL-10a) was specifically generated for this project from Origene. Coding region of RPL10a was sub cloned into precision shuttle mammalian vector with N-terminal GFP. The vector inserts or contig is as described in Appendix 7.

#### 6.3.2. Affinity purification and isolation of polysomes bound mRNAs.

The TRAP method of RNA purification was performed as previously described [205], and it involves 3 major steps; lysate preparation, immuno-purification, and RNA clean-up. The cells were transfected with mGFP-RPL10 (tagging 60S ribosomes) or by the control vector (mGFP). The TRAP was performed direct conjugation method and as described below.

*Cell culture lysate preparation*

The cells expressing RPL10 or control were grown in monolayers at their confluency. After aspirating the culture medium, the plates were washed three time with ice-cold PBS. After the complete removal of PBS, the cold lysis buffer- supplemented homogenization buffer (HB-S) was added to the monolayer cells and incubated the plates on ice for 5 mins. Polysome stabilization and inhibition of RNAse activity is critical during lysis process. Polysome stabilization was achieved by adding cycloheximide (100µg/ml final concentration, Sigma, cat # C7698) and magnesium (12mM final concentration) in HB-S buffer and addition of recombinant RNasin (400u/µl final concentration, Promega, cat # N2115) minimise the

activity of RNAse. Cells were scraped using a pre-chilled cell scraper, and the lysates were transferred to a pre-cooled microcentrifuge tubes. The lysates spun down at 13000g for 15 mins at $4^0$C. The resulting supernatants were transferred to new microcentrifuge tubes and small aliquots (1% total volume) of each sample were saved as 'INPUT' to compare it with the sample after enrichment of transcript. The remaining lysates were processed for target enrichment.

*Immunopurification (IP)*

Direct conjugation method is used for IP, where the antibody pre-coated with magnetic beads was used for affinity purification. To each 350µl supernatant, 5µl of 1mg/ml mGFP antibody pre-coated with dynabeads (Origene, cat # TA183038) was added. The lysate-antibody-bead solution was incubated at $4^0$C for 12-15 hrs with gentle end-over-end mixing in a tube rotator. After incubation beads were collected on a magnetic rack at $4^0$C and the 'supernatant' was collected and stored at $-80^0$C for later analysis. The beads were resuspended thoroughly in high salt buffer and washed three times at $4^0$C for 10 mins per each wash and resuspension for reducing background.

*RNA isolation and clean-up*

The mRNAs bound to polysomes are now attached to the beads and RNeasy mini kit (Qiagen, Cat # 74104) or Trizol-LS reagent (Life technologies, cat # 10296-028) is used for the isolation of mRNA from the antibody-beads-RNA complex. Lysis buffer (buffer RLT) added immediately after the last wash and vortexed the lysate for 30 seconds to break the bond and to dissolve the RNA in to the lysis buffer. RNA purification was performed as per manufacture's instruction. The integrity of the purified RNA analysed using 2100

Bioanalyzer (Aligent, DE04103620) and the yield was measured by Qubit Flurometer (Thermo-fisher scientific) and is further confirmed by Bioanalyzer.

## 6.4. Results

### 6.4.1. Establishment of mRNA purification by translating ribosome affinity purification (TRAP) in HEK293T cells

In order to validate the plasmid vector expression system and also the method of TRAP, all preliminary experiments were conducted in HEK293T cells transiently transfected with the mGFP - RPL10 or mGFP control vector. The first step of the validation process was to check the expression pattern of these vectors in HEK293T cells. As described in the introduction, ribosomal subunits are assembled in the nucleolus to form complete ribosome complex and then exported to the cytoplasm as a single unit (80S) where it facilitates the translation process. Consistent with the previous report, GFP fluorescence for ribosomal protein fusion was detected both in the nucleolus and in the cytoplasm of the HEK293T cells (Figure 6.3). Next, immunoprecipitation using anti-GFP antibody and western blot analysis demonstrated that enrichment of target protein (fusion of mGFP-L10a) in the inbound (IP) fraction of the sample compared to the whole cell lysate (INPUT) fraction, suggesting that the immuno-precipitation process is efficient in HEK293T cells (Figure 6.4). Further, TRAP followed by total RNA purification was performed in transiently transfected cells and analysis of RNA samples were performed using a Bioanalyser (Figure 6.5). The RNA yield from cells transfected with the mGFP - RPL10 vector was 890pg/ µl, whilst the yield was 390pg/ µl for the same amount of starting material of the control (mGFP transfected cells) sample. This translates into >2 fold enrichment of the translated mRNA yield compared to the background yield. RNA integrity (RIN) value for these samples were >9 indicating that RNA is intact and are suitable for downstream application including genome wide microarray. From

bioanalyser electrophoresis, the size distribution also confirming the presence of intact mRNA in RPL10 with the matching ratio is 1.6 for 18S to 28S. Further the detection of smaller size bands (between 25 - 200nt) in the RPL10 samples and the corresponding peaks in the electropherogram suggesting the presence of small RNAs, mainly tRNAs associated with translational process in ribosomes, which are absent in IP-mGFP control samples. The above results confirming the process of TRAP methodology of isolation and purification of translating mRNA is satisfactorily performing in HEK293T cells, and increasing the starting material (the number of cells) will be the key in deciding the amount of TRAP isolated mRNA.
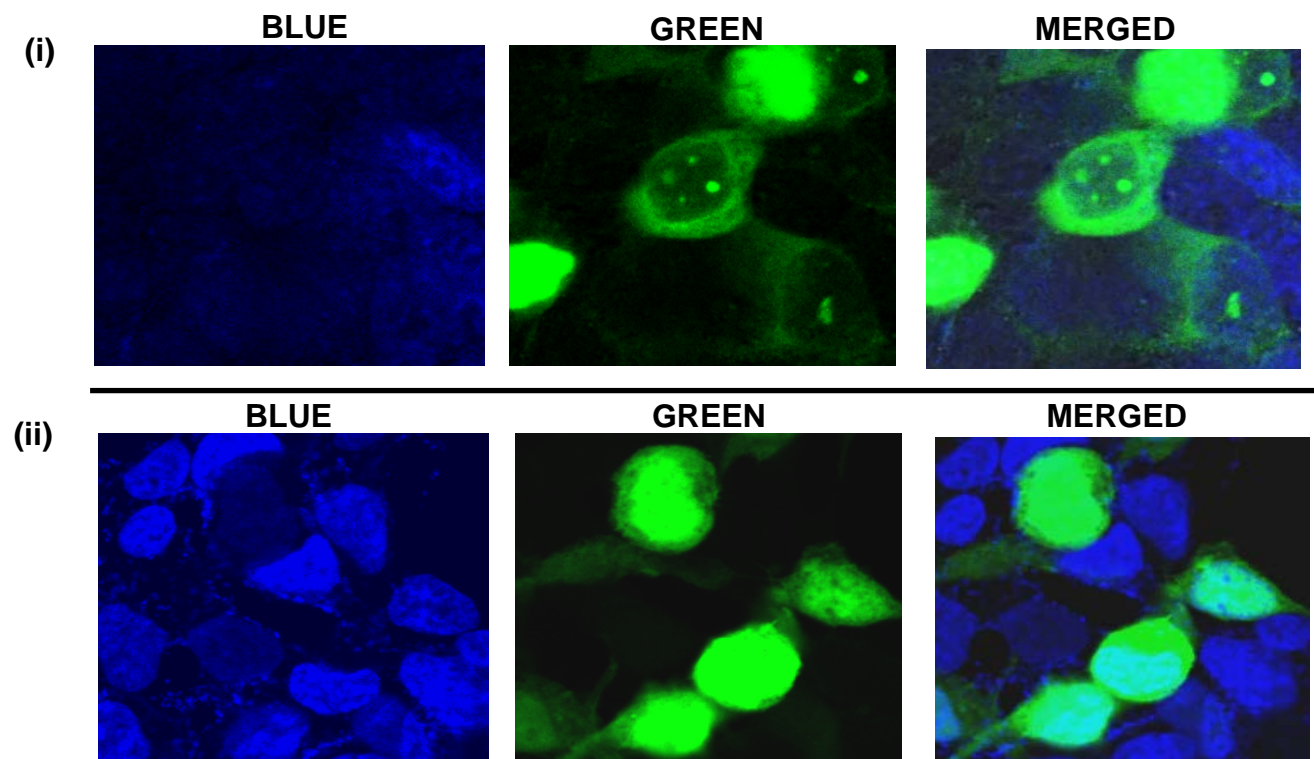
**Figure 6.3:** *mGFP-L10a or mGFP expression in HEK293T cells.* Representative images of HEK293T cells were grown monolayer on coverslip were transiently transfected with mGFP-L10 vector or mGFP vector control. Cells were grown for 48 hrs post-transfection, fixed with paraformaldehyde and mounted with DAPI to stain the DNA.( n=2) (i) Cells transfected with mGFP-L10a or (ii) mGFP both driven from CMV promoter.
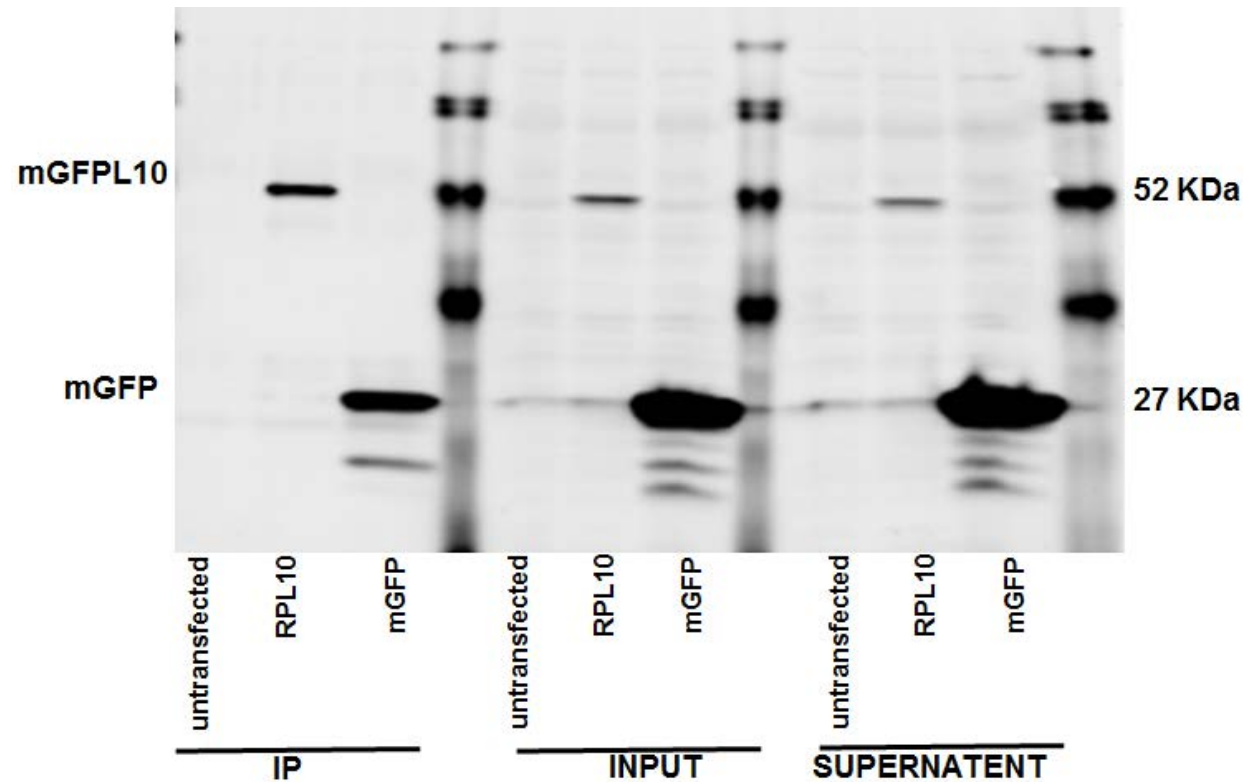
**Figure 6.4:** *Immunoprecipitation of mGFP tagged 60S ribosomal protein L10a in HEK293T cells.* HEK293T cells grown on 60mm culture dish were transiently transfected with mGFP-L10 vector tagging ribosomal protein or mGFP vector control. The immunoprecipitation was performed using magnetic beads coated anti-GFP antibody and analysed on western blot. Target protein mGFP-L10a was enriched IP fraction of

the sample compared to the whole lysate (INPUT). Fusion protein mGFP-L10a is 52KDa and control mGFP is 27KDa. Untransfected sample lysates served as an internal control (n= 3).

**A**

Lanes

1 - RPL10 IP

2 - mGFP IP

3 - RP10 INPUT

4 - mGFP INPUT

**B**

**(i)** 1-RPLIO IP

RIN: 9.40

RNA Concentration: 890 pg/µl

rRNA Ratio [28s / 18s]: 1.6

**(ii)** 2-MGFP IP

RIN: 9.30

RNA Concentration: 390 pg/µl

rRNA Ratio [28s / 18s]: 1.3

**(iii)** 3-RPLIO INPUT

1-88.5
RIN: 7.30

rRNA Ratio [28s / 18s]: 1.1

**(iv)** 4-MGFP INPUT

1-96.5
RIN: 7.60

rRNA Ratio [28s / 18s]: 1.2

127
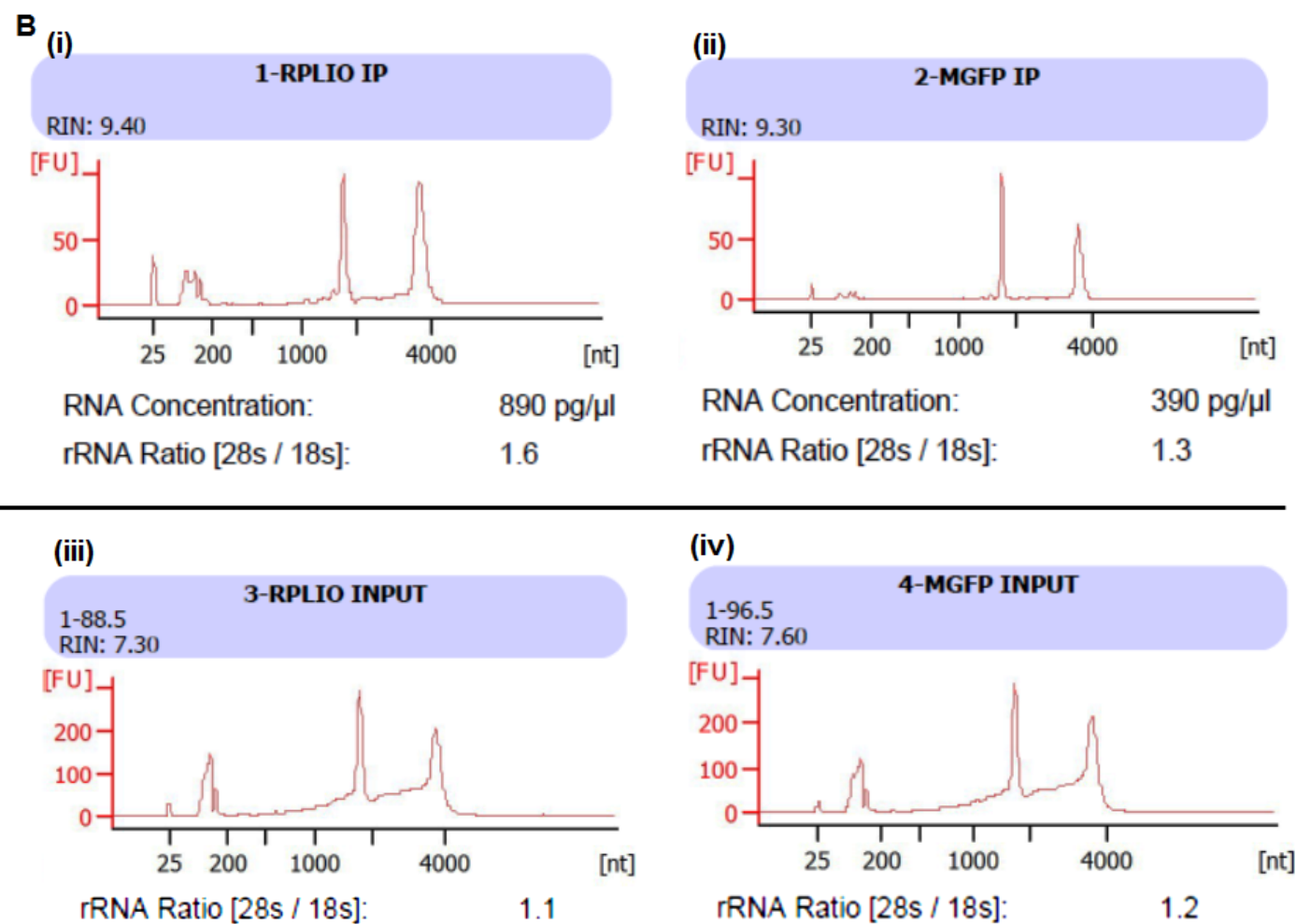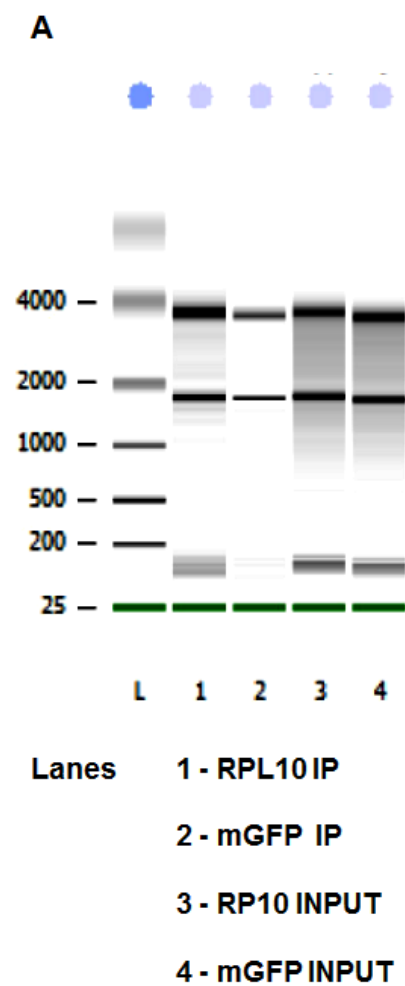
**Figure 6.5: TRAP *mRNA purification and analysis from HEK293T cells.*** Total RNA was extracted from HEK293T cells grown in a 60mm (two dishes per sample) culture dish and analysis was performed by Bioanalyser PicoChips (n=3) **(A)** Electropherogram showing the size distribution of RNA fragment from four samples. **(B)** Top panel, bioanalyser results for IP samples of RPL10 and mGFP and bottom panel has their corresponding INPUT samples. RNA ratios of the 18S to 28S were 1.6 and 1.3 for L10a and GFP control respectively. RNA integrity number (RIN) for IP samples were 9.4 (target) and 9.3 (control) whilst RIN values for the whole cell lysate were 7.3 (INPUT - RPL10) and 7.6 (INPUT - mGFP). The RNA concentration of the target RPL10 - IP sample was 890pg/µl whereas for the control mGFP the concentration was 390pg/µl. The ladder was at 1000pg/ µl.

### 6.4.2. Screening bladder cancer cell lines to identify optimal ATF3 mRNA induction, Pracinostat dosage, and ideal treatment period.

After establishing the method of TRAP and mRNA purification in HEK293T cells, I sought to identify the bladder cell line which has optimal induction of ATF3 mRNA expression on Pracinostat treatment to affinity purify translatomes and identify genes associated with ATF3. As demonstrated in previous chapters, all five cancer cell lines I have used in this study restored ATF3 expression both at mRNA and protein level depending on Pracinostat dosage and duration of the treatment; but at different degrees of reactivation in different cell lines. Due to this difference between cell lines, it is highly critical to set the optimal parameters to avoid biased insight of target genes for genome wide RNA sequencing analysis of ATF3 related genes involved in restoring the non-malignant phenotype. These parameters involve selecting cells with optimal induction of ATF3 mRNA expression, optimal dosage of Pracinostat and the duration of the treatment. In order to set the optimal parameters for the downstream analysis, four of the five bladder cancer cells (5637, T24, TSU-Pr1, and J82) were treated with four different concentrations of Pracinostat (50nM, 100nM, 200nM, and 500nM) and analysed at three different time points (6hrs, 12hrs, and 24hrs) (Figure 6.6). Although all four cell lines demonstrated a significant restoration of ATF3 at mRNA level, TSU-Pr1 cells exhibited a steady increase in all four dosages (50nM, 100nM, 200nM and 500nM) of Pracinostat at three time-points of analysis. Further, to choose the ideal dosage and time in TSU-Pr1 cells, I compared the level of ATF3 reactivation at each time points. Pracinostat at a concentration of 500nM showed a gradual increase of ATF3 over the three time points, and at 12hrs of treatment reactivation was significant with > 2 fold for the same dosage at 6hrs (~4 fold increase compared to control and ~9 fold at 12hrs). Because of the consistent results obtained for TSU-Pr1 cells from replicative experiments, I chose TSU-Pr1

cells for TRAP mRNA purification and RNA sequencing analysis using cells treated for12

hrs with 500nM Pracinostat to give optimal restoration of ATF3 levels.
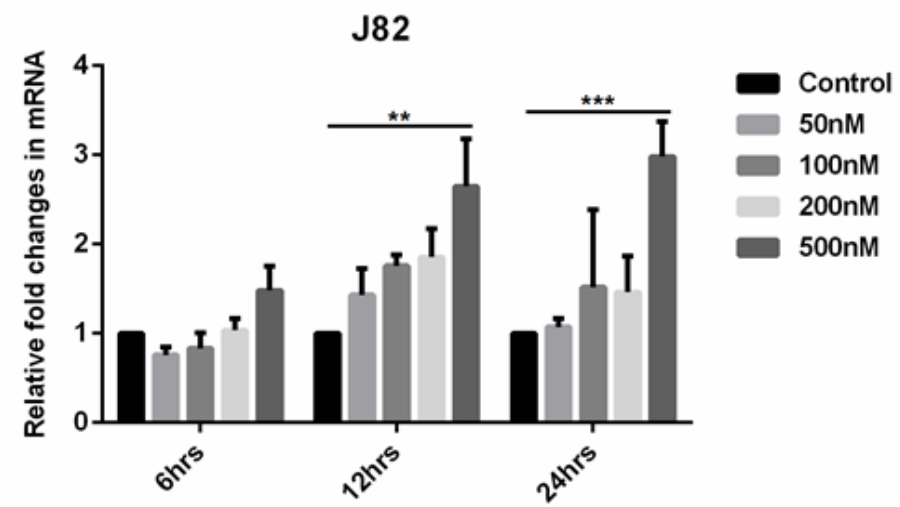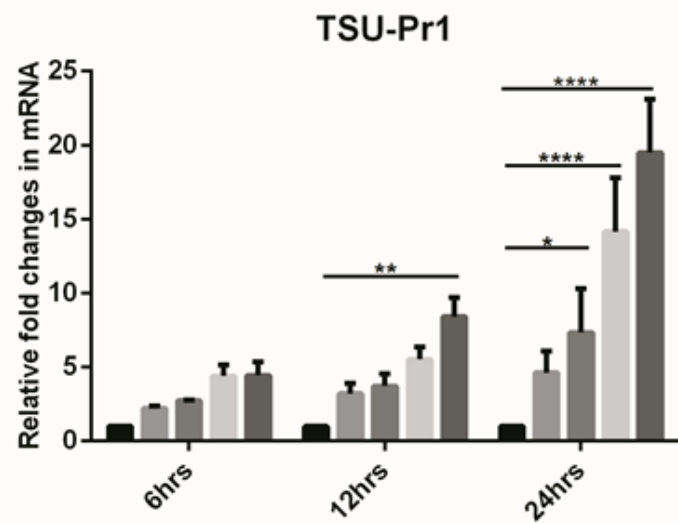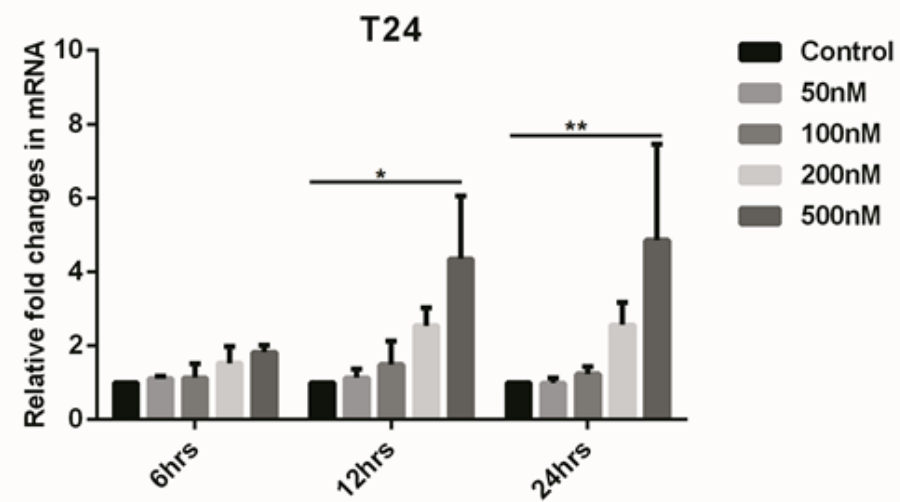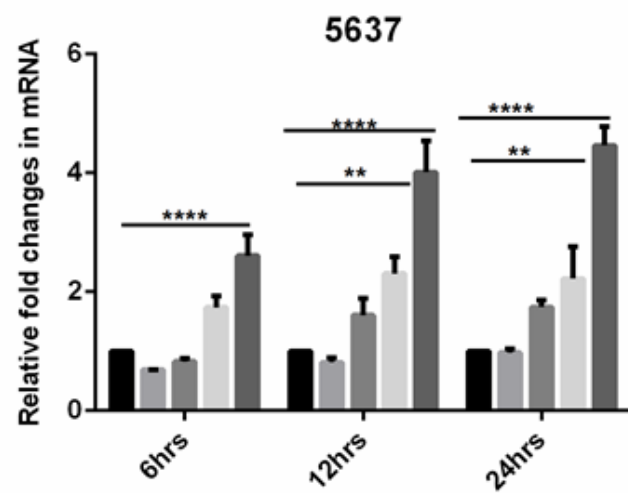
**Figure 6.6:** *qRT- PCR screening of bladder cancer cell lines for mRNA reactivation of ATF3 with different dosages of Pracinostat over three time points.* Quantitative real-time PCR for detecting relative fold changes ATF3 reactivation in bladder cancer cell lines - 5637, T24, TSU-Pr1, and J82 at 6 hours 12 hours and 24 hours of treatment with Pracinostat of varying concentrations (50nM - 500nM) (***$P \leq 0.001$) (**$P \leq 0.01$) (*$P \leq 0.05$) ( n= 3).

### 6.4.3. TRAP and mRNA purification in TSU-Pr1 cells stably transfected with RPL10a failed to enrich the translated mRNA.

With the aim of increasing the amount of total RNA yield for sequencing after the TRAP process, I decided to generate stable TSU-Pr1 cells expressing mGFP-RPL10 vector or control vector and selected under G418 (400µg/ml) for 3 - 4 weeks (Figure 6.7). The stable cells were grown in 100cm dishes (3 flasks per sample) to confluency and the TRAP and mRNA purification and the analysis were performed on Bioanalyser Pico chips and the data representing replicate experiments is shown in Figure 6.8 A and 6.8 B (n =3). The RIN value for all six (both IP and INPUT) samples were >9 suggesting that isolated RNAs are intact and suitable for the sequence analysis. But the total RNA yields obtained from TSU-Pr1-L10 cells were unpredictably low and the concentrations (~600pg/µl) were similar to that of the background level or the controls (mGFP) (Figure 6.8A (i) and (ii)). A Number of repeated experiments did not improve the RNA yield in RPL10 tagged TSU-Pr1 stable cells indicating that the TRAP method of translating mRNA enrichment was not efficiently performing in these cells.
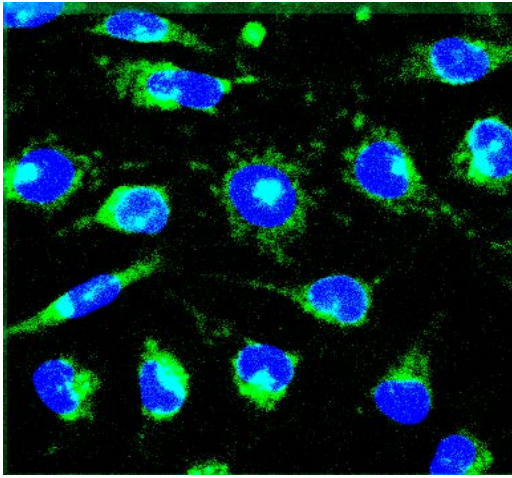
**mGFP- RP10a**                                    **mGFP**
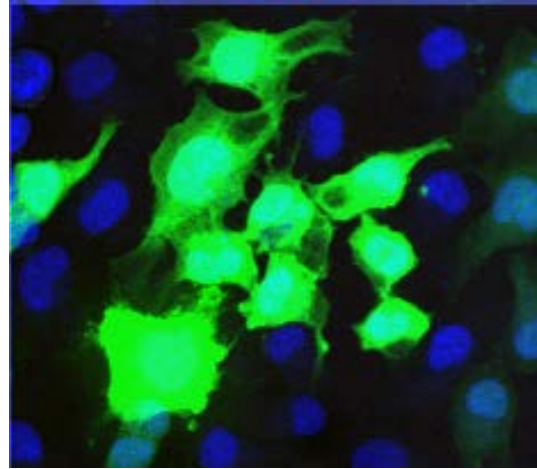


**Figure 6.7:** *Stable TSU-Pr1 cells transfected with mGFP-RPL10 vector or mGFP vector.* Cells under selection of G418.

**A**



**(i) RPLID-IP**
RIN: 9.10

RNA Concentration: 679 pg/µl
rRNA Ratio [28s / 18s]: 1.6

**(ii) mGFP-IP**
RIN: 9.70

RNA Concentration: 628 pg/µl
rRNA Ratio [28s / 18s]: 3.0

**(iii) Untransfected-IP**
RIN: 9.60

RNA Concentration: 466 pg/µl
rRNA Ratio [28s / 18s]: 1.6

**(iv) RPLIO-INPUT**
RIN: 9.90

RNA Concentration: 3,831 pg/µl
rRNA Ratio [28s / 18s]: 1.9

**(v) mGFP-INPUT**
RIN:10

RNA Concentration: 3,715 pg/µl
rRNA Ratio [28s / 18s]: 2.0

**(vi) Untransfected-INPUT**
RIN: 9.90

RNA Concentration: 3,197 pg/µl
rRNA Ratio [28s / 18s]: 1.8

**B**



**Figure 6.8: TRAP** *mRNA purification and analysis of TSU-Pr1 cells.* TRAP followed by mRNA purification of stable TSU-Pr1 cells with mGFP-L10a or mGFP vector or un-transfected cells and analysis was performed with Bioanalyser PicoChips. (**A**) Top panel, bioanalyser results for IP samples of RPL10 (i), mGFP (ii), and un-transfected (iii) and bottom panel has their corresponding INPUT results. The ladder was at 1000pg/µl. (**B**) Electropherogram showing the size distribution of RNA fragments from six samples.
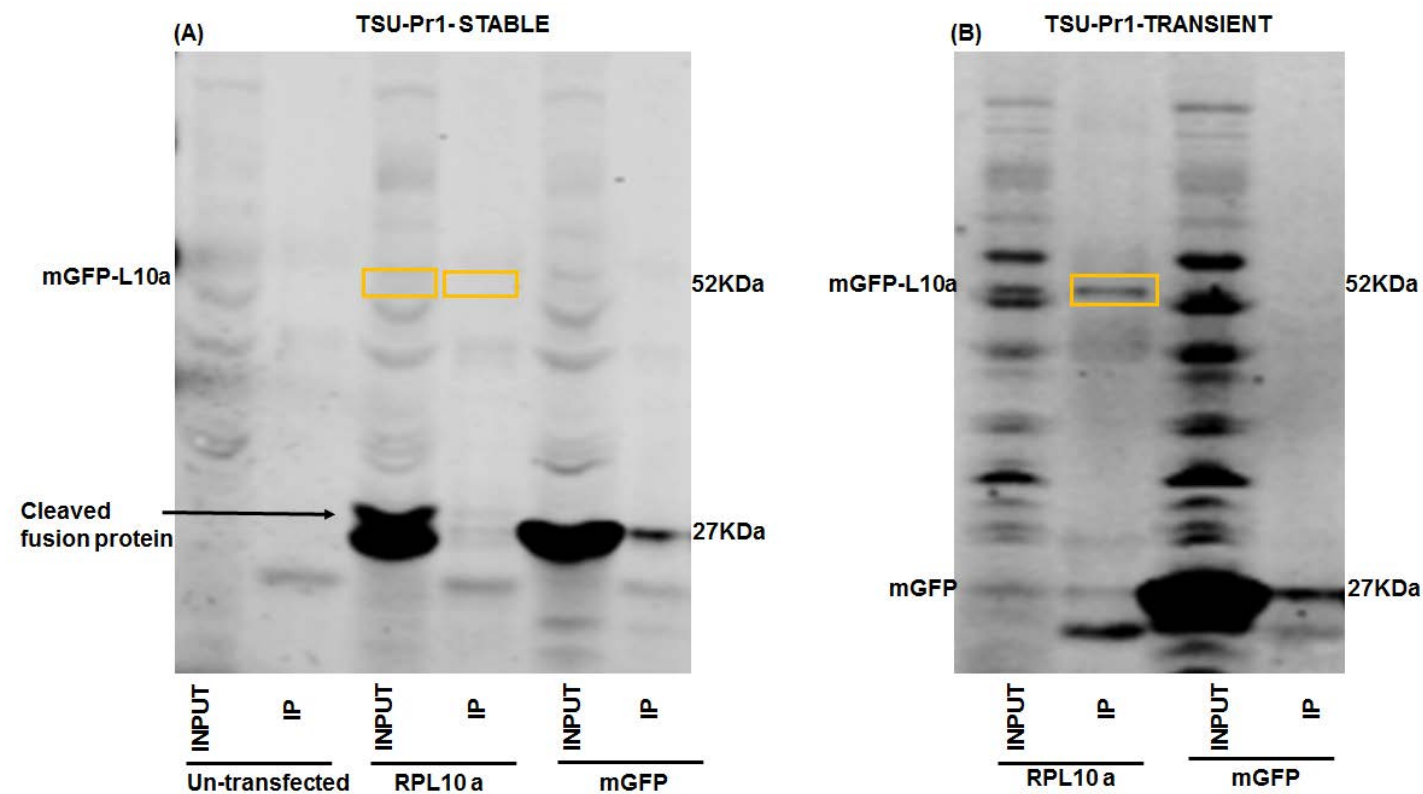
**Figure 6.9:** *Immunoprecipitation of mGFP tagged 60S ribosomal protein L10a in TSU-Pr1 cells.* (**A**) TSU-Pr1 cells stably expressing mGFP-L10 vector tagging ribosomal protein or mGFP vector control. (**B**) TSU-Pr1 cells transiently transfected with mGFPL10 vector or mGFP vector control. The immunoprecipitation was performed using magnetic beads coated anti-GFP antibody and analysed on western blot. Fusion protein

mGFP-L10a is 52KDa and control mGFP is 27KDa. Yellow box marking the fusion protein in transiently expressing TSU-Pr1 cells and expected size in stable cells. Data shown is representation of two replicative experiments.

## 6.5.     Discussion

The TRAP and mRNA profiling method is a powerful tool to profile translated mRNAs which will accurately reflect the actual protein levels rather than conventional gene expression profiling, which relies on the total mRNA pool. A series of non-malignant phenotypical changes were observed in bladder cancer cells upon reactivation of ATF3 expression followed by Pracinostat treatment. Polysomes-associated RNA profiling enables the identification of functionally relevant ATF3 depended genes during the restoration of the non-malignant status and potentially would identify other candidates to add more impact to the prognostic and therapeutic potential value to this model.

In this chapter, I successfully recapitulated the method of TRAP and mRNA isolation as described previously [198] [205]. I was able to demonstrate that the TRAP method and mRNA purification is effectively working in HEK293T cells with >2 fold enrichment of the translating mRNA compared to the controls in transiently transfected cells. After optimising the parameters including identifying the candidate bladder cancer cell lines (TSU-Pr1), in order to improve the RNA yield, I decided to stably tag the ribosomes (polysomes) in the candidate cells. Replicate experiments demonstrated that the TRAP method was unsuccessful in enriching the translated mRNA in the stable TSU-Pr1 cells, where the IP purified mRNA yield of RPL10 tagged cells were no difference to the controls. Further investigations in the stable cells demonstrated that the stable cells lose the expression of the fusion protein (mGFP-L10, expected size 52KDa) on immunoblot analysis (Figure 6.9 (A) and (B)). In stable TSU-Pr1 cells, the GFP antibody recognises two fragments close to the size of the GFP protein (~27KDa) in the whole lysate (INPUT) samples. But IP samples failed to show a mGFP-L10a band, in contrast to transiently tagged TSU-Pr1 cells (Figure 6.9 (B)). Considering the fact that the fusion protein was readily detectable on immunoblot for both

TSU-Pr1 cells and in HEK293T cells when transiently transfected this indicates that the plasmid vector expresses the fusion protein driven by constitutive promoter CMV as expected. Over-expressing the RPL10a gene fused with GFP previously performed by other groups in mammalian cell types, although using different systems, resulted in no toxicity. While this does not eliminate the possibility of any toxic effect from this fusion protein in bladder cancer cells, impaired translational machinery and aberrant ribosomal biogenesis has been widely reported in various cancer models [206] [207]. A number of events including mutations in ribosomal proteins (including RPL10) and presence of activated oncogenes evidently contributed instability to ribosomal biogenesis and ultimately to altered translational programs in cancer[208]. However, to investigate whether the aberrant cleavage of RPL10 is due to any altered translational machinery in TSU-Pr1 cells when it is stably integrated is beyond the scope of this study.

# CHAPTER - 7

*General discussions and future directions*

Cancer is the leading cause of illness in Australia, and bladder cancer ranks 2nd common among uro-genital related cancers [1]. Surgery followed by chemotherapy remains the standard of care for advanced bladder cancers including metastatic tumors, but the survival rate has been less than 50% for many decades [9]. Because of the economic burden posed from low-grade tumors, which require lifelong surveillance and the poor survival rates from high grade and metastatic tumors, there is always a greater demand for better alternative therapies [209].

In addition to genetic abnormalities, chromatin alterations (altered epigenetic changes) are also associated with all stages of tumor formation and progression [210]. These epigenetic alterations involve the altered pattern of histone modifications and both losses and gains of DNA methylation. The first direct evidence of epigenetic gene silencing came from studies in retinoblastoma tumors, where there was 92% reduction in RB1 expression in tumors with promoter hyper-methylation [211]. Earlier studies in various solid cancer models have shown that abnormal epigenetic silencing of genes can occur at any stage of tumor progression; (a) it occurs in the early stages of neoplastic process (loss of imprinting of IGF2 in colorectal cancers and in inherited predisposition to Wilms tumor); (b) abnormal silencing can also occur in the pre-invasive stage of the tumor progression (breast and lung cancers) [212] [213-215]. Previous studies in bladder cancer demonstrated that epigenetic inactivation of SFRP (secreted frizzled receptor protein) and altered P53 expression in combination can be utilised as a marker of invasive disease [216]. Our study focuses on exploring the therapeutical benefits of restoring the expression of ATF3, a transcription factor found to be lost/silenced in advanced bladder cancers, using a HDACi Pracinostat.

## 7.1. Pracinostat treatment reactivates the expression of epigenetically silenced ATF3 and restored non-malignant phenotypes in bladder cancer models

In tumor biology, numerous studies demonstrated that ATF3 functions both as a tumor suppressor and an oncogenic inducer depends on the degree of malignancy, and cellular context [131] [135]. Studies by our group previously showed that as the tumor progress the expression of ATF3 is reduced and in advanced bladder cancers loss of ATF3 expression correlates with poor clinical survival rate [139]. So we hypothesized that restoring ATF3 expression using an HDACi may have significant therapeutic benefits in patients with advanced bladder cancer.

Treating with Pracinostat in a series of bladder cancer cells of different grades and origins *in vitro*, demonstrated that treatment reactivated the expression of ATF3 both mRNA and protein level, concomitantly restoring the acetylation patterns in these cells. Increased acetylation of core-histone molecules in-parallel with nuclear re-expression of ATF3 was also observed in *in vivo* xenograft tumor models, upon oral administration of HDACi. These results suggesting that, the Pracinostat treatment re-established the normal acetylation pattern which subsequently activated the expression of ATF3. As a consequence of this reactivation, we observed a cascade of phenotypic alterations in the malignant behaviour both *in vitro* and *in vivo* bladder cancer models. Significant reduction in their capacity to proliferate, migrate and clone formation in a dose dependent manner was observed in all Pracinostat treated cells compared to their matched control *in vitro*. Treatment with Pracinostat also induced cell cycle arrest across all cell types, and increased their *in vitro* sensitivity to platinum treatment. *In vivo*, treatment with Pracinostat for 3 weeks resulted in 98% reduction in tumor volume compared to the controls. Further, detailed histological studies on xenograft tumors demonstrated a significant reduction in the angiogenic properties in Pracinostat treated

samples compared to vehicle controls, including the reduction in blood vessels, collapsed vasculatures, reduced production of pro-angiogenic factors. These observations indicated to us a less reactive stromal support for the growth of tumors in Pracinostat treated mice which also showed marked induction of cleaved caspase-3. Together, both *in vitro* and *in vivo* data clearly demonstrated that treating with HDACi altered the epigenetic silencing of ATF3 expression, and subsequently restored the non-malignant properties in bladder cancer models. Studies in other disease models previously shown that the expression of ATF3 has a significant role in regulating the expression of HDACs. Previous studies in innate immune system demonstrated that HDACs are recruited by ATF3 to regulate the chromatin structure, where it protects the host from chronic TLR (Toll-like receptor) stimulated inflammatory responses [118]. Similar observations were made in acute kidney injury, where ATF3 mediated epigenetic regulation resulted in euchromatin and subsequently protects against chronic inflammation associated with acute renal injury [192] [217]. Studies in non-small cell lung cancer (NSCLC) were the first in cancer to identify the HDACs association in regulating ATF3 expression [218]. Our study is the first in cancer models demonstrating that epigenetic re-activation of ATF3 by HDACi Pracinostat plays a tumor suppressor role in bladder cancer.

### 7.2.    ATF3 re-activation is pivotal in determining the treatment response in bladder cancer

Our studies using xenograft models demonstrated that the oral administration of Pracinostat re-activated the expression of ATF3 in bladder tumors. The cells expressing nuclear ATF3 were located in the treatment responding core of the tumor, where the majority of the cells were marked for necrosis or late apoptosis. The cells, which were in active proliferation, were remote from the treatment responding core, and located towards the outer edge of the tumor. Further analysis confirmed that cells expressing ATF3 were negatively correlated to

Ki67 expressing cells. These observations suggested to us that the re-expression of ATF3 is a marker of tumor response to Pracinostat mediated treatment. The role of ATF3 in determining the treatment outcome was further investigated by comparing the functional significance of loss of ATF3 expression with Pracinostat treatment both *in vitro* and *in vivo*. *In vitro*, the rate of proliferation, migration and colony formation were significantly higher in Pracinostat treated ATF3 knockdown cells compared to Pracinostat treated control cells. Further, *in vivo* studies using xenograft tumors demonstrated that upon Pracinostat treatment, though there was a delay in tumor growth, the rate of growth was significantly higher in ATF3 depleted xenografts compared to the shcontrol tumors. This was also reflected in the survival analysis of those mice in the shcontrol group where 100% of the mice responded to the Pracinostat treatment and survived until the end of the experiment. Together, these data clearly depicting that reactivation of ATF3 by Pracinostat, are pivotal in defining the tumor response to the HDACi therapy and confirm ATF3 as biomarker of response.

Though, some previous studies recognized the importance of expression of ATF3 in association with HDACi mediated treatment in cancers, our study is the first to demonstrate a mechanistic insight into crucial role of ATF3 reactivation in determining the treatment response. Earlier studies in colorectal cancer using HDACi M344 as a cytotoxic agent, demonstrated that expression of ATF3 play as a mediator of co-operative synergistic effect of HDACi in combination with cisplatin [193]. Similarly, another study in colorectal cancer also demonstrated that ATF3 induction by HDACi is required for efficient induction of DR-5 (death receptor-5) gene transcription and pro-apoptotic effect in p53 deficient human colon cancer cells [219]. Here, we have identified a novel biomarker of tumor response in HDACi mediated cancer therapy, and propose that regulating the expression of ATF3 by Pracinostat may have therapeutic utility for bladder cancer patients.

## 7.3.    Regulation of RB1 expression by ATF3

The retinoblastoma (RB) gene RB is the first identified tumor suppressor gene and inactivation of RB1 is the most frequent molecular hallmark of cancers [189]. Previous studies identified that RB1 is implicated in many biological process including cell cycle control and apoptosis. Alteration of RB1 results in cancer development and progression including bladder cancer [220] [221-223]. RB1 expression is regulated at both the transcriptional and post-translational levels but when the function of the RB protein is regulated by phosphorylation it was proposed that the transcriptional regulation of RB gene might not be essential [224] [225]. There are 3 different circumstances (involving both genetic and epigenetic events) in cancers where RB1 is functionally inactive in regulating cell cycle machinery, one of its primary functions [226]. (a) RB1 when hyper-phosphorylated is unable to bind to the E2F transcription factor, which subsequently results in transcription of E2F target genes and increased proliferation [227]. (b) Loss or aberrant RB expression results in uncontrolled growth [221]. (c) Class 1 HDAC binds to RB1 in the nucleus resulting RB1 silencing [228]. Pracinostat treatment in the four cell lines we tested demonstrated significant growth arrest. Further, immunoblot analysis showed that 5637, T24, and TSU-Pr1 cells have hyper-phosphorylated RB and upon Pracinostat treatment there was observed a clear switch from hyper-phosphorylated (inactive) to hypo-phosphorylated (active) form of RB1 in a dose depended manner. In the case of J82 (high grade) cell line, RB expression is completely lost but the treatment with Pracinostat restored the expression of RB. To check whether the reactivation of ATF3 has a direct impact on RB1 expression, over-expression of ATF3 in J82 cell line correlated with induced expression of RB1 and subsequently resulted in G0/G1 phase arrest. Further, in-silico analysis of RB1 promoter confirms the presence of ATF binding site in the RB1 promoter. Additionally, *in vivo* observation of ATF3 expressing cells

located in the treatment responding core of the tumor which are negatively correlated to Ki67 expressing cells also reaffirm ATF3 regulated cell cycle arrest. Previously a study explored the tumor suppressor role of ATF3 and identified cyclin D1 (a component of the cell-cycle regulators) as a target gene in regulating tumorigenesis [126]. Here we have identified a new potential ATF3 target gene - RB1 and the role of ATF3 in regulating the transcription of RB1.

## 7.4. TRAP and RNA sequencing to identify the potential partners of ATF3 in restoring non-malignancy in bladder cancers

Translational control is known to play crucial role in gene expression program, and as such analysis of translating mRNA is critical in understanding the functional significance of gene expression. The TRAP method is to isolate the mRNA under the translation process from affinity-tagged ribosomes and analyse translated mRNA to make the direct match to the protein products that will drive any phenotypic changes associated with any treatments or disease models. Implementation of TRAP method and successful isolation of translating mRNA from HEK293T cells is described in chapter 6. The central purpose of this experiment was to isolate polysomes associated mRNA profiled by RNA sequencing for genome wide analysis, which will enable us to identify all functionally relevant ATF3 depended genes at the time of the extraction, where ATF3 expression is reactivated upon Pracinostat treatment. The mRNA enrichment from the candidate cell line, TSU-Pr1 cells stably expressing RPL10 was unpredictably low, and profound investigations into this uncovered that the cleavage of fusion protein (RPL10-mGFP) in stable cell line was responsible for this low yield.

## 7.5. Conclusions

The purpose of this study was to identify a better alternative potential therapy to improve the treatment outcome and therapeutic management of patients with bladder cancer. An earlier

study in bladder cancer from our laboratory identified that the transcription factor ATF3 expression is reduced as the tumor progress. We utilised a HDACi mediated treatment strategy to re-establish the chromatin alterations associated with cancer progression. Treatment with Pracinostat in *in vivo* and *in vitro* bladder tumor models re-established the acetylation patterns. Most importantly, treatment with Pracinostat re-stored the expression of ATF3, which subsequently correlated with non-malignant phenotypes in *in vivo* and *in vitro* bladder cancer models. Further, the observation of ATF3 re-expressing cells located in the treatment responding core from the early to late stage of therapy in *in vivo* xenografts models suggest that re-expression of ATF3 is an indication of treatment response. Additionally, the reduced sensitivity of ATF3 expression depleted xenograft tumors confirmed the crucial role of ATF3 expression in predicting the treatment outcome. This study identified ATF3 as a biomarker of tumor response and provides a rationale for therapeutic utility of HDACi mediated treatments for bladder cancers.

## 7.6.    Future Directions

Treatment with HDACi Pracinostat reactivated epigenetically silenced ATF3 expression in bladder cancer models *in vitro* and *in vivo* and restored the non-malignant phenotype. To provide mechanistic insight into the transcriptional regulation of ATF3, Chromatin Immuno-Precipitation (ChIP) can be performed on the ATF3 promoter with antibodies against acetyl histone H3 and H4 following treatment with Pracinostat. Pracinostat treatment also increased the sensitivity of bladder cancer cells to platinum treatment. The mechanism of HDAC inhibition in sensitizing cancer cells can be further explored using markers of DNA repair process such as γH2AX. The significance of this increased *in vitro* sensitivity has to be further validated using pre-clinical mouse modals, since the future of the HDACi based therapy would be in combination with chemotherapeutic agents currently part of the standard

of care as this would enable the full potential of these inhibitors to be realized. Treatment of mouse models with bladder xenografts with 1 or 2 oral dosages of Pracinostat to initiate the response followed by single dose of Carboplatin aided with monitoring tumor growth pattern and histological studies would validate the current *in vitro* findings.

Transcriptional regulation of RB1 by ATF3 can be further confirmed by experiments utilising ChIP assays to demonstrate binding of ATF3 to the RB1 promoter upon treatment with Pracinostat. RB1 promoter reporter assays comparing the gene promoter activity between 'wild type' and 'ATF3 binding site mutant' RB promoter under the treatment will confirm the direct transcriptional regulation of RB1 by ATF3. Post-translation modifications of RB1 (hyper to hypo-phosphorylation) were also observed upon treatment with Pracinostat and the role of ATF3 in de-phosphorylation of RB1 remains to be investigated.

To identify ATF3 depended genes driving the phenotypic changes, future optimization experiments in stable cells will be performed using increased concentration of the antibiotics and also conducting multiple transfections to generate the stably expressing RPL10 gene before setting up transiently expressing RPL10 in larger number of cells to improve the mRNA yield for RNA sequence analysis. Expression profiles generated by RNA sequencing will be compared between untreated cells with that of treated cells, where ATF3 expression has been reactivated. The RNA sequencing data will be verified using the TSU-Pr1 cell line stably depleted for the expression of ATF3 to the control line in the presence of Pracinostat treatment for identifying key partners of ATF3 driving tumor suppression activity. The target genes and other regulatory proteins identified from the RNA sequencing data will be further validated by immunoblots and the functional significance confirmed using *in vivo* mouse models and clinical specimens which will ultimately add more predictability for this model.

# BIBLIOGRAPHY

1.      AIHW, *Cancer in Australia: an overview*, in *Cancer series no. 90. Cat. no. CAN 88.* 2014. p. 1-216.

2.      AIHW, *Health expenditure Australia 2007–08*, in *Health and Welfare Expenditure.* 2009. p. 1-191.

3.      Ferlay, J., et al., *Estimates of worldwide burden of cancer in 2008: GLOBOCAN 2008.* Int J Cancer, 2010. **127**(12): p. 2893-917.

4.      Figueroa, J.D., et al., *Genome-wide interaction study of smoking and bladder cancer risk.* Carcinogenesis, 2014. **35**(8): p. 1737-44.

5.      Letasiova, S., et al., *Bladder cancer, a review of the environmental risk factors.* Environ Health, 2012. **11 Suppl 1**: p. S11.

6.      Kiemeney, L.A., et al., *Sequence variant on 8q24 confers susceptibility to urinary bladder cancer.* Nat Genet, 2008. **40**(11): p. 1307-12.

7.      Kiriluk, K.J., et al., *Bladder cancer risk from occupational and environmental exposures.* Urol Oncol, 2012. **30**(2): p. 199-211.

8.      Luke, C., et al., *Exploring contrary trends in bladder cancer incidence, mortality and survival: implications for research and cancer control.* Intern Med J, 2010. **40**(5): p. 357-62.

9.      Knowles, M.A. and C.D. Hurst, *Molecular biology of bladder cancer: new insights into pathogenesis and clinical diversity.* Nat Rev Cancer, 2015. **15**(1): p. 25-41.

10.     Fajkovic, H., et al., *Impact of gender on bladder cancer incidence, staging, and prognosis.* World J Urol, 2011. **29**(4): p. 457-63.

11.     Bostrom, P.J., et al., *Sex differences in bladder cancer outcomes among smokers with advanced bladder cancer.* BJU Int, 2012. **109**(1): p. 70-6.

12.     National Collaborating Centre for Cancer, *National Institute for Health and Clinical Excellence: Guidance*, in *Bladder Cancer: Diagnosis and Management*. 2015, National Institute for Health and Care Excellence (UK): London.

13.     Bassett, J.C., et al., *Knowledge of the harms of tobacco use among patients with bladder cancer.* Cancer, 2014. **120**(24): p. 3914-22.

14.     Golka, K., et al., *Occupational exposure and urological cancer.* World J Urol, 2004. **21**(6): p. 382-91.

15.     Koutros, S., et al., *Hair dye use and risk of bladder cancer in the New England bladder cancer study.* Int J Cancer, 2011. **129**(12): p. 2894-904.

16.     American Cancer Society, *Cancer Facts & Figures*. 2016: Atlanta, Ga.

17.     Burger, M., et al., *Epidemiology and risk factors of urothelial bladder cancer.* Eur Urol, 2013. **63**(2): p. 234-41.

18.     Cazier, J.B., et al., *Whole-genome sequencing of bladder cancers reveals somatic CDKN1A mutations and clinicopathological associations with mutation burden.* Nat Commun, 2014. **5**: p. 3756.

19.     Rothman, N., et al., *A multi-stage genome-wide association study of bladder cancer identifies multiple susceptibility loci.* Nat Genet, 2010. **42**(11): p. 978-84.

20.     The Cancer Genome Atlas Research, N., *Comprehensive molecular characterization of urothelial bladder carcinoma.* Nature, 2014. **507**(7492): p. 315-322.

21.     Hemminki, K., et al., *Familial bladder cancer and the related genes.* Curr Opin Urol, 2011. **21**(5): p. 386-92.

22.     Garcia-Closas, M., et al., *NAT2 slow acetylation, GSTM1 null genotype, and risk of bladder cancer: results from the Spanish Bladder Cancer Study and meta-analyses.* Lancet, 2005. **366**(9486): p. 649-59.

23. Prout, G.R., Jr., et al., *Treated history of noninvasive grade 1 transitional cell carcinoma. The National Bladder Cancer Group.* J Urol, 1992. **148**(5): p. 1413-9.

24. Kluth, L.A., et al., *Prognostic and Prediction Tools in Bladder Cancer: A Comprehensive Review of the Literature.* Eur Urol, 2015. **68**(2): p. 238-53.

25. Zargar, H., et al., *Multicenter assessment of neoadjuvant chemotherapy for muscle-invasive bladder cancer.* Eur Urol, 2015. **67**(2): p. 241-9.

26. Zargar, H., et al., *Optimizing intravesical mitomycin C therapy in non-muscle-invasive bladder cancer.* Nat Rev Urol, 2014. **11**(4): p. 220-30.

27. Fuge, O., et al., *Immunotherapy for bladder cancer.* Res Rep Urol, 2015. **7**: p. 65-79.

28. Anastasiadis, A. and T.M. de Reijke, *Best practice in the treatment of nonmuscle invasive bladder cancer.* Ther Adv Urol, 2012. **4**(1): p. 13-32.

29. Richards, K.A., N.D. Smith, and G.D. Steinberg, *The importance of transurethral resection of bladder tumor in the management of nonmuscle invasive bladder cancer: a systematic review of novel technologies.* J Urol, 2014. **191**(6): p. 1655-64.

30. Apolo, A.B., et al., *Practical use of perioperative chemotherapy for muscle-invasive bladder cancer: summary of session at the Society of Urologic Oncology annual meeting.* Urol Oncol, 2012. **30**(6): p. 772-80.

31. Vishnu, P., J. Mathew, and W.W. Tan, *Current therapeutic strategies for invasive and metastatic bladder cancer.* Onco Targets Ther, 2011. **4**: p. 97-113.

32. Sundi, D., et al., *Extent of pelvic lymph node dissection during radical cystectomy: is bigger better?* Rev Urol, 2014. **16**(4): p. 159-66.

33. Zlotta, A.R., N.E. Fleshner, and M.A. Jewett, *The management of BCG failure in non-muscle-invasive bladder cancer: an update.* Can Urol Assoc J, 2009. **3**(6 Suppl 4): p. S199-205.

34.     Dovedi, S.J. and B.R. Davies, *Emerging targeted therapies for bladder cancer: a disease waiting for a drug.* Cancer Metastasis Rev, 2009. **28**(3-4): p. 355-67.

35.     Shen, Z., et al., *Intravesical treatments of bladder cancer: review.* Pharm Res, 2008. **25**(7): p. 1500-10.

36.     Kim, H.S., et al., *Pathological T0 following cisplatin-based neo-adjuvant chemotherapy for muscle-invasive bladder cancer: a network meta-analysis.* Clin Cancer Res, 2015.

37.     Apolo, A.B., N.J. Vogelzang, and D. Theodorescu, *New and promising strategies in the management of bladder cancer.* Am Soc Clin Oncol Educ Book, 2015: p. 105-12.

38.     Sio, T.T., et al., *Chemotherapeutic and targeted biological agents for metastatic bladder cancer: a comprehensive review.* Int J Urol, 2014. **21**(7): p. 630-7.

39.     Lohrisch, C., et al., *Small cell carcinoma of the bladder: long term outcome with integrated chemoradiation.* Cancer, 1999. **86**(11): p. 2346-52.

40.     Abrahams, N.A., et al., *Small cell carcinoma of the bladder: a contemporary clinicopathological study of 51 cases.* Histopathology, 2005. **46**(1): p. 57-63.

41.     Anastasiadis, A., et al., *Follow-up procedures for non-muscle-invasive bladder cancer: an update.* Expert Rev Anticancer Ther, 2012. **12**(9): p. 1229-41.

42.     Di Pierro, G.B., et al., *Bladder cancer: a simple model becomes complex.* Curr Genomics, 2012. **13**(5): p. 395-415.

43.     Goebell, P.J. and M.A. Knowles, *Bladder cancer or bladder cancers? Genetically distinct malignant conditions of the urothelium.* Urol Oncol, 2010. **28**(4): p. 409-28.

44.     Pollard, C., S.C. Smith, and D. Theodorescu, *Molecular genesis of non-muscle-invasive urothelial carcinoma (NMIUC).* Expert Rev Mol Med, 2010. **12**: p. e10.

45.     Kobayashi, T., et al., *Modelling bladder cancer in mice: opportunities and challenges.* Nat Rev Cancer, 2015. **15**(1): p. 42-54.

46.     Schulz, W.A., et al., *Epigenetics of urothelial carcinoma.* Methods Mol Biol, 2015. **1238**: p. 183-215.

47.     Venugopal, B. and T.R. Evans, *Developing histone deacetylase inhibitors as anti-cancer therapeutics.* Curr Med Chem, 2011. **18**(11): p. 1658-71.

48.     Tsai, H.C. and S.B. Baylin, *Cancer epigenetics: linking basic biology to clinical medicine.* Cell Res, 2011. **21**(3): p. 502-17.

49.     Portela, A. and M. Esteller, *Epigenetic modifications and human disease.* Nat Biotechnol, 2010. **28**(10): p. 1057-68.

50.     Javierre, B.M., et al., *Changes in the pattern of DNA methylation associate with twin discordance in systemic lupus erythematosus.* Genome Res, 2010. **20**(2): p. 170-9.

51.     Kanwal, R., K. Gupta, and S. Gupta, *Cancer epigenetics: an introduction.* Methods Mol Biol, 2015. **1238**: p. 3-25.

52.     Lo, P.K. and S. Sukumar, *Epigenomics and breast cancer.* Pharmacogenomics, 2008. **9**(12): p. 1879-902.

53.     Yates, D.R., et al., *Promoter hypermethylation identifies progression risk in bladder cancer.* Clin Cancer Res, 2007. **13**(7): p. 2046-53.

54.     Aleman, A., et al., *Identification of DNA hypermethylation of SOX9 in association with bladder cancer progression using CpG microarrays.* Br J Cancer, 2008. **98**(2): p. 466-73.

55.     Habuchi, T., et al., *Structure and methylation-based silencing of a gene (DBCCR1) within a candidate bladder cancer tumor suppressor region at 9q32-q33.* Genomics, 1998. **48**(3): p. 277-88.

56. Sanchez-Carbayo, M., *Hypermethylation in bladder cancer: biological pathways and translational applications.* Tumour Biol, 2012. **33**(2): p. 347-61.

57. Sana, J., et al., *Novel classes of non-coding RNAs and cancer.* J Transl Med, 2012. **10**: p. 103.

58. Hauptman, N. and D. Glavac, *Long non-coding RNA in cancer.* Int J Mol Sci, 2013. **14**(3): p. 4655-69.

59. Saito, Y., et al., *Specific activation of microRNA-127 with downregulation of the proto-oncogene BCL6 by chromatin-modifying drugs in human cancer cells.* Cancer Cell, 2006. **9**(6): p. 435-43.

60. Sun, X., et al., *Long non-coding RNA HOTAIR regulates cyclin J via inhibition of microRNA-205 expression in bladder cancer.* Cell Death Dis, 2015. **6**: p. e1907.

61. Wang, C., et al., *Up-regulation of p21(WAF1/CIP1) by miRNAs and its implications in bladder cancer cells.* FEBS Lett, 2014. **588**(24): p. 4654-64.

62. Liu, Y., et al., *Synthetic miRNA-mowers targeting miR-183-96-182 cluster or miR-210 inhibit growth and migration and induce apoptosis in bladder cancer cells.* PLoS One, 2012. **7**(12): p. e52280.

63. Peter, S., et al., *Identification of differentially expressed long noncoding RNAs in bladder cancer.* Clin Cancer Res, 2014. **20**(20): p. 5311-21.

64. Kornberg, R.D. and Y. Lorch, *Twenty-five years of the nucleosome, fundamental particle of the eukaryote chromosome.* Cell, 1999. **98**(3): p. 285-94.

65. Luger, K., et al., *Crystal structure of the nucleosome core particle at 2.8 A resolution.* Nature, 1997. **389**(6648): p. 251-60.

66.     Hadnagy, A., R. Beaulieu, and D. Balicki, *Histone tail modifications and noncanonical functions of histones: perspectives in cancer epigenetics.* Mol Cancer Ther, 2008. **7**(4): p. 740-8.

67.     Dillon, N., *Gene regulation and large-scale chromatin organization in the nucleus.* Chromosome Res, 2006. **14**(1): p. 117-26.

68.     Epping, M.T. and R. Bernards, *Molecular basis of the anti-cancer effects of histone deacetylase inhibitors.* Int J Biochem Cell Biol, 2009. **41**(1): p. 16-20.

69.     Hanahan, D. and R.A. Weinberg, *The hallmarks of cancer.* Cell, 2000. **100**(1): p. 57-70.

70.     Jones, P.A. and S.B. Baylin, *The epigenomics of cancer.* Cell, 2007. **128**(4): p. 683-92.

71.     Shahbazian, M.D. and M. Grunstein, *Functions of site-specific histone acetylation and deacetylation.* Annu Rev Biochem, 2007. **76**: p. 75-100.

72.     Ververis, K., et al., *Histone deacetylase inhibitors (HDACIs): multitargeted anticancer agents.* Biologics, 2013. **7**: p. 47-60.

73.     Gregoretti, I.V., Y.M. Lee, and H.V. Goodson, *Molecular evolution of the histone deacetylase family: functional implications of phylogenetic analysis.* J Mol Biol, 2004. **338**(1): p. 17-31.

74.     Barneda-Zahonero, B. and M. Parra, *Histone deacetylases and cancer.* Mol Oncol, 2012. **6**(6): p. 579-89.

75.     Li, X. and N. Kazgan, *Mammalian sirtuins and energy metabolism.* Int J Biol Sci, 2011. **7**(5): p. 575-87.

76.     Haigis, M.C. and L.P. Guarente, *Mammalian sirtuins--emerging roles in physiology, aging, and calorie restriction.* Genes Dev, 2006. **20**(21): p. 2913-21.

77.     van Haaften, G., et al., *Somatic mutations of the histone H3K27 demethylase gene UTX in human cancer.* Nat Genet, 2009. **41**(5): p. 521-3.

78.     Pasqualucci, L., et al., *Inactivating mutations of acetyltransferase genes in B-cell lymphoma.* Nature, 2011. **471**(7337): p. 189-95.

79.     Gui, Y., et al., *Frequent mutations of chromatin remodeling genes in transitional cell carcinoma of the bladder.* Nat Genet, 2011. **43**(9): p. 875-8.

80.     Fraga, M.F., et al., *Loss of acetylation at Lys16 and trimethylation at Lys20 of histone H4 is a common hallmark of human cancer.* Nat Genet, 2005. **37**(4): p. 391-400.

81.     Weichert, W., et al., *Class I histone deacetylase expression has independent prognostic impact in human colorectal cancer: specific role of class I histone deacetylases in vitro and in vivo.* Clin Cancer Res, 2008. **14**(6): p. 1669-77.

82.     Halkidou, K., et al., *Upregulation and nuclear recruitment of HDAC1 in hormone refractory prostate cancer.* Prostate, 2004. **59**(2): p. 177-89.

83.     Weichert, W., et al., *Association of patterns of class I histone deacetylase expression with patient prognosis in gastric cancer: a retrospective analysis.* Lancet Oncol, 2008. **9**(2): p. 139-48.

84.     Oehme, I., et al., *Targeting of HDAC8 and investigational inhibitors in neuroblastoma.* Expert Opin Investig Drugs, 2009. **18**(11): p. 1605-17.

85.     Weichert, W., et al., *Expression of class I histone deacetylases indicates poor prognosis in endometrioid subtypes of ovarian and endometrial carcinomas.* Neoplasia, 2008. **10**(9): p. 1021-7.

86.     Yang, X.J. and E. Seto, *The Rpd3/Hda1 family of lysine deacetylases: from bacteria and yeast to mice and men.* Nat Rev Mol Cell Biol, 2008. **9**(3): p. 206-18.

87.     Yang, X.J. and E. Seto, *HATs and HDACs: from structure, function and regulation to novel strategies for therapy and prevention.* Oncogene, 2007. **26**(37): p. 5310-8.

88.     Liang, G., et al., *Distinct localization of histone H3 acetylation and H3-K4 methylation to the transcription start sites in the human genome.* Proc Natl Acad Sci U S A, 2004. **101**(19): p. 7357-62.

89.     Olumi, A.F., *A critical analysis of the use of p53 as a marker for management of bladder cancer.* Urol Clin North Am, 2000. **27**(1): p. 75-82, ix.

90.     Ozawa, A., et al., *Inhibition of bladder tumour growth by histone deacetylase inhibitor.* BJU Int, 2010. **105**(8): p. 1181-6.

91.     Richon, V.M., et al., *Histone deacetylase inhibitor selectively induces p21WAF1 expression and gene-associated histone acetylation.* Proc Natl Acad Sci U S A, 2000. **97**(18): p. 10014-9.

92.     Butler, L.M., et al., *Inhibition of transformed cell growth and induction of cellular differentiation by pyroxamide, an inhibitor of histone deacetylase.* Clin Cancer Res, 2001. **7**(4): p. 962-70.

93.     Canes, D., et al., *Histone deacetylase inhibitors upregulate plakoglobin expression in bladder carcinoma cells and display antineoplastic activity in vitro and in vivo.* Int J Cancer, 2005. **113**(5): p. 841-8.

94.     Glaser, K.B., et al., *Gene expression profiling of multiple histone deacetylase (HDAC) inhibitors: defining a common gene set produced by HDAC inhibition in T24 and MDA carcinoma cell lines.* Mol Cancer Ther, 2003. **2**(2): p. 151-63.

95.     Ellinger, J., et al., *Alterations of global histone H3K9 and H3K27 methylation levels in bladder cancer.* Urol Int, 2014. **93**(1): p. 113-8.

96. Schneider, A.C., et al., *Global histone H4K20 trimethylation predicts cancer-specific survival in patients with muscle-invasive bladder cancer.* BJU Int, 2011. **108**(8 Pt 2): p. E290-6.

97. Telu, K.H., et al., *Alterations of histone H1 phosphorylation during bladder carcinogenesis.* J Proteome Res, 2013. **12**(7): p. 3317-26.

98. Weikert, S., et al., *Expression levels of the EZH2 polycomb transcriptional repressor correlate with aggressiveness and invasive potential of bladder carcinomas.* Int J Mol Med, 2005. **16**(2): p. 349-53.

99. West, A.C. and R.W. Johnstone, *New and emerging HDAC inhibitors for cancer treatment.* J Clin Invest, 2014. **124**(1): p. 30-9.

100. Li, Z. and W.G. Zhu, *Targeting histone deacetylases for cancer therapy: from molecular mechanisms to clinical implications.* Int J Biol Sci, 2014. **10**(7): p. 757-70.

101. Nebbioso, A., et al., *Trials with 'epigenetic' drugs: an update.* Mol Oncol, 2012. **6**(6): p. 657-82.

102. Dokmanovic, M., C. Clarke, and P.A. Marks, *Histone deacetylase inhibitors: overview and perspectives.* Mol Cancer Res, 2007. **5**(10): p. 981-9.

103. Sharma, N.L., et al., *The emerging role of histone deacetylase (HDAC) inhibitors in urological cancers.* BJU Int, 2013. **111**(4): p. 537-42.

104. Elaut, G., V. Rogiers, and T. Vanhaecke, *The pharmaceutical potential of histone deacetylase inhibitors.* Curr Pharm Des, 2007. **13**(25): p. 2584-620.

105. Duvic, M., et al., *Phase 2 trial of oral vorinostat (suberoylanilide hydroxamic acid, SAHA) for refractory cutaneous T-cell lymphoma (CTCL).* Blood, 2007. **109**(1): p. 31-9.

106. Piekarz, R.L., et al., *Phase II multi-institutional trial of the histone deacetylase inhibitor romidepsin as monotherapy for patients with cutaneous T-cell lymphoma.* J Clin Oncol, 2009. **27**(32): p. 5410-7.

107. Wang, H., et al., *Discovery of (2E)-3-{2-butyl-1-[2-(diethylamino)ethyl]-1H-benzimidazol-5-yl}-N-hydroxyacrylami de (SB939), an orally active histone deacetylase inhibitor with a superior preclinical profile.* J Med Chem, 2011. **54**(13): p. 4694-720.

108. Novotny-Diermayr, V., et al., *SB939, a novel potent and orally active histone deacetylase inhibitor with high tumor exposure and efficacy in mouse models of colorectal cancer.* Mol Cancer Ther, 2010. **9**(3): p. 642-52.

109. Jayaraman, R., et al., *Preclinical metabolism and disposition of SB939 (Pracinostat), an orally active histone deacetylase inhibitor, and prediction of human pharmacokinetics.* Drug Metab Dispos, 2011. **39**(12): p. 2219-32.

110. Novotny-Diermayr, V., et al., *Pharmacodynamic evaluation of the target efficacy of SB939, an oral HDAC inhibitor with selectivity for tumor tissue.* Mol Cancer Ther, 2011. **10**(7): p. 1207-17.

111. Yong, W.P., et al., *Phase I and pharmacodynamic study of an orally administered novel inhibitor of histone deacetylases, SB939, in patients with refractory solid malignancies.* Ann Oncol, 2011. **22**(11): p. 2516-22.

112. Zorzi, A.P., et al., *A phase I study of histone deacetylase inhibitor, pracinostat (SB939), in pediatric patients with refractory solid tumors: IND203 a trial of the NCIC IND program/C17 pediatric phase I consortium.* Pediatr Blood Cancer, 2013. **60**(11): p. 1868-74.

113.    Eigl, B.J., et al., *A phase II study of the HDAC inhibitor SB939 in patients with castration resistant prostate cancer: NCIC clinical trials group study IND195.* Invest New Drugs, 2015. **33**(4): p. 969-76.

114.    Hai, T., C.C. Wolford, and Y.S. Chang, *ATF3, a hub of the cellular adaptive-response network, in the pathogenesis of diseases: is modulation of inflammation a unifying component?* Gene Expr, 2010. **15**(1): p. 1-11.

115.    Kang, Y., C.R. Chen, and J. Massague, *A self-enabling TGFbeta response coupled to stress signaling: Smad engages stress response factor ATF3 for Id1 repression in epithelial cells.* Mol Cell, 2003. **11**(4): p. 915-26.

116.    Yin, X., et al., *ATF3, an adaptive-response gene, enhances TGF{beta} signaling and cancer-initiating cell features in breast cancer cells.* J Cell Sci, 2010. **123**(Pt 20): p. 3558-65.

117.    Jiang, H.Y., et al., *Activating transcription factor 3 is integral to the eukaryotic initiation factor 2 kinase stress response.* Mol Cell Biol, 2004. **24**(3): p. 1365-77.

118.    Gilchrist, M., et al., *Systems biology approaches identify ATF3 as a negative regulator of Toll-like receptor 4.* Nature, 2006. **441**(7090): p. 173-8.

119.    Whitmore, M.M., et al., *Negative regulation of TLR-signaling pathways by activating transcription factor-3.* J Immunol, 2007. **179**(6): p. 3622-30.

120.    Rosenberger, C.M., et al., *ATF3 regulates MCMV infection in mice by modulating IFN-gamma expression in natural killer cells.* Proc Natl Acad Sci U S A, 2008. **105**(7): p. 2544-9.

121.    Zmuda, E.J., et al., *Deficiency of Atf3, an adaptive-response gene, protects islets and ameliorates inflammation in a syngeneic mouse transplantation model.* Diabetologia, 2010. **53**(7): p. 1438-50.

122.    Chen, H., et al., *Amino acid deprivation induces the transcription rate of the human asparagine synthetase gene through a timed program of expression and promoter binding of nutrient-responsive basic region/leucine zipper transcription factors as well as localized histone acetylation.* J Biol Chem, 2004. **279**(49): p. 50829-39.

123.    Park, H.J., et al., *ATF3 negatively regulates adiponectin receptor 1 expression.* Biochem Biophys Res Commun, 2010. **400**(1): p. 72-7.

124.    Qi, L., et al., *Adipocyte CREB promotes insulin resistance in obesity.* Cell Metab, 2009. **9**(3): p. 277-86.

125.    Wang, J., Y. Cao, and D.F. Steiner, *Regulation of proglucagon transcription by activated transcription factor (ATF) 3 and a novel isoform, ATF3b, through the cAMP-response element/ATF site of the proglucagon gene promoter.* J Biol Chem, 2003. **278**(35): p. 32899-904.

126.    Lu, D., C.D. Wolfgang, and T. Hai, *Activating transcription factor 3, a stress-inducible gene, suppresses Ras-stimulated tumorigenesis.* J Biol Chem, 2006. **281**(15): p. 10473-81.

127.    Huang, X., X. Li, and B. Guo, *KLF6 induces apoptosis in prostate cancer cells through up-regulation of ATF3.* J Biol Chem, 2008. **283**(44): p. 29795-801.

128.    Bottone, F.G., Jr., et al., *The anti-invasive activity of cyclooxygenase inhibitors is regulated by the transcription factor ATF3 (activating transcription factor 3).* Mol Cancer Ther, 2005. **4**(5): p. 693-703.

129.    Fan, F., et al., *ATF3 induction following DNA damage is regulated by distinct signaling pathways and over-expression of ATF3 protein suppresses cells growth.* Oncogene, 2002. **21**(49): p. 7488-96.

130. Pelzer, A.E., et al., *The expression of transcription factor activating transcription factor 3 in the human prostate and its regulation by androgen in prostate cancer.* J Urol, 2006. **175**(4): p. 1517-22.

131. Bandyopadhyay, S., et al., *The tumor metastasis suppressor gene Drg-1 down-regulates the expression of activating transcription factor 3 in prostate cancer.* Cancer Res, 2006. **66**(24): p. 11983-90.

132. Wang, Z., et al., *Loss of ATF3 promotes Akt activation and prostate cancer development in a Pten knockout mouse model.* Oncogene, 2015. **34**(38): p. 4975-84.

133. Yin, X., J.W. Dewille, and T. Hai, *A potential dichotomous role of ATF3, an adaptive-response gene, in cancer development.* Oncogene, 2008. **27**(15): p. 2118-27.

134. Thompson, M.R., D. Xu, and B.R. Williams, *ATF3 transcription factor and its emerging roles in immunity and cancer.* J Mol Med (Berl), 2009. **87**(11): p. 1053-60.

135. Wang, A., et al., *The transcription factor ATF3 acts as an oncogene in mouse mammary tumorigenesis.* BMC Cancer, 2008. **8**: p. 268.

136. Wu, X., et al., *Opposing roles for calcineurin and ATF3 in squamous skin cancer.* Nature, 2010. **465**(7296): p. 368-72.

137. Janz, M., et al., *Classical Hodgkin lymphoma is characterized by high constitutive expression of activating transcription factor 3 (ATF3), which promotes viability of Hodgkin/Reed-Sternberg cells.* Blood, 2006. **107**(6): p. 2536-9.

138. Xie, J.J., et al., *ATF3 functions as a novel tumor suppressor with prognostic significance in esophageal squamous cell carcinoma.* Oncotarget, 2014. **5**(18): p. 8569-82.

139. Yuan, X., et al., *ATF3 suppresses metastasis of bladder cancer by regulating gelsolin-mediated remodeling of the actin cytoskeleton.* Cancer Res, 2013. **73**(12): p. 3625-37.

140. Yu, L., et al., *Selective regulation of p38beta protein and signaling by integrin-linked kinase mediates bladder cancer cell migration.* Oncogene, 2014. **33**(6): p. 690-701.

141. St Germain, C., et al., *Cisplatin induces cytotoxicity through the mitogen-activated protein kinase pathways and activating transcription factor 3.* Neoplasia, 2010. **12**(7): p. 527-38.

142. Hai, T. and M.G. Hartman, *The molecular biology and nomenclature of the activating transcription factor/cAMP responsive element binding family of transcription factors: activating transcription factor proteins and homeostasis.* Gene, 2001. **273**(1): p. 1-11.

143. Vigushin, D.M., et al., *Trichostatin A is a histone deacetylase inhibitor with potent antitumor activity against breast cancer in vivo.* Clin Cancer Res, 2001. **7**(4): p. 971-6.

144. Yoshida, M., et al., *Potent and specific inhibition of mammalian histone deacetylase both in vivo and in vitro by trichostatin A.* J Biol Chem, 1990. **265**(28): p. 17174-9.

145. Hagelkruys, A., et al., *The biology of HDAC in cancer: the nuclear and epigenetic components.* Handb Exp Pharmacol, 2011. **206**: p. 13-37.

146. Takahashi, R., et al., *The retinoblastoma gene functions as a growth and tumor suppressor in human bladder carcinoma cells.* Proc Natl Acad Sci U S A, 1991. **88**(12): p. 5257-61.

147. Diyabalanage, H.V., M.L. Granda, and J.M. Hooker, *Combination therapy: histone deacetylase inhibitors and platinum-based chemotherapeutics for cancer.* Cancer Lett, 2013. **329**(1): p. 1-8.

148. Jin, K.L., et al., *The effect of combined treatment with cisplatin and histone deacetylase inhibitors on HeLa cells.* J Gynecol Oncol, 2010. **21**(4): p. 262-8.

149.     Bandyopadhyay, D., A. Mishra, and E.E. Medrano, *Overexpression of histone deacetylase 1 confers resistance to sodium butyrate-mediated apoptosis in melanoma cells through a p53-mediated pathway.* Cancer Res, 2004. **64**(21): p. 7706-10.

150.     Wang, L., et al., *Targeting HDAC with a novel inhibitor effectively reverses paclitaxel resistance in non-small cell lung cancer via multiple mechanisms.* Cell Death Dis, 2016. **7**: p. e2063.

151.     Piekarz, R.L., et al., *T-cell lymphoma as a model for the use of histone deacetylase inhibitors in cancer therapy: impact of depsipeptide on molecular markers, therapeutic targets, and mechanisms of resistance.* Blood, 2004. **103**(12): p. 4636-43.

152.     Okada, T., et al., *Involvement of P-glycoprotein and MRP1 in resistance to cyclic tetrapeptide subfamily of histone deacetylase inhibitors in the drug-resistant osteosarcoma and Ewing's sarcoma cells.* Int J Cancer, 2006. **118**(1): p. 90-7.

153.     Rosato, R.R., et al., *Histone deacetylase inhibitors activate NF-kappaB in human leukemia cells through an ATM/NEMO-related pathway.* J Biol Chem, 2010. **285**(13): p. 10064-77.

154.     Fantin, V.R. and V.M. Richon, *Mechanisms of resistance to histone deacetylase inhibitors and their therapeutic implications.* Clin Cancer Res, 2007. **13**(24): p. 7237-42.

155.     Newbold, A., et al., *The role of p21(waf1/cip1) and p27(Kip1) in HDACi-mediated tumor cell death and cell cycle arrest in the Emu-myc model of B-cell lymphoma.* Oncogene, 2014. **33**(47): p. 5415-23.

156.     Qiu, L., et al., *Histone deacetylase inhibitors trigger a G2 checkpoint in normal cells that is defective in tumor cells.* Mol Biol Cell, 2000. **11**(6): p. 2069-83.

157.	Lee, J.H., et al., *Role of checkpoint kinase 1 (Chk1) in the mechanisms of resistance to histone deacetylase inhibitors.* Proc Natl Acad Sci U S A, 2011. **108**(49): p. 19629-34.

158.	Ungerstedt, J.S., et al., *Role of thioredoxin in the response of normal and transformed cells to histone deacetylase inhibitors.* Proc Natl Acad Sci U S A, 2005. **102**(3): p. 673-8.

159.	Wang, D. and S.J. Lippard, *Cellular processing of platinum anticancer drugs.* Nat Rev Drug Discov, 2005. **4**(4): p. 307-20.

160.	Lin, J., et al., *Downregulation of HIPK2 increases resistance of bladder cancer cell to cisplatin by regulating Wip1.* PLoS One, 2014. **9**(5): p. e98418.

161.	Gottesman, M.M., T. Fojo, and S.E. Bates, *Multidrug resistance in cancer: role of ATP-dependent transporters.* Nat Rev Cancer, 2002. **2**(1): p. 48-58.

162.	Bolden, J.E., M.J. Peart, and R.W. Johnstone, *Anticancer activities of histone deacetylase inhibitors.* Nat Rev Drug Discov, 2006. **5**(9): p. 769-84.

163.	Ramalingam, S.S., et al., *Carboplatin and Paclitaxel in combination with either vorinostat or placebo for first-line therapy of advanced non-small-cell lung cancer.* J Clin Oncol, 2010. **28**(1): p. 56-62.

164.	Shen, J., et al., *Enhancement of cisplatin induced apoptosis by suberoylanilide hydroxamic acid in human oral squamous cell carcinoma cell lines.* Biochem Pharmacol, 2007. **73**(12): p. 1901-9.

165.	Erlich, R.B., et al., *Valproic acid as a therapeutic agent for head and neck squamous cell carcinomas.* Cancer Chemother Pharmacol, 2009. **63**(3): p. 381-9.

166.	Valentini, A., et al., *Valproic acid induces apoptosis, p16INK4A upregulation and sensitization to chemotherapy in human melanoma cells.* Cancer Biol Ther, 2007. **6**(2): p. 185-91.

167. Min, K.J., et al., *The effects of DNA methylation and epigenetic factors on the expression of CD133 in ovarian cancers.* J Ovarian Res, 2012. **5**(1): p. 28.

168. Yoon, C.Y., et al., *The histone deacetylase inhibitor trichostatin A synergistically resensitizes a cisplatin resistant human bladder cancer cell line.* J Urol, 2011. **185**(3): p. 1102-11.

169. Stronach, E.A., et al., *HDAC4-regulated STAT1 activation mediates platinum resistance in ovarian cancer.* Cancer Res, 2011. **71**(13): p. 4412-22.

170. Khabele, D., *The therapeutic potential of class I selective histone deacetylase inhibitors in ovarian cancer.* Front Oncol, 2014. **4**: p. 111.

171. Razak, A.R., et al., *Phase I clinical, pharmacokinetic and pharmacodynamic study of SB939, an oral histone deacetylase (HDAC) inhibitor, in patients with advanced solid tumours.* Br J Cancer, 2011. **104**(5): p. 756-62.

172. Kerbel, R.S., *Human tumor xenografts as predictive preclinical models for anticancer drug activity in humans: better than commonly perceived-but they can be improved.* Cancer Biol Ther, 2003. **2**(4 Suppl 1): p. S134-9.

173. Sausville, E.A. and A.M. Burger, *Contributions of human tumor xenografts to anticancer drug development.* Cancer Res, 2006. **66**(7): p. 3351-4, discussion 3354.

174. Davies, B.R., et al., *AZD6244 (ARRY-142886), a potent inhibitor of mitogen-activated protein kinase/extracellular signal-regulated kinase kinase 1/2 kinases: mechanism of action in vivo, pharmacokinetic/pharmacodynamic relationship, and potential for combination in preclinical models.* Mol Cancer Ther, 2007. **6**(8): p. 2209-19.

175. Porter, A.G. and R.U. Janicke, *Emerging roles of caspase-3 in apoptosis.* Cell Death Differ, 1999. **6**(2): p. 99-104.

176.    Wang, D., et al., *Immunohistochemistry in the evaluation of neovascularization in tumor xenografts.* Biotech Histochem, 2008. **83**(3-4): p. 179-89.

177.    Montecinos, V.P., et al., *Primary xenografts of human prostate tissue as a model to study angiogenesis induced by reactive stroma.* PLoS One, 2012. **7**(1): p. e29623.

178.    Nishida, N., et al., *Angiogenesis in cancer.* Vasc Health Risk Manag, 2006. **2**(3): p. 213-9.

179.    Ellis, L., H. Hammers, and R. Pili, *Targeting tumor angiogenesis with histone deacetylase inhibitors.* Cancer Lett, 2009. **280**(2): p. 145-53.

180.    Deroanne, C.F., et al., *Histone deacetylases inhibitors as anti-angiogenic agents altering vascular endothelial growth factor signaling.* Oncogene, 2002. **21**(3): p. 427-36.

181.    Kim, M.S., et al., *Histone deacetylases induce angiogenesis by negative regulation of tumor suppressor genes.* Nat Med, 2001. **7**(4): p. 437-43.

182.    Michaelis, M., et al., *Valproic acid inhibits angiogenesis in vitro and in vivo.* Mol Pharmacol, 2004. **65**(3): p. 520-7.

183.    Chlenski, A., et al., *Anti-angiogenic SPARC peptides inhibit progression of neuroblastoma tumors.* Mol Cancer, 2010. **9**: p. 138.

184.    Fletcher, O., et al., *Lifetime risks of common cancers among retinoblastoma survivors.* J Natl Cancer Inst, 2004. **96**(5): p. 357-63.

185.    Cooper, G.M., *The Cell: A Molecular Approach*. Tumor Suppressor Genes, ed. S. (MA). Vol. 2nd edition. 2000: Sinauer Associates.

186.    Crawford, J.M., *The origins of bladder cancer.* Lab Invest, 2008. **88**(7): p. 686-93.

187.    Miyamoto, H., et al., *Retinoblastoma gene mutations in primary human bladder cancer.* Br J Cancer, 1995. **71**(4): p. 831-5.

188.    Sherr, C.J., *Cancer cell cycles.* Science, 1996. **274**(5293): p. 1672-7.

189.    Di Fiore, R., et al., *RB1 in cancer: different mechanisms of RB1 inactivation and alterations of pRb pathway in tumorigenesis.* J Cell Physiol, 2013. **228**(8): p. 1676-87.

190.    Welch, P.J. and J.Y. Wang, *A C-terminal protein-binding domain in the retinoblastoma protein regulates nuclear c-Abl tyrosine kinase in the cell cycle.* Cell, 1993. **75**(4): p. 779-90.

191.    Siddiqui, H., et al., *Histone deacetylation of RB-responsive promoters: requisite for specific gene repression but dispensable for cell cycle inhibition.* Mol Cell Biol, 2003. **23**(21): p. 7719-31.

192.    Li, H.F., et al., *ATF3-mediated epigenetic regulation protects against acute kidney injury.* J Am Soc Nephrol, 2010. **21**(6): p. 1003-13.

193.    St Germain, C., A. O'Brien, and J. Dimitroulakos, *Activating Transcription Factor 3 regulates in part the enhanced tumour cell cytotoxicity of the histone deacetylase inhibitor M344 and cisplatin in combination.* Cancer Cell Int, 2010. **10**: p. 32.

194.    Sakai, T., et al., *Oncogenic germ-line mutations in Sp1 and ATF sites in the human retinoblastoma gene.* Nature, 1991. **353**(6339): p. 83-6.

195.    Park, K., et al., *The human retinoblastoma susceptibility gene promoter is positively autoregulated by its own product.* J Biol Chem, 1994. **269**(8): p. 6083-8.

196.    Yan, C. and D.D. Boyd, *ATF3 regulates the stability of p53: a link to cancer.* Cell Cycle, 2006. **5**(9): p. 926-9.

197.    Taketani, K., et al., *Key role of ATF3 in p53-dependent DR5 induction upon DNA damage of human colon cancer cells.* Oncogene, 2012. **31**(17): p. 2210-21.

198.    Heiman, M., et al., *A translational profiling approach for the molecular characterization of CNS cell types.* Cell, 2008. **135**(4): p. 738-48.

199. Doyle, J.P., et al., *Application of a translational profiling approach for the comparative analysis of CNS cell types.* Cell, 2008. **135**(4): p. 749-62.

200. King, H.A. and A.P. Gerber, *Translatome profiling: methods for genome-scale analysis of mRNA translation.* Brief Funct Genomics, 2016. **15**(1): p. 22-31.

201. Tian, Q., et al., *Integrated genomic and proteomic analyses of gene expression in Mammalian cells.* Mol Cell Proteomics, 2004. **3**(10): p. 960-9.

202. Alberts, B., A. Johnson, and J. Lewis, *Molecular Biology of the Cell*, in *From RNA to Protein*. 2002, Graland Science: Nwe York.

203. Wilson, D.N. and J.H. Doudna Cate, *The structure and function of the eukaryotic ribosome.* Cold Spring Harb Perspect Biol, 2012. **4**(5).

204. Jackson, R.J., C.U. Hellen, and T.V. Pestova, *The mechanism of eukaryotic translation initiation and principles of its regulation.* Nat Rev Mol Cell Biol, 2010. **11**(2): p. 113-27.

205. Heiman, M., et al., *Cell type-specific mRNA purification by translating ribosome affinity purification (TRAP).* Nat Protoc, 2014. **9**(6): p. 1282-91.

206. Ruggero, D. and P.P. Pandolfi, *Does the ribosome translate cancer?* Nat Rev Cancer, 2003. **3**(3): p. 179-92.

207. Shenoy, N., et al., *Alterations in the ribosomal machinery in cancer and hematologic disorders.* J Hematol Oncol, 2012. **5**: p. 32.

208. Girardi, T. and K. De Keersmaecker, *T-ALL: ALL a matter of Translation?* Haematologica, 2015. **100**(3): p. 293-5.

209. Yeung, C., T. Dinh, and J. Lee, *The health economics of bladder cancer: an updated review of the published literature.* Pharmacoeconomics, 2014. **32**(11): p. 1093-104.

210. Baylin, S.B. and J.E. Ohm, *Epigenetic gene silencing in cancer - a mechanism for early oncogenic pathway addiction?* Nat Rev Cancer, 2006. **6**(2): p. 107-16.

211. Ohtani-Fujita, N., et al., *CpG methylation inactivates the promoter activity of the human retinoblastoma tumor-suppressor gene.* Oncogene, 1993. **8**(4): p. 1063-7.

212. Riccio, A., *Wilms tumor and constitutional epigenetic defects.* Nat Genet, 2008. **40**(11): p. 1272-3.

213. Feinberg, A.P. and B. Tycko, *The history of cancer epigenetics.* Nat Rev Cancer, 2004. **4**(2): p. 143-53.

214. Cui, H., et al., *Loss of IGF2 imprinting: a potential marker of colorectal cancer risk.* Science, 2003. **299**(5613): p. 1753-5.

215. Belinsky, S.A., et al., *Aberrant methylation of p16(INK4a) is an early event in lung cancer and a potential biomarker for early diagnosis.* Proc Natl Acad Sci U S A, 1998. **95**(20): p. 11891-6.

216. Marsit, C.J., et al., *Epigenetic inactivation of SFRP genes and TP53 alteration act jointly as markers of invasive bladder cancer.* Cancer Res, 2005. **65**(16): p. 7081-5.

217. Cheng, C.F. and H. Lin, *Acute kidney injury and the potential for ATF3-regulated epigenetic therapy.* Toxicol Mech Methods, 2011. **21**(4): p. 362-6.

218. Zhong, S., et al., *Pharmacologic inhibition of epigenetic modifications, coupled with gene expression profiling, reveals novel targets of aberrant DNA methylation and histone deacetylation in lung cancer.* Oncogene, 2007. **26**(18): p. 2621-34.

219. Liu, J., et al., *Role of ATF3 in synergistic cancer cell killing by a combination of HDAC inhibitors and agonistic anti-DR5 antibody through ER stress in human colon cancer cells.* Biochem Biophys Res Commun, 2014. **445**(2): p. 320-6.

220. Indovina, P., et al., *RB1 dual role in proliferation and apoptosis: cell fate control and implications for cancer therapy.* Oncotarget, 2015. **6**(20): p. 17873-90.

221. Rieger, K.M., et al., *Human bladder carcinoma cell lines as indicators of oncogenic change relevant to urothelial neoplastic progression.* Br J Cancer, 1995. **72**(3): p. 683-90.

222. Sourvinos, G., et al., *Genetic detection of bladder cancer by microsatellite analysis of p16, RB1 and p53 tumor suppressor genes.* J Urol, 2001. **165**(1): p. 249-52.

223. Acikbas, I., et al., *Detection of LOH of the RB1 gene in bladder cancers by PCR-RFLP.* Urol Int, 2002. **68**(3): p. 189-92.

224. Sowa, Y., et al., *Retinoblastoma binding factor 1 site in the core promoter region of the human RB gene is activated by hGABP/E4TF1.* Cancer Res, 1997. **57**(15): p. 3145-8.

225. Gill, R.M., et al., *Characterization of the human RB1 promoter and of elements involved in transcriptional regulation.* Cell Growth Differ, 1994. **5**(5): p. 467-74.

226. DeCaprio, J.A., et al., *The product of the retinoblastoma susceptibility gene has properties of a cell cycle regulatory element.* Cell, 1989. **58**(6): p. 1085-95.

227. Ozono, E., S. Yamaoka, and K. Ohtani, *To grow, stop or die? - novel tumor suppressive mechanism regulated by the transcription factor E2F*, in *Future aspects of tumor suppressor gene*, Y. Cheng, Editor. 2013, Intech.

228. Youn, J.I., et al., *Epigenetic silencing of retinoblastoma gene regulates pathologic differentiation of myeloid cells in cancer.* Nat Immunol, 2013. **14**(3): p. 211-20.

# *APPENDICES*

**1. Appendix: Sequence of primers used for quantitative real time PCR**

| | | |
|---|---|---|
| **ATF3** | Forward | AACCTGACGCCCTTTGTCAAG |
| | Reverse | TACCTCGGCTTTTGTGATGGA |
| **Actin** | Forward | CATCCACGAAACTACCTTCAACTCC |
| | Reverse | GAGCCGCCGATCCACACG |
| **HDAC1** | Forward | ACCGGGCAACGTTACGAAT |
| | Reverse | CTATCAAAGGACACGCCAAGTG |
| **HDAC2** | Forward | TCAAGGAGGCGGCAAAAA |
| | Reverse | TGCGGATTCTATGAGGCTTCA |
| **HDAC3** | Forward | TTGAGTTCTGCTCGCGTTACA |
| | Reverse | CCCAGTTAATGGCAATATCACAGAT |
| **HDAC4** | Forward | AATCTGAACCACTGCATTTCCA |
| | Reverse | GGTGGTTATAGGAGGTCGACACT |
| **HDAC5** | Forward | CCATTGGAGACGTGGAGTACCT |
| | Reverse | GCGGAGACTAGGACCACATCA |
| **HDAC6** | Forward | GGAATGGCATGGCCATCATTAG |
| | Reverse | CGTGGTTGAACATGCAATAGC |
| **HDAC7** | Forward | CTGCATTGGAGGAATGAAGCT |

| | | |
|---|---|---|
| | Reverse | CTGGCACAGCGGATGTTTG |
| **HDAC8** | Forward | GACCGTGTCCCTGCACAAA |
| | Reverse | CAACATCAGACACGTCACCTGTT |
| **HDAC9** | Forward | AGTGTGAGACGCAGACGCTTAG |
| | Reverse | TTTGCTGTCGCATTTGTTCTTT |
| **HDAC10** | Forward | GCTTCACTGTCAACCTGCCC |
| | Reverse | AGTCAGCGTTTCCCATCCC |
| **HDAC11** | Forward | TGGGCATGAGCGAGACTTC |
| | Reverse | GCGGTTGTAAACATCCATGATG |

**2. Appendix: Immunoblot for ATF3, Acetyl H3, Acetyl H4**
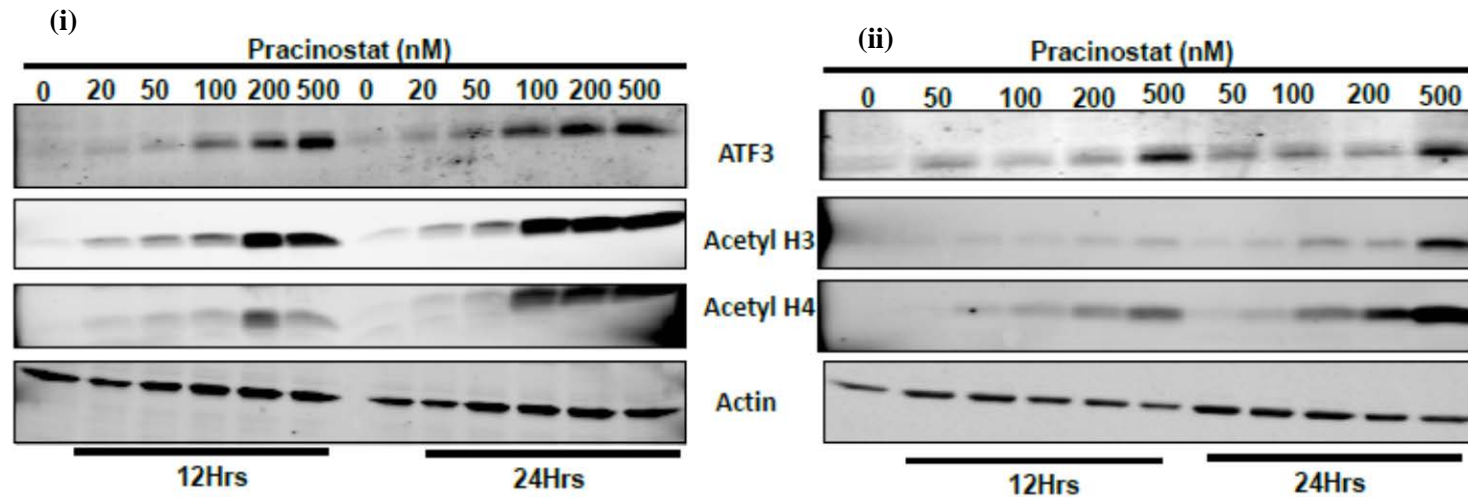


**Pracinostat reactivates ATF3 protein expression *in vitro* in a dose- and time-dependent manner**. Western blot analysis of (i) T24 and (ii) TCC-SUP cell lines treated with increasing concentration (20-500 nM) of Pracinostat for 12 hours and 24 hours. Reactivation of ATF3 in a dose- and time-dependent manner also coincides with progressive increase in acetylation of H3 and H4 (i). Actin is used as an internal control to standardize the relative expression of ATF3 at the protein level.
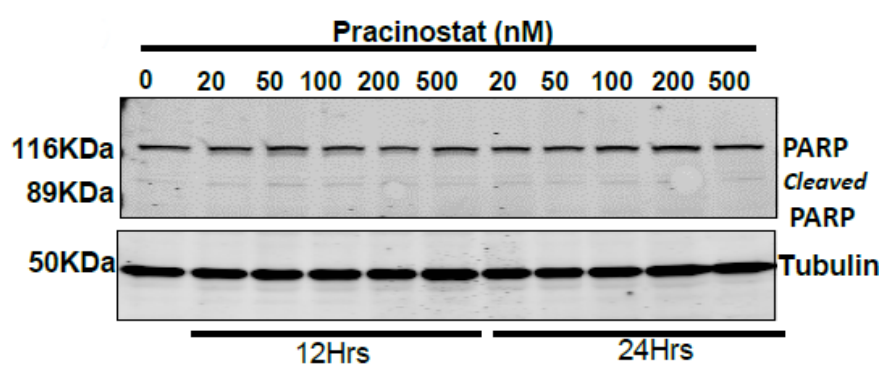
### 3. Appendix: Immunoblot for PARP

**(i)**
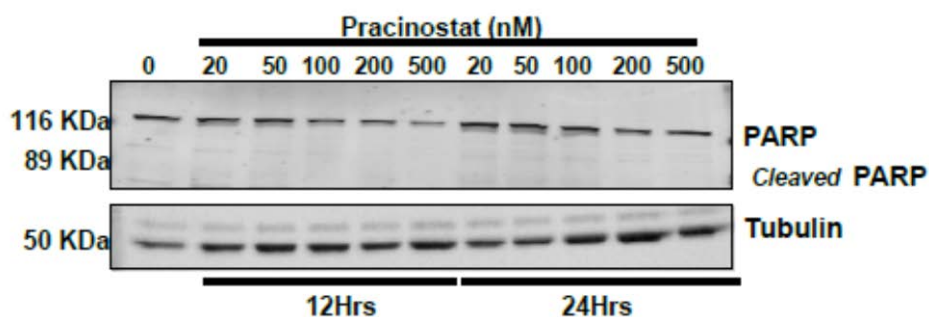


**(ii)**
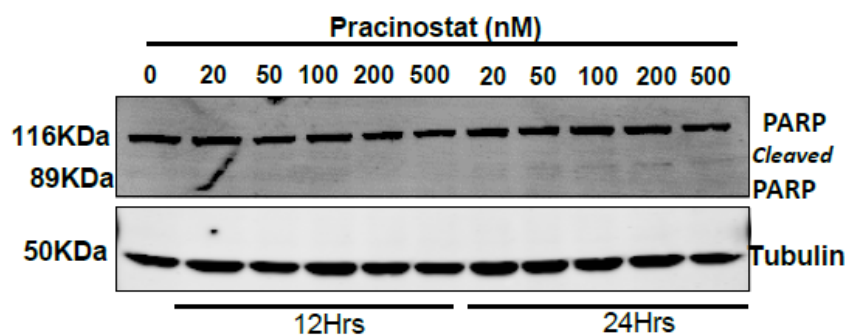


**(iii)**



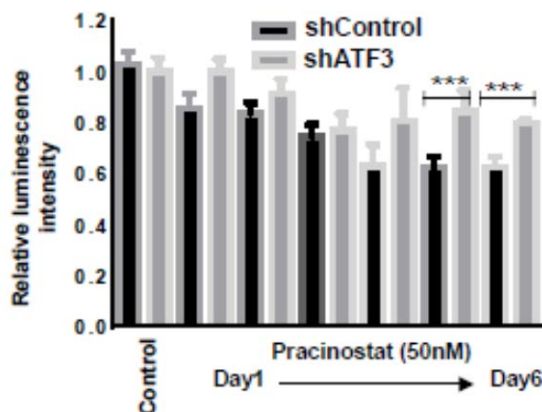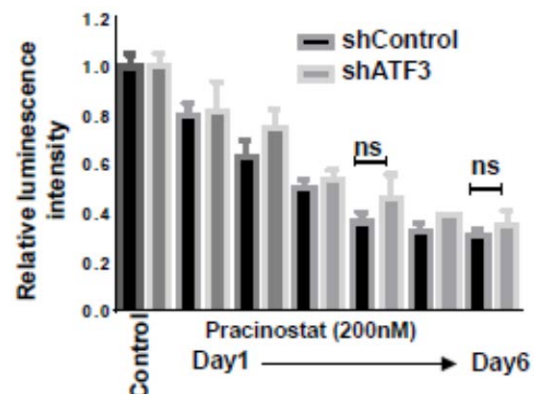**Pracinostat treatment does not induce cell death.** Immunoblot analysis of PARP (116 KDa) and cleaved PARP (89KDa) in 5637 (i), TSU-Pr1 (ii) and in J82 cell lines (iii) treated with Pracinostat for 12 and 24 hrs (n=2).

## 4. Appendix: Assessment of viability in stable control cells and ATF-3 depleted cells with 50nM and 200nM Pracinostat over 6 days.

**(i)**                                                    **(ii)**



**Assessment of viability.** Vialight assay on stable control cells and ATF3-depleted cells treated with Pracinostat over a period of 6 days at a concentration of 50 nM (i) and 200 nM (ii). From day 5, the proliferation rate was significantly higher in knockdown cells compared to control cells at 50 nM Pracinostat treatment (***$P \leq 0.001$). Though the rate of proliferation of shcontrol cells was slower than that of the cells with depleted ATF3 expression in 200 nM Pracinostat-treated cells, the difference was non-significant (ns). Data shown are representative of three replicative experiments.

**5.** **Appendix: Quantification of spheres in ATF3 depleted and matched control cells in soft agar colony formation assay.**
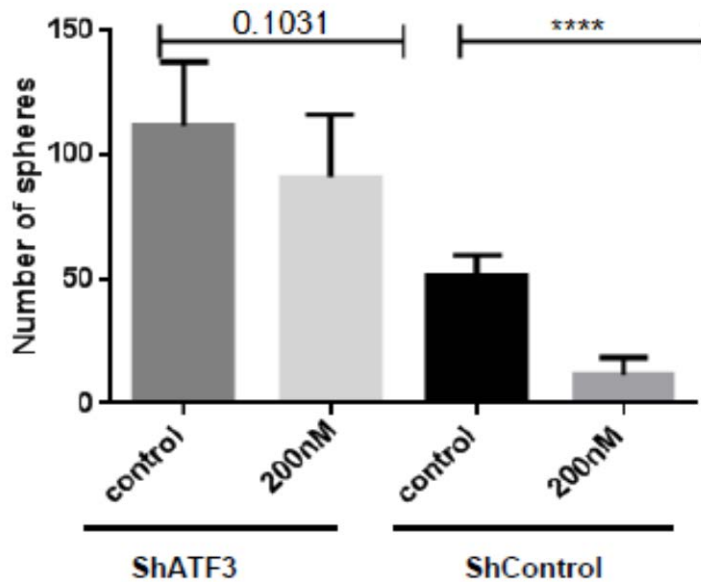


**Quantification of spheres from soft agar assay**: No significant reduction in the colony number was observed in stable ATF3 knockdown cells treated with Pracinostat compared to the untreated shATF3 cells (P = 0.1031). Colony numbers were significantly reduced, > 4 fold (P< 0.001) in control cells treated with 200 nM Pracinostat compared to the untreated control cells. Data shown are representative of three independent experiments and represents mean $\pm$ SEM.

### 6. Appendix: Quantification of scratch wound assay in ATF3 depleted and matched control cells.
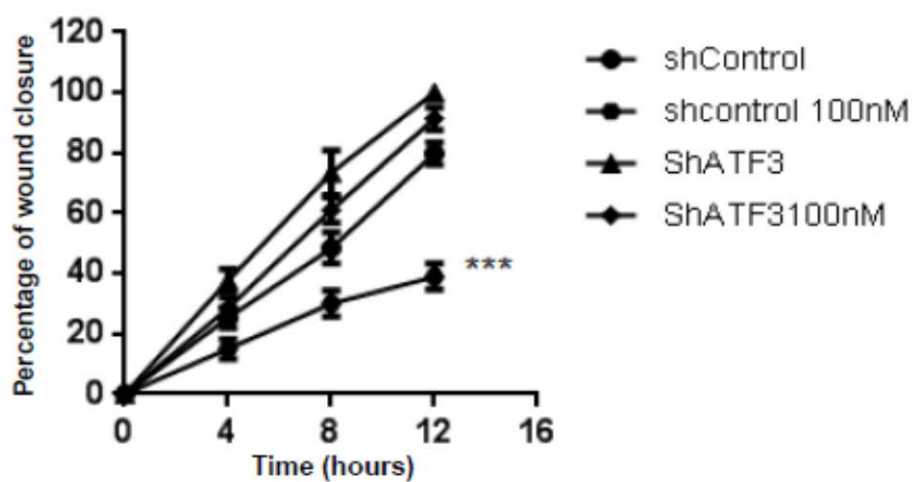


Quantification of monolayer wound healing in control cells and in ATF3 depleted cells +/ -
Pracinostat (100nM). Data represent mean ± SEM (n=3; ***P≤0.001).

## 7. Appendix: Vector sequence

**pCMV6 - AN - mGFP -RPL10a (monomeric GFP fused to the 'N'-terminus of the large-subunit ribosomal protein L10a)**

(7235bp)

```
AACAAAATATTAACGCTTACAATTTCCATTCGCCATTCAGGCTGCGCAACTGTTGGGAAGGGCGATCG
GTGCGGGCCTCTTCGCTATTACGCCAGCTGGCGAAAGGGGGATGTGCTGCAAGGCGATTAAGTTGGGT
AACGCCAGGGTTTTCCCAGTCACGACGTTGTAAAACGACGGCCAGTGCCAAGCTGATCTATACATTGA
ATCAATATTGGCAATTAGCCATATTAGTCATTGGTTATATAGCATAAATCAATATTGGCTATTGGCCA
TTGCATACGTTGTATCTATATCATAATATGTACATTTATATTGGCTCATGTCCAATATGACCGCCATG
TTGACATTGATTATTGACTAGTTATTAATAGTAATCAATTACGGGGTCATTAGTTCATAGCCCATATA
TGGAGTTCCGCGTTACATAACTTACGGTAAATGGCCCGCCTGGCTGACCGCCCAACGACCCCCGCCCA
TTGACGTCAATAATGACGTATGTTCCCATAGTAACGCCAATAGGGACTTTCCATTGACGTCAATGGGT
GGAGTATTTACGGTAAACTGCCCACTTGGCAGTACATCAAGTGTATCATATGCCAAGTCCGCCCCCTA
TTGACGTCAATGACGGTAAATGGCCCGCCTGGCATTATGCCCAGTACATGACCTTACGGGACTTTCCT
ACTTGGCAGTACATCTACGTATTAGTCATCGCTATTACCATGGTGATGCGGTTTTGGCAGTACACCAA
TGGGCGTGGATAGCGGTTTGACTCACGGGGATTTCCAAGTCTCCACCCCATTGACGTCAATGGGAGTT
TGTTTTGGCACCAAAATCAACGGGACTTTCCAAAATGTCGTAATAACCCCGCCCCGTTGACGCAAATG
GGCGGTAGGCGTGTACGGTGGGAGGTCTATATAAGCAGAGCTCGTTTAGTGAACCGTCAGAATTTTGT
AATACGACTCACTATAGGGCGGCCGGGAATTCGTCGACTGGATCCGGTACCGAGGAGATCTGCCACC```A```
```ATGAGCGGGGGCGAGGAGCTGTTCGCCGGCATCGTGCCCGTGCTGATCGAGCTGGACGGCGACGTGCAC```
```GGCCACAAGTTCAGCGTGCGCGGCGAGGGCGAGGGCGACGCCGACTACGGCAAGCTGGAGATCAAGTT```
```CATCTGCACCACCGGCAAGCTGCCCGTGCCCTGGCCCACCCTGGTGACCACCCTCTGCTACGGCATCC```
```AGTGCTTCGCCCGCTACCCCGAGCACATGAAGATGAACGACTTCTTCAAGAGCGCCATGCCCGAGGGC```
```TACATCCAGGAGCGCACCATCCAGTTCCAGGACGACGGCAAGTACAAGACCCGCGGCGAGGTGAAGTT```
```CGAGGGCGACACCCTGGTGAACCGCATCGAGCTGAAGGGCAAGGACTTCAAGGAGGACGGCAACATCC```
```TGGGCCACAAGCTGGAGTACAGCTTCAACAGCCACAACGTGTACATCCGCCCCGACAAGGCCAACAAC```
```GGCCTGGAGGCTAACTTCAAGACCCGCCACAACATCGAGGGCGGCGGCGTGCAGCTGGCCGACCACTA```
```CCAGACCAACGTGCCCCTGGGCGACGGCCCCGTGCTGATCCCCATCAACCACTACCTGAGCACTCAGA```
```CCAAGATCAGCAAGGACCGCAACGAGGCCCGCGACCACATGGTGCTCCTGGAGTCCTTCAGCGCCTGC```
```TGCCACACCCACGGCATGGACGAGCTGTACAGGTCCGGACTCAGA```GCGATCGCC```ATGGGCCGCCGCCCC```
CGCCCGTTGTTACCGGTATTGTAAGAACAAGCCGTACCCAAAGTCTCGCTTCTGCCGAGGTGTCCCTG
ATGCCAAGATTCGCATTTTTGACCTGGGGCGGAAAAAGGCAAAAGTGGATGAGTTTCCGCTTTGTGGC
CACATGGTGTCAGATGAATATGAGCAGCTGTCCTCTGAAGCCCTGGAGGCTGCCCGAATTTGTGCCAA
TAAGTACATGGTAAAAAGTTGTGGCAAAGATGGCTTCCATATCCGGGTGCGGCTCCACCCCTTCCACG
TCATCCGCATCAACAAGATGTTGTCCTGTGCTGGGGCTGACAGGCTCCAAACAGGCATGCGAGGTGCC
TTTGGAAAGCCCCAGGGCACTGTGGCCAGGGTTCACATTGGCCAAGTTATCATGTCCATCCGCACCAA
GCTGCAGAACAAGGAGCATGTGATTGAGGCCCTGCGCAGGGCCAAGTTCAAGTTTCCTGGCCGCCAGA
AGATCCACATCTCAAAGAAGTGGGGCTTCACCAAGTTCAATGCTGATGAATTTGAAGACATGGTGGCT
GAAAAGCGGCTCATCCCAGATGGCTGTGGGGTCAAGTACATCCCCAGTCGTGGCCCTCTGGACAAGTG
GCGGGCCCTGCACTCA```ACGCGT```TAAGCGGCCGCACTCGAGGTTTAAACGGCCGGCCGCGGTCATAGCT
GTTTCCTGAACAGATCCCAGGTGGCATCCCTGTGACCCCTCCCCAGTGCCTCTCCTGGCCCTGGAAGT
TGCCACTCCAGTGCCCACCAGCCTTGTCCTAATAAAATTAAGTTGCATCATTTTGTCTGACTAGGTGT
CCTTCTATAATATTATGGGGTGGAGGGGGGTGGTATGGAGCAAGGGGCAAGTTGGGAAGACAACCTGT
AGGGCCTGCGGGGTCTATTGGGAACCAAGCTGGAGTGCAGTGGCACAATCTTGGCTCACTGCAATCTC
CGCCTCCTGGGTTCAAGCGATTCTCCTGCCTCAGCCTCCCGAGTTGTTGGGATTCCAGGCATGCATGA
```

CCAGGCTCAGCTAATTTTTGTTTTTTTGGTAGAGACGGGGTTTCACCATATTGGCCAGGCTGGTCTCC
AACTCCTAATCTCAGGTGATCTACCCACCTTGGCCTCCCAAATTGCTGGGATTACAGGCGTGAACCAC
TGCTCCCTTCCCTGTCCTTCTGATTTTAAAATAACTATACCAGCAGGAGGACGTCCAGACACAGCATA
GGCTACCTGGCCATGCCCAACCGGTGGGACATTTGAGTTGCTTGCTTGGCACTGTCCTCTCATGCGTT
GGGTCCACTCAGTAGATGCCTGTTGAATTGGGTACGCGGCCAGCTTGGCTGTGGAATGTGTGTCAGTT
AGGGTGTGGAAAGTCCCCAGGCTCCCCAGCAGGCAGAAGTATGCAAAGCATGCATCTCAATTAGTCAG
CAACCAGGTGTGGAAAGTCCCCAGGCTCCCCAGCAGGCAGAAGTATGCAAAGCATGCATCTCAATTAG
TCAGCAACCATAGTCCCGCCCCTAACTCCGCCCATCCCGCCCCTAACTCCGCCCAGTTCCGCCCATTC
TCCGCCCCATGGCTGACTAATTTTTTTTTATTTATGCAGAGGCCGAGGCCGCCTCGGCCTCTGAGCTAT
TCCAGAAGTAGTGAGGAGGCTTTTTTGGAGGCCTAGGCTTTTGCAAAAAGCTCCCGGGAGCTTGTATA
TCCATTTTCGGATCTGATCAAGAGACAGGATGAGGATCGTTTCGCATGATTGAACAAGATGGATTGCA
CGCAGGTTCTCCGGCCGCTTGGGTGGAGAGGCTATTCGGCTATGACTGGGCACAACAGACAATCGGCT
GCTCTGATGCCGCCGTGTTCCGGCTGTCAGCGCAGGGGCGCCCGGTTCTTTTTGTCAAGACCGACCTG
TCCGGTGCCCTGAATGAACTGCAGGACGAGGCAGCGCGGCTATCGTGGCTGGCCACGACGGGCGTTCC
TTGCGCAGCTGTGCTCGACGTTGTCACTGAAGCGGGAAGGGACTGGCTGCTATTGGGCGAAGTGCCGG
GGCAGGATCTCCTGTCATCTCACCTTGCTCCTGCCGAGAAAGTATCCATCATGGCTGATGCAATGCGG
CGGCTGCATACGCTTGATCCGGCTACCTGCCCATTCGACCACCAAGCGAAACATCGCATCGAGCGAGC
ACGTACTCGGATGGAAGCCGGTCTTGTCGATCAGGATGATCTGGACGAAGAGCATCAGGGGCTCGCGC
CAGCCGAACTGTTCGCCAGGCTCAAGGCGCGCATGCCCGACGGCGAGGATCTCGTCGTGACCCATGGC
GATGCCTGCTTGCCGAATATCATGGTGGAAAATGGCCGCTTTTCTGGATTCATCGACTGTGGCCGGCT
GGGTGTGGCCGACCGCTATCAGGACATAGCGTTGGCTACCCGTGATATTGCTGAAGAGCTTGGCGGCG
AATGGGCTGACCGCTTCCTCGTGCTTTACGGTATCGCCGCTCCCGATTCGCAGCGCATCGCCTTCTAT
CGCCTTCTTGACGAGTTCTTCTGAGCGGGACTCTGGGGTTCGAAATGACCGACCAAGCGACGCCCAAC
CTGCCATCACGAGATTTCGATTCCACCGCCGCCTTCTATGAAAGGTTGGGCTTCGGAATCGTTTTCCG
GGACGCCGGCTGGATGATCCTCCAGCGCGGGGATCTCATGCTGGAGTTCTTCGCCCACCCCAACTTGT
TTATTGCAGCTTATAATGGTTACAAATAAAGCAATAGCATCACAAATTTCACAAATAAAGCATTTTTT
TCACTGCATTCTAGTTGTGGTTTGTCCAAACTCATCAATGTATCTTATCATGTCTGTATACCGTCGAC
CTCTAGCTAGAGCTTGGCGTAATCATGGTCATAGCTGTTTCCTGTGTGAAATTGTTATCCGCTCACAA
TTCCACACAACATACGAGCCGGAAGCATAAAGTGTAAAGCCTGGGGTGCCTAATGAGTGAGCTAACTC
ACATTAATTGCGTTGCGCTCACTGCCCGCTTTCCAGTCGGGAAACCTGTCGTGCCAGCTGCATTAATG
AATCGGCCAACGCGCGGGGAGAGGCGGTTTGCGTATTGGGCGCTCTTCCGCTTCCTCGCTCACTGACT
CGCTGCGCTCGGTCGTTCGGCTGCGGCGAGCGGTATCAGCTCACTCAAAGGCGGTAATACGGTTATCC
ACAGAATCAGGGGATAACGCAGGAAAGAACATGTGAGCAAAAGGCCAGCAAAAGGCCAGGAACCGTAA
AAAGGCCGCGTTGCTGGCGTTTTTCCATAGGCTCCGCCCCCCTGACGAGCATCACAAAAATCGACGCT
CAAGTCAGAGGTGGCGAAACCCGACAGGACTATAAAGATACCAGGCGTTTCCCCCTGGAAGCTCCCTC
GTGCGCTCTCCTGTTCCGACCCTGCCGCTTACCGGATACCTGTCCGCCTTTCTCCCTTCGGGAAGCGT
GGCGCTTTCTCATAGCTCACGCTGTAGGTATCTCAGTTCGGTGTAGGTCGTTCGCTCCAAGCTGGGCT
GTGTGCACGAACCCCCCGTTCAGCCCGACCGCTGCGCCTTATCCGGTAACTATCGTCTTGAGTCCAAC
CCGGTAAGACACGACTTATCGCCACTGGCAGCAGCCACTGGTAACAGGATTAGCAGAGCGAGGTATGT
AGGCGGTGCTACAGAGTTCTTGAAGTGGTGGCCTAACTACGGCTACACTAGAAGAACAGTATTTGGTA
TCTGCGCTCTGCTGAAGCCAGTTACCTTCGGAAAAAGAGTTGGTAGCTCTTGATCCGGCAAACAAACC
ACCGCTGGTAGCGGTGGTTTTTTTGTTTGCAAGCAGCAGATTACGCGCAGAAAAAAAGGATCTCAAGA
AGATCCTTTGATCTTTTCTACGGGGTCTGACGCTCAGTGGAACGAAAACTCACGTTAAGGGATTTTGG
TCATGAGATTATCAAAAAGGATCTTCACCTAGATCCTTTTAAATTAAAAATGAAGTTTTAAATCAATC
TAAAGTATATATGAGTAAACTTGGTCTGACAGTTACCAATGCTTAATCAGTGAGGCACCTATCTCAGC
GATCTGTCTATTTCGTTCATCCATAGTTGCCTGACTCCCCGTCGTGTAGATAACTACGATACGGGAGG
GCTTACCATCTGGCCCCAGTGCTGCAATGATACCGCGAGACCCACGCTCACCGGCTCCAGATTTATCA
GCAATAAACCAGCCAGCCGGAAGGGCCGAGCGCAGAAGTGGTCCTGCAACTTTATCCGCCTCCATCCA
GTCTATTAATTGTTGCCGGGAAGCTAGAGTAAGTAGTTCGCCAGTTAATAGTTTGCGCAACGTTGTTG
CCATTGCTACAGGCATCGTGGTGTCACGCTCGTCGTTTGGTATGGCTTCATTCAGCTCCGGTTCCCAA

182

CGATCAAGGCGAGTTACATGATCCCCCATGTTGTGCAAAAAAGCGGTTAGCTCCTTCGGTCCTCCGAT
CGTTGTCAGAAGTAAGTTGGCCGCAGTGTTATCACTCATGGTTATGGCAGCACTGCATAATTCTCTTA
CTGTCATGCCATCCGTAAGATGCTTTTCTGTGACTGGTGAGTACTCAACCAAGTCATTCTGAGAATAG
TGTATGCGGCGACCGAGTTGCTCTTGCCCGGCGTCAATACGGGATAATACCGCGCCACATAGCAGAAC
TTTAAAAGTGCTCATCATTGGAAAACGTTCTTCGGGGCGAAAACTCTCAAGGATCTTACCGCTGTTGA
GATCCAGTTCGATGTAACCCACTCGTGCACCCAACTGATCTTCAGCATCTTTTACTTTCACCAGCGTT
TCTGGGTGAGCAAAAACAGGAAGGCAAAATGCCGCAAAAAAGGGAATAAGGGCGACACGGAAATGTTG
AATACTCATACTCTTCCTTTTTCAATATTATTGAAGCATTTATCAGGGTTATTGTCTCATGAGCGGAT
ACATATTTGAATGTATTTAGAAAAATAAACAAATAGGGGTTCCGCGCACATTTCCCCGAAAAGTGCCA
CCTGACGCGCCCTGTAGCGGCGCATTAAGCGCGGCGGGTGTGGTGGTTACGCGCAGCGTGACCGCTAC
ACTTGCCAGCGCCCTAGCGCCCGCTCCTTTCGCTTTCTTCCCTTCCTTTCTCGCCACGTTCGCCGGCT
TTCCCCGTCAAGCTCTAAATCGGGGGCTCCCTTTAGGGTTCCGATTTAGTGCTTTACGGCACCTCGAC
CCCAAAAAACTTGATTAGGGTGATGGTTCACGTAGTGGGCCATCGCCCTGATAGACGGTTTTTCGCCC
TTTGACGTTGGAGTCCACGTTCTTTAATAGTGGACTCTTGTTCCAAACTGGAACAACACTCAACCCTA
TCTCGGTCTATTCTTTTGATTTATAAGGGATTTTGCCGATTTCGGCCTATTGGTTAAAAAATGAGCTG
ATTTAACAAAAATTTAACGCGAATTTT
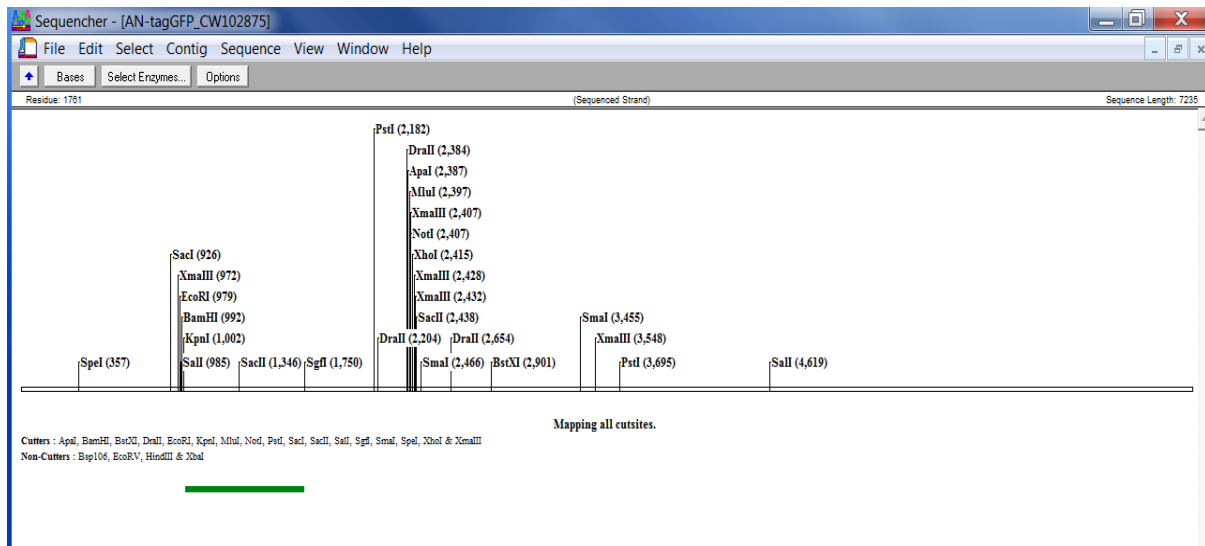
## 8. Appendix: Solution recipes

| Name | Recipe | Description |
|---|---|---|
| Resolving gel (12%)  20 ml for 2 gels | 6.6 ml de-ionized H2O  8 ml 30% acrylamide  5 ml 1.5M Tris (pH 8.8)  0.2 ml 10% Sodium dodecyl sulfate  0.2 ml 10% Ammonium per sulfate  0.008 ml TEMED | Immunoblotting |
| Stacking gel (5%)  6 ml for 2 gels | 4.1 ml de-ionized H2O  1 ml 30% acrylamide  0.75 ml 0.5M Tris (pH 6.8)  0.06 ml 10% Sodium dodecyl sulfate  0.06 ml 10% Ammonium per sulfate  0.006 ml TEMED | Immunoblotting |
| RIPA lysis buffer  (30ml stock  - ⁻20  freezer) | 1.5 ml sodium fluoride (NaF)  1.5 ml sodium orthovanadate  200µl 100x protease inhibitor cocktail  26.7 ml RIPA buffer | Protein lysis buffer |

| | | |
|---|---|---|
| SDS running buffer (10x) | 30.3 g Tris base<br><br>144 g glycine<br><br>10 g SDS<br><br>make to IL with dH2O | Western blot running buffer |
| Transfer buffer storage $4^0$C | 14.4 g glycine<br><br>3 g Tris base<br><br>Make to 800 ml with dH2O<br><br>200 ml methanol | Western blot transfer buffer |
| Tris buffered saline | 2.42 g Tris base<br><br>8 g sodium chloride<br><br>3.8 ml 1M HCL to 1L to make the pH 7.6 | Dilution / wash buffer - western blot |
| Homogenization Buffer (HB) 20 ml | 0.666 ml Tris 1.5 M pH 7.4<br><br>2 ml KCL 1M<br><br>0.24 ml MgCl$_2$ 1M<br><br>2 ml 10% NP-40<br><br>15.09 ml RNase-free H2O | Lysis buffer for translatomes |
| Supplemented | 19.08 ml Homogenization buffer | Homogenisation and lysis |

| homogenization buffer (HB-S) 20 ml | 0.020 ml DTT (1M)<br><br>0.2 ml protease inhibitor (1x)<br><br>0.1 ml RNAsin (200 Units/ml)<br><br>0.4 ml cyclohexamide ( 5mg/ ml)<br><br>0.2 ml Heparin ( 100 mg/ ml) | buffer for translatomes in TRAP mRNA methods |
|---|---|---|
| High salt buffer 20 ml | 0.666 ml  Tris 1.5M pH 7.4<br><br>6 ml KCl 1M<br><br>0.240 ml $MgCl_2$ 1M<br><br>2 ml 10% NP-40<br><br>0.02 ml DTT 1M<br><br>0.4 ml cyclohexamide (5mg/ ml)<br><br>10.67 ml RNAse free H2O | Wash buffer to remove unbound protein to beads in TRAP methods |